

# THE FUTURE OF NUCLEAR PHYSICS IN EUROPE AND THE DEMANDS ON ACCELERATOR TECHNIQUES

Walter F. Henning, GSI, 64291 Darmstadt, Germany

## INTRODUCTION

Nuclear physics has undergone a major reorientation in its research goals during the last decade or so [1]. There are two, or maybe three major reasons for that.

The first one results from the fact that nucleons and mesons, the basic building of nuclei and their fields, have substructure. Understanding the quark-gluon structure of hadrons, how and to what extent this partonic substructure affects the behavior of nuclei and nuclear matter, and to what extent we have a full and quantitative understanding of these features through the theory of strong interaction, quantum-chromo-dynamics (QCD), is at the center of much of the activity in nuclear physics. The length and energy dimensions involved with hadrons and nuclei require the non-perturbative treatment within QCD, and also the extension to finite temperature and chemical potential.

A second important new area has been the development of accelerated beams of short-lived nuclei (sometimes called ‘radioactive’, ‘rare isotope’ or ‘exotic’ beams) at useful intensities. Much of what we know about nuclei comes from nuclear reactions. Consequently these studies have been essentially restricted to stable nuclei where reaction targets could be built and exposed to beams of particles, in particular light ones (protons, deuterons, helium nuclei etc.). Energetic beams of short-lived nuclei now allow to reverse the reaction kinematics and thus, with targets of light nuclei, to study nuclei away from, and up to the limits of stability in nuclear reactions.

galactic neutrinos as well as neutrinos from high-intensity accelerators are of broad interest now. Rare decays and direct symmetry violation studies requiring intense primary and secondary beams are also pushing accelerator performance and design.

The areas of interest just described have overlap and intersections with each other. One way of summarizing the overall situation could be the schematic shown in Figure 1.

## RESEARCH AREAS, FACILITIES AND BEAMS

The new research programs require new experimental capabilities and new facilities and beams, and these then, in turn, define new and very challenging requirements for accelerator instrumentation, in particular beam diagnostics - the subject of this conference.

The substructure of the stable nucleons, protons and neutrons, and of stable nuclei is directly accessible via studies with beams of hadrons, leptons and photons. Other hadrons, mesons and excited baryons, need to be produced in reactions.

Beams of leptons, and in particular electrons, are preferred probes for the ground state structure of nucleons since they are point-like and the electromagnetic interaction is well understood. Structure functions, including in particular spin, have been and are intensely studied. Quark and gluon contributions to the spin are being studied at existing high-energy facilities (HERMES at DESY [3] and COMPASS at CERN [4] for example) but in particular also at the dedicated high-intensity cw electron-beam facility CEBAF at JLAB [5]. Current interest is being focussed on skewed parton distributions and the measurements of DVCS, deep virtual Compton scattering, which promises to provide information on parton correlations and, possibly, structure functions of excited hadrons. These studies, plus the exploration of the transition from perturbative to non-perturbative QCD, are asking for high-duty cycle electron machines up to several tens of GeV laboratory energy. In addition, concepts are being developed for future e-A colliders at tens to 100 GeV center-of-mass energy [6,7].

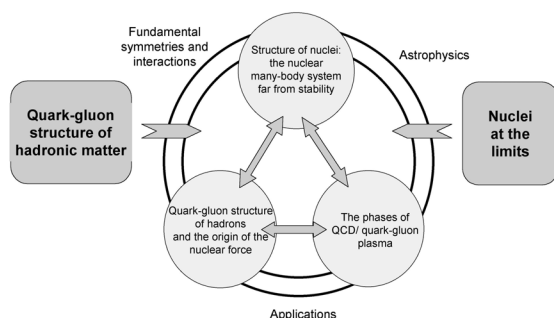


Figure 1: Current research frontiers in nuclear physics.

The third area of interest is the exploration of the limits of the Standard Model. For the strong interaction sector this connects to the QCD discussion above. For the weak sector, the discovery of neutrino oscillations and mass has placed new emphasis on an area which started with Davis’ solar neutrino searches in radiochemical experiments several decades ago [2]. Both solar and

Facilities for studies of QCD with intense hadronic probes are being developed in Japan and Europe: the Japanese Hadron Facility (J-PARC) [8] with intense proton beams and primary interest in research with secondary beams of kaons and neutrinos; the future facility proposed for the GSI Laboratory in Germany with intense antiproton beams and in particular a high-energy antiproton storage ring with electron cooling [9]. The

## Overview of the Diagnostics Systems of SOLEIL and DIAMOND

J.-C. Denard, L. Cassinari, SOLEIL, Societé Synchrotron Soleil, Saint-Aubin, France  
e-mail: Jean-Claude.Denard@synchrotron-soleil.fr  
M. Dykes, R. Smith, ASTeC, Daresbury Laboratory, Daresbury, UK

### *Abstract*

SOLEIL and DIAMOND are two third-generation light sources in construction in France and in Great Britain respectively. SOLEIL is scheduled to deliver its first photons to its users in 2006 and DIAMOND in 2007. This talk will present the beam diagnostic systems of both projects with emphasizing technological novelties and the instruments that are essential to their performances: BPM system, profile monitors and feedback systems.

Paper not received

(See slides of talk on  
following pages)

## SINGLE PASS OPTICAL PROFILE MONITORING

R. Jung, G. Ferioli, S. Hutchins, CERN, Geneva, Switzerland

### Abstract

Beam profiles are acquired in transfer lines to monitor extracted beams and compute their emittance. Measurements performed on the first revolutions of a ring will evaluate the matching of a chain of accelerators. Depending on the particle type and energy, these measurements are in general performed with screens, making either use of Luminescence or Optical Transition Radiation [OTR], and the generated beam images are acquired with sensors of various types. Sometimes the beam position is also measured this way. The principle, advantages and disadvantages of both families of screens will be discussed in relation with the detectors used. Test results with beam and a possible evaluation method for luminescent screens will be presented. Finally other optical methods used will be mentioned for completeness.

### SCREEN MONITORS

Screen monitors are the most popular instruments for single pass profile measurements. A typical monitor is depicted in Fig. 1. It consists of a vacuum vessel with Input and Exit ports for the beam, a mechanism holding several screens, 2 or 3 are usual numbers, a window to extract the light produced by the screen, an optical set-up to image the screen onto a sensor and to control the quantity of light transmitted, and finally a detector to convert the photons into an electrical signal, be it a TV standard signal or a digital acquisition.

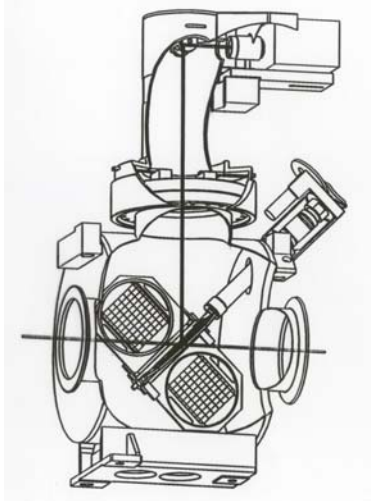


Figure 1: Typical screen monitor.

In the following, we shall review the various types of screens and mention the most important features of the sensors for this type of monitor. The match of these two constituents will largely define the performance of the monitor.

### SCREENS

Two types of screens are in general use: Luminescent screens and Optical Transition Radiation [OTR] screens. The first produce light by excitation of the molecules of the screen by the passage of a charged particle beam followed by de-excitation, which is a bulk phenomenon, whereas the second produce light by an electromagnetic phenomenon initiated by the passage of the beam at the interface of two regions with different dielectric constants, and is hence a pure surface phenomenon.

#### Luminescent screens

When a molecule is excited by an external electromagnetic field, it can emit light via two processes. The first is characterised by a direct jump to the base level with a short decay time constant of a few tens of nanoseconds and will be called fluorescence. In the second process, the de-excitation passes via an intermediate receiver level and takes much longer, typically microseconds to seconds. It will be called phosphorescence. If both processes are present, which is the case with many screens, or in case of doubt, the light emission will be called luminescence.

A first screen type is manufactured from ceramics or glass in which activators have been introduced for controlling the emitted wavelength. The most popular dopant for ceramics is Cr, which results in an emission in the red, well matched to solid-state detectors: see Fig. 8. The concentration of activator, of a few per mil, controls the emitted intensity. Typically, such screens are made from  $\text{Al}_2\text{O}_3$  powder, with grains of the order of  $5\ \mu\text{m}$ , to which silica magnesia lime and the activator, here  $\text{Cr}_2\text{O}_3$ , are added to arrive at a concentration of 99.4% of  $\text{Al}_2\text{O}_3$ . This powder is mixed and pressed, before being fired to sinter, process in which the glassy phase fills up the voids between the grains. After machining to the final shape and finish, typically to  $R_a \sim 1\ \mu\text{m}$ , there is another firing. Microscope observations show large structures, up to  $\sim 30\ \mu\text{m}$ , in the finished product.

Another type of screen uses crystalline materials, where dopants also control the emitted wavelength. These screens are in general more expensive, but as will be seen later, have a better resolution as well as a higher light yield, i.e. sensitivity. There is experience with two types: Thallium doped CsI [1] and Cerium doped YAG [2].

As the light is generated in the bulk of the material, if the screens are placed at  $45^\circ$  with respect to the beam and if they are not infinitely thin or made of opaque material, there will be a collection of light generated in the depth of the material which will create instrument generated tails [3], in the vertical direction in the case of the Fig.1 set-up. To counteract this degradation, monitors have been built [4] with the luminescent screen perpendicular to the beam

## Challenges for LHC and Demands on Beam Instrumentation

J. Wenninger, CERN, Geneva, Switzerland

### Abstract

The LHC machine presently under construction at CERN will exceed existing super-conducting colliders by about one order of magnitude for luminosity and beam energies for pp collisions. To achieve this performance the bunch frequency is as large as 40 MHz and the range in beam intensity covers  $5 \cdot 10^9$  protons to  $3 \cdot 10^{14}$  protons with a normalized beam emittance as small as  $3 \mu\text{rad}$ . This puts very stringent demands on the beam instrumentation to be able to measure beam parameters like beam positions, profiles, tunes, chromaticity, beam losses or luminosity.

This document highlights selected topics in the field of LHC beam instrumentation. The examples will be chosen to cover new detection principles or new numerical data treatments, which had to be developed for the LHC as well as aspects of operational reliability for instrumentation, which will be used for machine protection systems.

### THE LHC MACHINE

The Large Hadron Collider (LHC) is a proton-proton collider scheduled to start operation in 2007. The LHC will be installed in the existing 26.7 km long LEP tunnel. Its nominal operating energy is 7 TeV/c, with injection from the Super Proton Synchrotron (SPS) at 450 GeV/c. The overall layout of the LHC is shown in Fig. 1. The two

chambers that cross in Interaction Regions (IR) 1,2,5 and 8. The two high luminosity experiments are installed in IR1 (ATLAS) and IR5 (CMS). IR3 and IR7 are devoted to beam collimation (beam cleaning). The 400 MHz RF system and most special beam instruments are installed in IR4. The beam dumping system is installed in IR6.

The LHC super-conducting magnets are immersed in a bath of super-fluid Helium at 1.9 K. The nominal operating field of the dipoles is 8.4 T. The main parameters of the LHC for proton operation are summarized in Table 1. Details on ion operation can be found in Ref [2].

Dipole field (at T=1.9 K)	8.39 T
Number of bunches	1 – 2808
Bunch spacing	25 ns
Bunch population	$1.1 \cdot 10^{11}$
R.M.S. normalized emittance $\gamma\epsilon_{x,y}$	$3.75 \mu\text{m}$
Peak luminosity $\mathcal{L}$	$10^{34} \text{ cm}^{-2} \text{ s}^{-1}$
Number of IPs (high $\mathcal{L}$ )	4(2)
Crossing angle at IP	$300 \mu\text{rad}$
Beam-beam tune shift	0.0034
R.M.S. beam size at high $\mathcal{L}$ IP	$16 \mu\text{m}$
R.M.S. bunch length	7.7 cm
Synchrotron rad. power	3.6 kW

Table 1: Nominal proton beam parameters at 7 TeV [1].

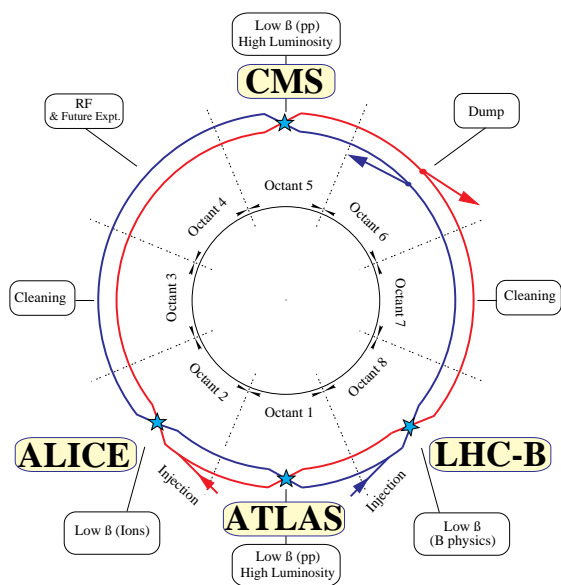


Figure 1: Layout of LHC ring and experiments.

beams (rings) of the LHC circulate in separated vacuum

### DYNAMIC EFFECTS OF SUPER-CONDUCTING MAGNETS

The transfer function at low field of super-conducting magnets shows a hysteresis caused by the persistent currents, long lasting eddy currents originating in the super-conducting filaments when they are subject to field changes, i.e. during ramps [3]. The effect of persistent currents is particularly strong at low field and their effects appear on all allowed multi-poles ( $b_1$  (dipole),  $b_3$  (sextupole),  $b_5$  (decapole) .. for dipole magnets).

The field contributions from the persistent currents decay during injection with a time constant of  $\sim 900$  s and result in systematic and random (magnet to magnet fluctuations) effects. Fig. 2 gives an example for the  $b_3$  component of the dipoles. The associated chromaticity change is  $\Delta Q' \simeq 80$  units. A field ramp of 20 to 30 mT of the dipole field re-establishes the persistent currents to their original configuration before decay. This so-called 'snapback' occurs therefore in the first tens of seconds of the ramp.

The main consequences of the persistent currents are:

## SINGLE SHOT ELECTRON-BEAM BUNCH LENGTH MEASUREMENTS

G. Berden\*, G.M.H. Knippels†, D. Oepts, A.F.G. van der Meer,  
FOM Institute Rijnhuizen / FELIX, Nieuwegein, The Netherlands

S.P. Jamison‡, X. Yan, A.M. MacLeod, W.A. Gillespie,  
School of Computing and Advanced Technologies, University of Abertay Dundee, Dundee, UK

J.L. Shen§, Dept. of Physics, Capital Normal University, Beijing, China

I. Wilke, Rensselaer Polytechnic Institute, Troy, NY, USA

### Abstract

It is recognised by the instrumentation community that 4th generation light sources (like TESLA, LCLS) pose some of the most stringent requirements on beam diagnostics. Of these diagnostics, electro-optic detection of the electric field of electron bunches offers a promising single-shot technique for the measurement of the bunch length and shape in the sub-picosecond domain. The electro-optic detection method makes use of the fact that the local electric field of a highly relativistic electron bunch moving in a straight line is almost entirely concentrated perpendicular to its direction of motion. This electric field induces birefringence in an electro-optic crystal placed in the vicinity of the beam. The amount of birefringence depends on the electric field and is probed by monitoring the change of polarization of a chirped, synchronized Ti:sapphire laser pulse. This paper will provide details of the experimental setup at the Free Electron Laser for Infrared eXperiments (FELIX) in Nieuwegein, The Netherlands, where single shot images of 1.7 ps long electron bunches have been obtained (beam energy 46 MeV, charge per bunch 200 pC). Future upgrading possibilities will be discussed.

### INTRODUCTION

An on-going research project at the Free Electron Laser for Infrared eXperiments (FELIX) [1] is the development of methods to measure the longitudinal shape of electron bunches via electro-optic detection of their transverse electric field. The electron bunch shape is measured inside the accelerator beam pipe at the entrance of the undulator of the FEL. A 0.5 mm thick  $\langle 110 \rangle$  ZnTe crystal is used as an electro-optic sensor and is placed with its  $4 \times 4$  mm<sup>2</sup> front face perpendicular to the propagation direction of the electron beam. The probe laser beam is linearly polarized and passes through the ZnTe crystal parallel to the electron beam.

\* berden@rijnh.nl

† present address: Picarro, Sunnyvale, CA, USA

‡ also at: University of Strathclyde, Glasgow, UK

§ also at: University of Strathclyde, Glasgow, UK

This paper describes three methods to measure the shape of an electron bunch with electro-optic detection. The electric field-induced birefringence in an electro-optic crystal is probed by

1. sweeping the pulse of the probe laser, with a probe pulse length that is shorter than the electron bunch length, over the electron bunch and recording the intensity of the light transmitted through a the crossed polarizer (analyzer) as a function of time [2]. Although this is not a single-shot method, it can be used for real-time monitoring.
2. using a linearly chirped pulse of the probe laser, with a pulse length longer than the electron bunch length, and recording the wavelength spectrum of the chirped pulse which is transmitted through an analyzer [3].
3. using a chirped pulse of the probe laser, with a pulse length longer than the electron bunch length, and recording the single-shot cross-correlation of the chirped pulse transmitted through an analyzer. An unchirped pulse is used as the reference in the cross-correlator.

### DELAY-SCAN METHOD

The probe laser for the “delay-scan method” (method 1) is a femtosecond Ti:Sapphire laser (wavelength 800 nm, pulse energy 5 nJ, repetition rate 100 MHz, pulse length 15 fs) which is actively synchronized to the accelerator rf clock [5] (see Figure 1). The delay between optical pulses and the electron bunches (beam energy 46 MeV, bunch charge 200 pC, micropulse repetition rate 25 MHz or 1 GHz, bunch length  $\sim 1.5$  ps) can be varied with a phase shifter. A balanced detection arrangement was used instead of a crossed-polarizer detection setup in order to increase the signal-to-noise ratio. The laser room, containing the femtosecond laser system and the detection system, is located approximately 30 meters from the FEL cavity. The probe pulse is relayed by means of lenses and mirrors to direct the pulse towards the ZnTe crystal (fibers would stretch the probe pulse). More details on the setup can be found in Refs. [2, 4].

## Short Bunch Beam Profiling

P. Krejcik, SLAC, Stanford Linear Accelerator, Stanford, CA, USA  
e-mail: pkr@slac.stanford.edu

### *Abstract*

The complete longitudinal profiling of short electron bunches is discussed in the context of 4th generation light sources. The high peak current required for the SASE lasing process is achieved by longitudinal compression of the electron bunch. The lasing process also depends on the preservation of the transverse emittance along the bunch during this manipulation in longitudinal phase space. Beam diagnostic instrumentation needs to meet several challenges: The bunch length and longitudinal profile should be measured on a single bunch to characterize the instantaneous, peak current along the bunch. Secondly, the transverse emittance and longitudinal energy spread should be measured for slices of charge along the bunch. Several techniques for invasive and noninvasive bunch profiling will be reviewed, using as examples recent measurements from the SLAC Sub Picosecond Photon Source (SPPS) and the planned diagnostics for the Linac Coherent Light Source (LCLS). These include transverse RF deflecting cavities for temporal streaking of the electron bunch, RF zero-phasing techniques for energy correlation measurements, and electro-optic measurements of the wake-field profile of the bunch.

Paper not received

(See slides of talk on  
following pages)

## DIGITAL SIGNAL PROCESSING IN BEAM INSTRUMENTATION: LATEST TRENDS AND TYPICAL APPLICATIONS

M. E. Angoletta, CERN, Geneva, Switzerland

### Abstract

The last decade has seen major improvements in digital hardware, algorithms and software, which have trickled down to the Beam Instrumentation (BI) area. An advantageous transition is taking place towards systems with an ever-stronger digital presence. Digital systems are assembled by means of a rather small number of basic building blocks, with improved speed, precision, signal-to-noise ratio, dynamic range, flexibility, and accompanied by a range of powerful and user-friendly development tools. The paper reviews current digital BI trends, including using Digital Signal Processors, Field Programmable Gate Arrays, Digital Receivers and General Purpose Processors as well as some useful processing algorithms. Selected digital applications are illustrated on control/feedback and beam diagnostics.

### INTRODUCTION

This review addresses latest years' developments in the use of digital techniques in BI. Owing to the large body of data available on this topic, the reader is also referred to the proceedings of various conferences and workshops such as the BIW, DIPAC, PAC, EPAC, ICALEPCS and LINAC, widely available on the web, and to previous reviews on some aspects of this subject [1,2,3].

A "Digital Engineering" perspective is adopted here, through the concept of "Digital Building Block" (DBB). This indicates the smallest digital unit, a chip, which can accomplish a given function. DBBs are now profusely used as part of recent digital systems. There are several DBBs, important for the evolution of the digital signal processing field. The treatment here is limited to only four major programmable DBBs, having great flexibility through programmability, providing multifunctionality hence causing continuing system size shrinkage.

The digital signal processing area has been steadily evolving since the '60s [4]. It is witnessing a slow transition from an all-analogue approach to an analogue/digital balance, primarily in control/feedback applications, with an ever-stronger digital presence.

### DIGITAL BUILDING BLOCKS IN BI

Nowadays, digital systems are assembled using a limited number of "miniaturised" DBBs, each accomplishing a range of functions and having a definite place in the signal processing chain (Figure 1). The four DBB considered in this paper, listed as one follows the signal from the detector, are 1) Digital Receiver (DRX), 2) Field Programmable Gate Array (FPGA), 3) Digital

Signal Processor (DSP) and 4) General Purpose Processor (GPP) and GPP-hybrid. DBB major functionalities include baseband translation and initial data reduction (for DRX), fast math-intensive processing (for DSP and FPGA), glue logic (for FPGA), slow processing, data management and high-level interfacing (for GPP). In general, system specification and final goal will influence and modify this generalised chain structure. For example, either the DSP or the FPGA may be absent depending on the type of processing and the time constraints the system imposes. Typically, FPGAs support faster sampling than DSPs. On-site availability of tools and expertise in DSP or FPGA development may tip the chain balance towards either a no-DSP or a no-FPGA implementation. A DBB not covered here is for example the Analogue-Digital Converter (ADC). This will also influence system

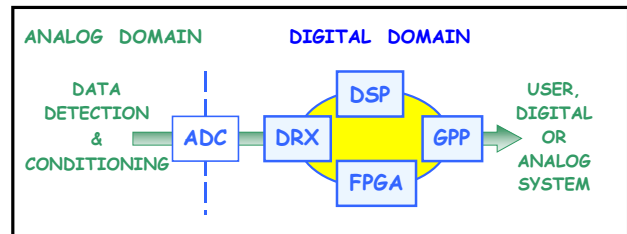


Figure 1: DAQ and processing chain DBBs.

architecture and its evolution will impact digital signal processing in the future. For example, the analogue/digital divide in the system signal chain may move closer and closer to the detector end as ADCs become faster and more powerful. Conceivably, future systems will directly feed the signal to the digitising ADC, without going through intermediate frequency (IF) translation.

Last but not least, developers should provide a digital system with enough diagnostic and troubleshoot access points, to avoid turning the system into a tightly sealed black box.

### Digital Receivers

The digital receiver chip, also called Digital Down Converter (DDC), is the evolution of the classical analogue superheterodyne receiver [1]. It extracts a narrow frequency band of interest from a wide-band input by down mixing, filtering and decimation. Figure 2 shows the block diagram for a generic DRX. Its main blocks are the local oscillator (LO), the complex (or I/Q) mixer and the low-pass filter. LO is a direct digital synthesiser generating a quadrature sinusoid, with programmable frequency and phase, from a look-up table. The mixer consists of two digital multipliers and outputs only the

## DIAGNOSTIC CHALLENGES AT SNS\*

M.A. Plum, Los Alamos National Laboratory, Los Alamos, NM, USA;  
 T. Shea and S. Assadi, Oak Ridge National Laboratory, Oak Ridge, TN, USA;  
 L. Doolittle, Lawrence Berkeley National Laboratory, Berkeley, CA, USA;  
 P. Cameron and R. Connolly, Brookhaven National Laboratory, Upton, NY, USA

### Abstract

The Spallation Neutron Source now being built in Oak Ridge, Tennessee, USA, accelerates an  $H^-$  ion beam to 1000 MeV with an average power of 1.4 MW. The  $H^-$  beam is then stripped to  $H^+$ , compressed in a storage ring to a pulse length of 695 ns, and then directed onto a liquid-mercury neutron spallation target. Most of the acceleration in the linac is accomplished with superconducting rf cavities. The presence of these cavities, the high average beam power, and the potential for the e-p instability in the storage ring, provide unique challenges to the beam diagnostics systems. In this talk we will discuss these challenges and some of our solutions, including the laser profile monitor system, the residual gas ionization profile monitors, and network attached devices. Measurements performed using prototype instrumentation will also be presented.

### INTRODUCTION

Most of the beam diagnostics [1] at the Spallation Neutron Source (SNS) are fairly standard: beam position monitors, beam loss monitors, wire scanners, beam current monitors, slit and collector emittance stations,

Faraday Cups, etc. However, there are several aspects about the SNS that create some special challenges, such as the superconducting rf cavities, the high beam power, and the potential for the e-p instability in the ring. The high beam power and the superconducting rf cavity challenges have led to the development of a laser profile monitor system that replaces the originally-envisioned wire scanner system in the superconducting linac (SCL). The challenges associated with the e-p instability and the expected beam loss in the ring have led to improvements in the gas ionization profile monitor design. We have also taken advantage of technology developments by basing many of our diagnostics instrumentation designs on the personal computer (PC) platform. A layout of the various diagnostics systems is shown in Fig. 1.

### LASER PROFILE MONITOR SYSTEM

The profile monitor system for the SCL was originally envisioned to be a carbon wire scanner system. However, linac designers were concerned about the possibility that carbon wire ablation, or broken wire fragments, could find their way into the superconducting cavities and cause them to fail. A high reliability wire scanner actuator was

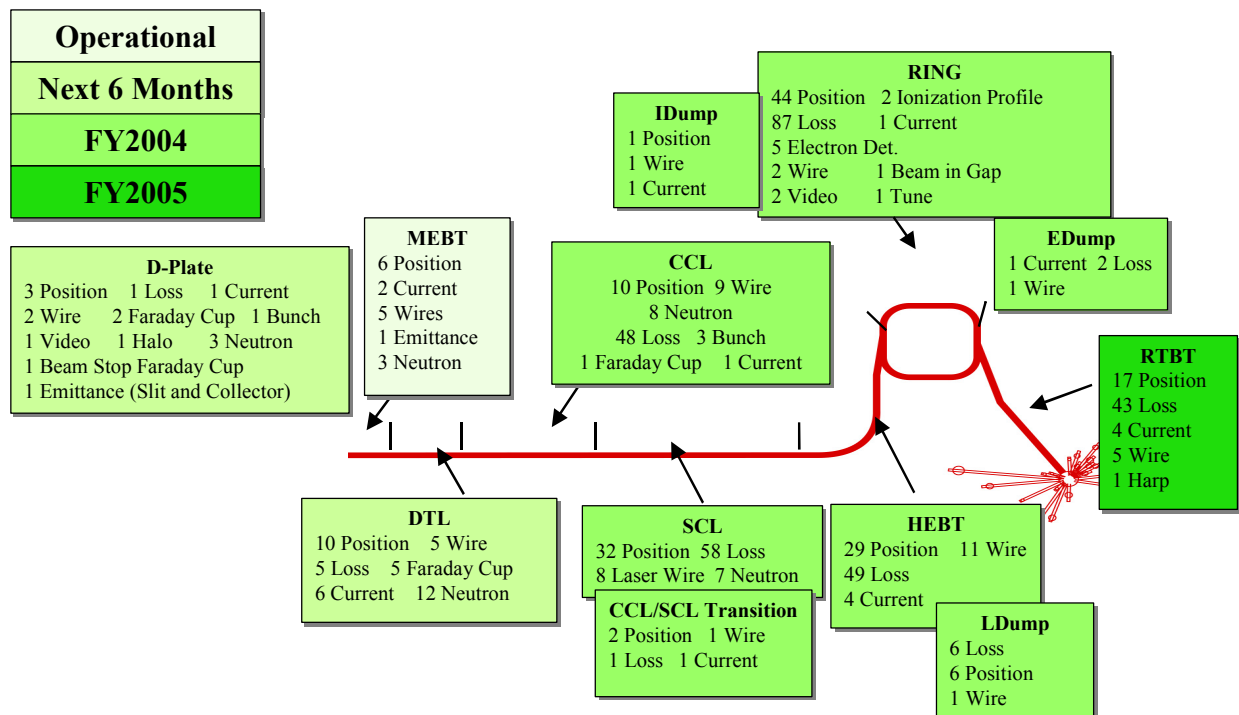


Fig. 1. (color) Layout of the diagnostics in the SNS facility, color-coded to indicate the staged installation dates.

\*Work supported by the Office of Science of the US Department of Energy.

## SMITH–PURCELL RADIATION IN VIEW OF PARTICLE BEAM DIAGNOSTICS

G. Kube \*, H. Backe, W. Lauth, H. Schöpe, Institut für Kernphysik, Mainz, Germany

### Abstract

During the last years Smith–Purcell radiation which is generated when a charged particle beam passes close to the surface of a diffraction grating became topic of interest as non–invasive tool for particle beam diagnostics. In some publications the use of Smith–Purcell radiation for longitudinal as well as for transversal monitoring was already considered. The proposed methods are based on the idea that the relevant beam parameters can be extracted by a comparison of the measured spectral intensity distribution with the theoretical one. In the case of Smith–Purcell radiation this is a non-trivial task because the spectral intensity distribution is strongly influenced by the form of the grating profile, and the theoretical description of the radiation factors describing this dependency require extensive numerical calculations. As consequence a careful choice of the grating is essential or methods are preferable by which the wavelength dependent influence can be minimized. In the case of longitudinal beam diagnostics it should be possible by a proper choice of the form of the grating profile. In the case of transversal beam monitoring it is demonstrated that direct imaging of the beam profile is possible with Smith–Purcell radiation taking advantage of the specific emission characteristics at ultra relativistic beam energies.

### INTRODUCTION

The development of the next generation high quality electron beams necessary for future high luminosity linear colliders and short wavelengths free electron lasers presents an enormous challenge for both the diagnostic measurement of beam parameters and the accurate positioning and control of these beams. The existing monitors are based on a number of different physical principles, and one technique is to use the radiation that can be produced by the beam itself. In this context nowadays the beam diagnostics based on optical transition radiation is widely used [1, 2, 3, 4]. However, the transition radiation technique entails the disadvantage of an interaction of the beam with the target leading to either the destruction of the high quality beam parameters due to small angle scattering of the electrons in the target foil or at high beam currents even of the screen. Hence the development of non–invasive, low cost, and compact beam monitors is demanded. Monitors based on synchrotron radiation, while non–invasive, are disadvantageous because they cannot be used in linear beam geometries. Another approach rather similar to the transition radiation technique is to exploit the radiation characteris-

tics of diffraction radiation which is emitted when the electrons pass close to an obstacle [5, 6, 7, 8, 9]. In recent publications beam diagnostics based on resonant diffraction radiation is proposed which originates from electrons moving through an ideally conducting tilted target which is made by strips separated by vacuum gaps [10, 11].

A rather similar and also non–destructive approach is to use Smith–Purcell (SP) radiation as a compact and inexpensive beam profile monitor. The radiation is generated when the electron beam passes a periodic structure like a diffraction grating at a fixed distance close to the surface. The radiation mechanism was predicted by Frank in 1942 [12] and observed in the visible spectral range for the first time by Smith and Purcell [13] using a 250–300 keV electron beam.

Soon after the discovery of the SP effect also potential applications became topic of interest. The possibility to use coherent SP radiation as bunch length diagnostic was proposed in [14, 15] and design studies of bunch length monitors were reported e.g. in reference [16]. The feasibility to use SP radiation for longitudinal bunch shape measurements was recently demonstrated in Frascati [17]. SP radiation as high resolution position sensor is discussed in view of possible applications for ultra relativistic beam energies up to 500 GeV in Ref. [18]. Experimental studies performed at the Mainz Microtron MAMI demonstrated that SP radiation from ultra relativistic energies can be used both as transversal beam size as well as beam position monitor. The investigations presented here were performed in context with the experiment reported in Ref. [19]. SP radiation generated with the MAMI low emittance 855 MeV electron beam [20] was investigated in the visible spectral range. By measuring the spatial intensity distribution emitted perpendicular to the grating surface beam position and beam size in the horizontal plane could be determined.

### SMITH–PURCELL RADIATION PROPERTIES

According to the theory of di Francia [21], the emission mechanism of SP radiation can be interpreted in analogy to the diffraction of light as the diffraction of the field of the electrons (virtual photons) which pass the grating at a distance  $d$  away from its surface by the grating grooves. One characteristic signature of SP radiation is that it must fulfill the dispersion relation [13]

$$\lambda = \frac{D}{|n|} (1/\beta - \cos \theta \sin \Phi). \quad (1)$$

In this equation  $\lambda$  is the wavelength of the emitted radiation,  $D$  the grating period,  $n$  the diffraction order,  $\beta = v/c$

\* corresponding author, present address: DESY, Hamburg, Germany, gero.kube@desy.de

# ADVANCED DIAGNOSTICS OF LATTICE PARAMETERS IN HADRON COLLIDERS

J.- P. Koutchouk, CERN, Geneva, Switzerland

## Abstract

With a beam stored energy exceeding by several orders of magnitude the quench level of the magnets and non-negligible non-linear field components, the control of the beam dynamics and losses in LHC must be very precise [1]. This is a strong incentive to strengthen as much as possible the potential of beam diagnostics. This paper reviews some of the developments in various laboratories that appear to have a large potential. They either allow for a much better access to classical beam parameters or for the measurement of quantities formerly not accessible. Examples are a fast measurement of the betatron tunes, the use of PLL for reliable tune tracking and feedback, new methods or ideas to measure the chromaticity with the potential of feedback systems and similarly for the betatron coupling, the measurement of high-order non-linear fields and resonances and the potential of AC dipole excitation. This list is bound to be incomplete as the field is fortunately very dynamic.

## FAST TUNE MEASUREMENTS

The most common method for tune measurement is to Fourier transform the transverse oscillation of a beam after a transverse kick. If observed over  $N$  turns, the tune resolution is  $1/2N$ . The tunes shall usually be controlled to some 0.001, requiring a measurement over 500 turns. This method has limitations. The decoherence due to non-linearities from various sources and the beating effect due to a non-vanishing chromaticity are often significant in the first 500 turns and degrade the accuracy. This is particularly the case when the purpose of the tune measurement is to fix a pathological situation which most often enhances the decoherence.

Methods have been available for some time to either improve the accuracy of the tune measurement for a given observation time or reduce the latter significantly to capture faster phenomena.

## Interpolation in the frequency domain

The measurement of the linear parameters like the tunes only requires small amplitude beam oscillations. A simple Fourier Transform does not take advantage of the knowledge that this oscillation is a simple sine wave. It is however possible to re-interpret the spectrum in the light of this hypothesis. This leads to an analytic interpolation between the FFT lines on either side of the true tune, improving significantly the precision [2]:

$$Q_{true} = \frac{1}{N} \left( k + \frac{|\phi_{k+1}|}{|\phi_k| + |\phi_{k+1}|} \right), \quad \text{where } \phi_k \text{ and } \phi_{k+1}$$

are the harmonics of largest amplitude and  $k/N$  the FFT approximation of the tune. The tune accuracy improves like  $1/N^2$  in the absence of noise.

## Cross-correlation in the time domain

Instead of Fourier transforming the data set and interpolating, it is possible to cross-correlate the measured time series with a sinusoidal model using a guessed tune. For continuous signals, the tune difference between the theoretical and measured tunes would simply be given by the abscissa of the peak of the cross-correlation function. For sampled signals, the tune shift is derived from two or more values of the cross-correlation function [3]. The analytical evaluation shows that this algorithm is robust against noise, with an error proportional to  $1/N\sqrt{N}$ . This method was experimented in LEP.

## Windowing in time domain

The transverse beam oscillation signal may be viewed as the product of an infinite sinusoidal signal with a rectangle window of length  $N$ . The resulting spectrum is the convolution of a Dirac function with the Fourier transform of the rectangle window i.e. merely the window spectrum shifted in frequency so that its main peak is centred on the tune. The signal power concentrated on the Dirac impulse of the Fourier transform of the infinite sine wave is spread over the main peak and the side lobes of the transform of the rectangle.

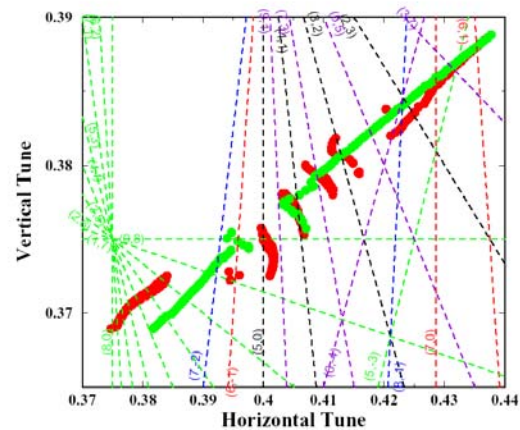


Figure 1: Experimental frequency map of the ESRF [5]

To study the non-linearities in the frequency domain, it is necessary to use the shortest possible window  $N$  (e.g.  $N < 1000$ ) and yet to measure the tune to high accuracy (e.g.  $10^{-5}$ ). Plotting the tunes for a range of oscillation amplitudes gives a representation of dynamical systems in the frequency space (Fig. 1). The method, developed for celestial mechanics [4] relies on *i*) windowing with a Hanning window of order 2, *ii*) interpolating in the frequency domain *iii*) followed by an iterative subtraction of the identified frequency components. The Hanning window significantly reduces the side lobes. In the

## AN INDUCTIVE PICK-UP FOR BEAM POSITION AND CURRENT MEASUREMENTS

M. Gasior, CERN, Geneva, Switzerland

### Abstract

An Inductive Pick-Up (IPU) senses the azimuthal distribution of the beam image current. Its construction is similar to a wall current monitor, but the pick-up inner wall is divided into electrodes, each of which forms the primary winding of a toroidal transformer. The beam image current component flowing along each electrode is transformed to a secondary winding, connected to a pick-up output. Four pick-up output signals drive an active hybrid circuit (AHC), producing one sum ( $\Sigma$ ) signal, proportional to the beam current, and two difference ( $\Delta$ ) signals proportional also to the horizontal and vertical beam positions. The bandwidth of these signals ranges from below 1 kHz to beyond 150 MHz, exceeding five decades. Each electrode transformer has an additional turn to which a pulse from a precise current source is applied to calibrate the sensor for accurate beam position and current measurements. The IPU has been developed for the drive beam linac (DBL) of the Third CLIC Test Facility (CTF3) [1]. For that purpose it had to be optimized for low longitudinal coupling impedance in the GHz range.

### CONSTRUCTION

The CTF3 DBL beam consists of a  $1.5 \mu\text{s}$  train of  $2.3 \text{ nC}$ ,  $5 \text{ ps}_{\text{RMS}}$  electron bunches paced at a 1.5 GHz repetition rate [1], as shown in Figure 1. A position monitor for such a beam should have a low cut-off frequency in the kHz range to limit signal droops, a high cut-off frequency beyond 100 MHz to observe fast beam movements and longitudinal coupling impedance  $Z_C$  low in the GHz range, containing important beam frequency components, to limit the monitor influence on the beam. These requirements implied significant improvements over the LEP Pre-Injector pick-ups [2] on which this IPU design is based.

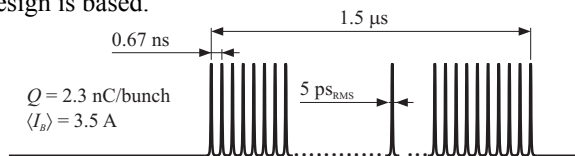


Figure 1: Time structure of the CTF3 DBL beam.

The IPU components and the assembly are shown in Figure 2 and 3 respectively. The 8 electrodes E have an internal diameter only 9 mm larger than the vacuum chamber of 40 mm and cover 75 % of the circumference in order to make the IPU as transparent to the beam as possible to minimize  $Z_C$ . The diameter step is occupied by the ceramic tube B of the vacuum assembly A; the tube is titanium coated on the inside. The electrodes are surrounded by the ferrite cylinder F inserted in the body C. The plates H accommodate the PCBs G on which the

transformers are mounted. A screw D passes through each transformer ring, connecting an electrode E to a plate H. The clamps I tighten the plates H with connectors screwed. To achieve good low frequency responses primary circuit parasitic resistances had to be kept below a  $\text{m}\Omega$ , thus the body C, the electrodes E and the plates H are made from copper. The plates as well as the beryllium copper screws D are gold plated. The electrodes and their supporting plate are machined as one piece to minimize contact resistances between small surfaces and to achieve good mechanical precision.

The four IPU outputs are connected to the AHC, which is followed by amplifiers housed in a common enclosure. The amplifiers, having two remotely switchable gains, amplify  $\Delta$  and  $\Sigma$  signals to a level suitable to be sent over long cables to an equipment room.

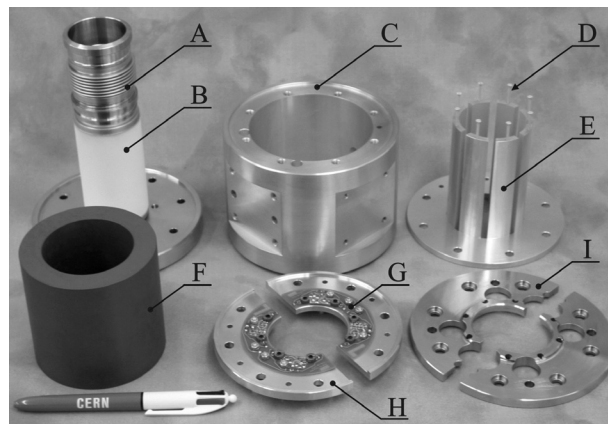


Figure 2: The IPU parts.



Figure 3: The IPU assembled. On the front there are four pick-up outputs and two calibration inputs.

**SINGLE-SHOT MEASUREMENTS OF THE 4-DIMENSIONAL TRANSVERSE PHASE SPACE DISTRIBUTION AT THE UNILAC AT GSI**

W. Barth and L. Groening, GSI, Darmstadt, Germany

D. Liakin, ITEP, Moscow, Russia

*Abstract*

The UNILAC is used as an injector for the synchrotron SIS. It is designed to fill the synchrotron up to its space charge limit. The upper limit for the useful beam emittance of the UNILAC is given by the finite acceptance of the SIS during the injection process. In order to remain within this acceptance the emittance growth during beam acceleration and transportation due to space charge effects must be minimized by applying an appropriate beam focusing. Therefore, the influence of the magnetic focusing strength on the beam emittance growth was investigated experimentally for different beam currents. Measurements of transverse phase space distributions were performed before and after the Alvarez accelerator with a periodic focusing channel, respectively. In order to perform such a wide parameter scan within a reasonable time with respect to machine stability, the pepper pot technique was applied. The pepper pot method allows for single-pulse measurements. For comparison several measurements using the slit-grid technique, which averages over many pulses, were performed. Both transverse planes were measured simultaneously. Using two pepper pot devices more than 60 single shot measurements of the full 4-dimensional transverse phase space distribution were performed within 8 hours. In this paper we report on the results of the measurements and we compare them to beam dynamic simulations and we give an outlook on further developments on pepper pot devices.

**INTRODUCTION**

The High Current Injector (HSI) of the UNILAC (Fig.1) comprises a RFQ and two IH-structures operated at 36 MHz. It accelerates intense ion beams generated by a MUCIS- or MEVVA- ion source to an energy of

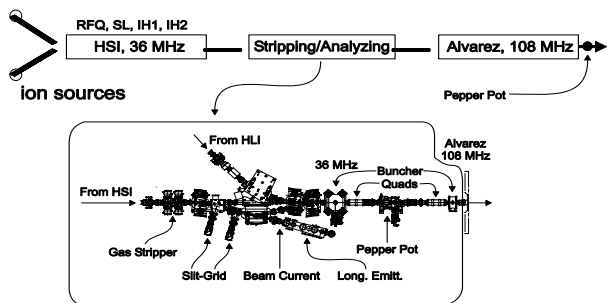


Fig. 1: Schematic overview of the Universal Linear Accelerator UNILAC at GSI.

1.4 MeV/u. After the HSI the ion charge state is increased by passing the beam through a gas jet stripper. A subsequent charge state separator selects the charge state for further acceleration in the Alvarez DTL (108 MHz) to 11.4 MeV/u. To match the periodic transverse focusing in this section, the beam size must be reduced significantly in all three dimensions. This leads to a strong increase of the space charge forces, which scale with the space charge parameter SCP [1]

$$SCP \sim I_p \cdot q^2 \cdot \beta^{-1} \cdot (XYZ)^{-1} ,$$

where  $I_p$  is the particle beam current,  $q$  is the ion charge state,  $\beta$  is the relative velocity, and  $(XYZ)$  is the bunch volume. As shown in Fig.2 the SCP has two maxima

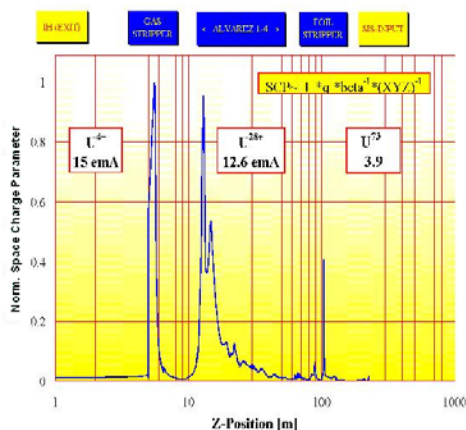


Fig. 2: The space charge parameter SCP along the UNILAC.

during the stripping process and at the entry to the Alvarez section, respectively. During acceleration it decreases due to the increase of  $\beta$ . For a given beam current the emittance growth along the section depends on the transverse focusing strength. According to theory the growth should be reduced by a stronger focusing. We aimed on the experimental investigation of this dependence for three different beam intensities.

**EXPERIMENTAL SET-UP**

Figure 1 shows the set-up of the experiment. Beam currents were measured before and after the Alvarez section. The 4-dimensional transverse phase distributions were measured during single-shots using a pepper pot device before and after the DTL, respectively. Additionally, a horizontal slit/grid set-up was employed,

## Beam Instrumentation for the Single Electron DAΦNE Beam Test Facility

G. Mazzitelli\*, F. Sannibale, P. Valente, M. Vescovi  
 Laboratori Nazionali di Frascati dell'INFN, Frascati, Italy  
 P. Privitera, V. Verzi  
 Dipartimento di Fisica & INFN Roma II, Roma, Italy

### Abstract

The DAΦNE Beam Test Facility (BTF) has been successfully commissioned in February 2002, and started operation in November of the same year. Although the BTF is a beam transfer line optimized for single particle production, mainly for high energy detectors calibration, it can provide electrons and positrons in a wide range of multiplicity: between  $1 \div 10^{10}$ , with energies from a few tens of MeV up to 800 MeV. The large multiplicity range requires many different diagnostic devices, from high-energy calorimeters and ionization/fluorescence chambers in the few particles range, to standard beam diagnostics systems. The schemes of operation, the commissioning results, as well as the beam diagnostics are presented.

### DESCRIPTION OF THE DAΦNE BTF

The Beam Test Facility (BTF) is a beam line optimized for the production of a pre-determined number of electrons or positrons, in a wide range of energies (up to 800 MeV) and multiplicity. The facility is particularly suitable for particle detector testing purposes, such as energy calibration and efficiency measurements, in single electron mode; while beam diagnostics devices and detector aging can be studied at higher intensities.

The BTF is part of the DAΦNE accelerator complex, consisting of a double ring electron-positron collider, a high current linear accelerator (LINAC), an intermediate damping ring (Accumulator) and a system of 180 m transfer lines connecting the four machines. The LINAC delivers electrons with energy up to 800 MeV, with a typical current of 500 mA/pulse, or positrons with energy up to 550 MeV, with a typical current of 100 mA/pulse; the pulse duration can be adjusted in the range  $1 \div 20$  ns with a maximum repetition rate of 50 Hz. When injecting for operation of the main rings at the  $\phi$  resonance, the beam energy is 510 MeV.

Since the minimum LINAC beam current that can be conveniently measured by the DAΦNE current monitors is  $I \approx 1$  mA, the corresponding number of electrons (positrons) is  $\approx 10^8$ /pulse. It is thus necessary to strongly reduce the number of particles to reach the few particles range. The reduction of the particle multiplicity can be achieved with different methods, the one chosen for the BTF operation is the following[1]: first the LINAC beam is

intercepted by a (variable depth) target in order to strongly increase the energy spread of the primary beam; then the out-coming particles are energy selected by means of a bending magnet and slit system. The energy selector only accepts a small fraction of the resulting energy distribution, thus reducing of the number of electrons by a large and tunable factor. The target is shaped in such a way that three different values of radiation length can be selected ( $1.7, 2.0, 2.3 X_0$ ) by inserting it at different depths into the beam-pipe. The attenuated beam is transported by a  $\approx 12$  m transfer line to the BTF hall, where the experimental setups can be installed. The dipole magnet, together with a downstream collimator, selects the momentum of the particles. At the end of the BTF line a second bending magnet allows to use two separate test lines: one directly from the straight section, the other from the magnet at  $45^\circ$ .

Due to the momentum dispersion introduced by the bending magnet, the relative energy spread  $\Delta E/E$  is essentially determined by the magnet/collimators configuration[2]; in the standard BTF operation for a wide range of slit apertures a resolution better than 1% can be obtained.

The number of transported electrons (or positrons) can be adjusted in a wide range, down to single particle, and is well below the sensitivity of any standard beam diagnostics device, so that many different particle detectors have been used to monitor the beam characteristics.

### BEAM COMMISSIONING AND DIAGNOSTICS

During 2002 the BTF has been successfully commissioned and started operation, delivering beam to the first user experiments, from Nov. 2002 to May 2003[3]. The facility has been operating both in the single electron production scheme and the high multiplicity operation mode, according to the different user requirements.

At low multiplicity a calorimeter has been used as main diagnostic device. The detector is a lead/scintillating fibers calorimeter of the KLOE type[4], with single side photomultiplier readout. The main features are a sampling fraction of  $\approx 15\%$ , a good energy resolution,  $\sigma_E/E = 4.7\%/\sqrt{E(\text{GeV})}$ , and excellent timing resolution,  $\sigma_t/t = 54\text{ps}/\sqrt{E(\text{GeV})}$ .

The LINAC setting has been optimized to provide a 510 MeV energy,  $4 \div 5$  mA intensity beam. The repetition rate of the LINAC was 24 Hz (+1 shot to the spectrometer line

\* giovanni.mazzitelli@lnf.infn.it

## The Beam Inhibit System For TTF II

D. Nölle, P. Göttlicher, R. Neumann, D. Pugachov, K. Wittenburg, M. Wendt, M. Werner, H. Schlarb, M. Staack, DESY, Hamburg, Germany  
 M. Desmons, A. Hamdi, M. Jablonka, M. Luong, CEA, DAPNIA, Saclay, France  
 e-mail: [dirk.noelle@desy.de](mailto:dirk.noelle@desy.de)

### Abstract

The new generation of light sources based on SASE Free-Electron-Lasers driven by LINACs operate with electron beams with high beam currents and duty cycles. This is especially true for the superconducting machines like TTF 2 and the X-RAY FEL, under construction or planning at DESY. Elaborate fast protections systems are required not only to protect the machine from electron beams hitting and destroying the vacuum chamber, but also to prevent the machine from running at high loss levels, dangerous for components like the FEL undulator.

This paper will give an overview over the different protection systems under construction for TTF 2. The very fast systems, based on transmission measurements and distributed loss detection monitors, will be described in detail. This description will include the fast electronics to collect and to transmit the different interlock signals.

### INTRODUCTION

The TESLA Test Facility phase 2 (**TTF 2**) is currently under construction at DESY in Hamburg. This machine has two main objectives [1]:

- a) serve as a test facility for accelerator components for the future TESLA and X-RAY FEL [2],
- b) operate as a 4<sup>th</sup> Generation Light Source to provide SASE FEL radiation in the range between 100 and 6 nm.

In order to demonstrate the requirements for the large machines for high luminosity in case of the collider and high peak and average brightness in case of the SASE light source, the TTF 2 is capable to run a 800  $\mu$ s long beam pulse at 10 Hz rep. rate with a 9 MHz bunch frequency. With the design charge of 1 nC this yields currents of 9 mA averaged over the bunch train, or a total average current of 72  $\mu$ A.

Although the average current of TTF II is rather small compared to a typical conventional 3<sup>rd</sup> generation light source, the intrinsic energy of this system is much higher (Table 1).

Table 1: Comparison of power and energy stored in the beam and losses for LINAC and storage ring driven light sources.

	Storage Ring	TTF 2
Average Current	200 mA	72 $\mu$ A
Circumference/Length	200 m	250 m
Beam Lifetime	10 h	-
Energy	2 GeV	1 GeV
Avg. Beam Power	400 MW	72 kW
Energy (Beam/Pulsetrain)	0.26 kJ	7.2 kJ
Loss Level	$10^{-7}$ (Undulator only)	$2 \cdot 10^{-11}$ (total, 1/Turn)

Therefore, effective protection systems are required to prevent the machine from serious damage due to the operation. These systems have to protect the machine from different damage mechanisms resulting in different damage levels at different time scales, e.g.:

- Beam hitting a part of the vacuum chamber. The beam has to be stopped as fast as possible. In the worst case less than 10 bunches can cause damage. Therefore, the reaction time of the system has to be as short as possible, and is mainly determined by signal transmission times.
- Beam halo or dark current is (partially) lost in the machine. Such losses would result in increased activation of components. In the undulator accumulated losses can degrade the performance of the magnets substantially. Therefore, losses have to be observed down to a level of  $10^{-7}$ .
- Invasive beam diagnostics or even obstacles are present in the beam pipe. Such an event has to be recognized by a protection system, to restrict the number of bunches within a bunch train to a number given by the sensitivity of the inserted object.

In order to allow safe machine operation, TTF 2 will have monitoring as well as interlock systems. There will be rather slow monitoring system based on Dosimetrie, using conventional Thermo-Luminescence-Dosimeters crystals and optical fibres. The fibre-based system can provide information about high dose rates in the machine with good spatial resolution and update rates of some minutes [3].

The active part of the protection system is taken by the Beam Inhibit System (**BIS**). This system was redesigned based on the experience with a predecessor system at TTF 1.

### THE BEAM INHIBIT SYSTEM

In order to deal with different machine settings a number of operation and beam modes are defined.

Operation modes define the path the electrons have to take, like gun mode (beam stopped by a Faraday cup before the first module), undulator and bypass mode.

The beam modes determine, whether short, long or even only single bunch operation is allowed. These modes depend on the machine setting, e.g. if a screen is inserted only single bunch mode is allowed. Furthermore, they depend on the performance of the machine, i.e. the beam mode is switched back from long to short pulse or even to single bunch in the case the losses get too high or transmission gets too bad.

## Beam Loss Detection at Radiation Source ELBE

P. Michel, J. Teichert, R. Schurig, H. Langenhagen  
Forschungszentrum Rossendorf (FZR), Dresden, Germany

### Abstract

The Rossendorf superconducting Electron Linac of high Brilliance and low Emittance (ELBE) delivers a 40 MeV, 1 mA cw-beam for different applications such as bremsstrahlung production, electron channeling, free- electron lasers or secondary particle beam generation. In this energy region in case of collisions of the electron beam with the pipe nearly all beam power will be deposited into the pipe material. Therefore a reliable beam loss monitoring is essential for machine protection at ELBE. Different systems basing on photo multipliers, compton diodes and long ionization chambers were studied. The pros and cons of the different systems will be discussed. Ionization chambers based on air-isolated RF cables installed some cm away parallel to the beam line turned out to be the optimal solution. The beam shut-off threshold was adjusted to 1  $\mu\text{C}$  integral charge loss during a 100 ms time interval. Due to the favourable geometry the monitor sensitivity varies less than  $\pm 50\%$  along the beam line (different shielding conditions).

### Introduction

The Forschungszentrum Rossendorf is constructing a superconducting Electron Linac with high Brilliance and low Emittance (ELBE) which can deliver a 1 mA cw beam of 40 MeV. The electron beam is used to generate infrared light (Free Electron Lasers), X-rays (electron channeling), MeV-bremsstrahlung, fast neutrons and positrons. [1] The safe and reliable operation of the accelerator is essential for a user facility like the ELBE radiation source. The machine should run over many shifts and for long periods with constant and reproducible parameters. The facility must be able to be operated by a minimum number of trained operators. Because of the high beam power (max. 40kW) and the electron energy range of 15-40 MeV the prevention of beam losses in the beam line plays a special role. Due to the average electron penetration depth at these energies approximately the full beam power can be deposited into the vacuum pipes. Apart from the production of ionizing radiation and activation, the vacuum pipes can be melted. It is inevitable that the vacuum system,

and in particular the superconducting accelerator cavities, would be contaminated. The result would be long down-times and substantial costs for repairs.

### Detectors

Multiple detectors for the measurement of the beam loss were tested at the ELBE beam line. These were photomultipliers (PM), Compton diodes (CD) [2] and long ionization chambers (LIC) [3] constructed from air-filled high frequency cables.

**Photo Multipliers:** Photomultipliers (Electron tubes P30P) were installed approximately 3m away from the beam line. The detector shows very short response time ( $\sim 1$  ns) and is able to detect extremely low levels of radiation ( $\sim 10$  nA beam loss). Due to the nonlinear behaviour of the PM signals saturation effects in the PM problems appear at very high dose rates. At very fast increasing and extremely high beam losses the PM saturate before the necessary signal level for the accelerator shut-off is reached. In addition, the continuous monitoring of the beam pipe can be guaranteed only when a large number of detectors ( $\sim$  one PM per meter) is used due to the strong dependence of the monitor signal on the distance between PM and the location of the beam loss.

**Compton Diodes:** Compton diodes were installed similar to the PM's. They showed a very good linear behaviour up to extremely high beam loss levels. The Compton diodes exhibit an angle dependent signal and thus a directional characteristic based on the geometry of the detector. This can be used in order to supervise certain segments of the beam line with increased sensitivity. Nevertheless, the crucial disadvantage remains the same as for the PM. A complete beam line monitoring with approximately constant sensitivity is attainable only with a very large number of detectors.

**Long Ion Chambers:** Air-filled high frequency cables of the type Andrew HJ5-50 (diameter 22.2mm) were mounted approx. 20cm away parallel to the beam pipe. The cables were operated as ionization chambers applying a high voltage to the outer conductor and

# TIMING SICKNESSES IN CONTROL SYSTEMS: CAUSES, CURE AND PREVENTION

M. Werner, DESY, Hamburg, Germany

## Abstract

In some cases, Trigger Generators or Data Acquisition Systems used for Beam Diagnostics show undefined or unreliable timing behavior. This presentation identifies common reasons, ways to fix the problems and some general rules to avoid them from the beginning. Examples will be given to discuss causes for e.g. double bunches and timing and trigger jumps, periodic as well as randomly. It will be discussed, how proper layout, timing calculations and timing measurements can avoid these inconvenient effects in advance.

## TRANSMITTING MEDIA

### Copper Cable

Copper cable is good for short and medium distances. Many electronic devices have **coaxial** input and output connectors and use TTL or NIM voltage levels.

Alternatively a signal can be transmitted **differentially over twisted pair** lines, decreasing the sensitivity to common mode noise. Two examples are **RS-422/RS-485** with a common mode immunity of at least  $\pm 7V$  or **LVDS** for high speed applications.

### Glass fibre

A **monomode** fibre works well for high speeds over long distances, while **multimode** fibres are suited for medium distances - look carefully on jitter specifications!

## ERROR SOURCES

### Noise

Noise is a major concern to limit the timing precision of a system. It ranges from the small electronic noise of every cable receiver, 50/60Hz ground noise and switching power supplies up to big spikes produced by switching electric devices like motors.

### Reflections

Some amount of reflection is always present on a cable transmission, but with proper topologies and proper termination it can be minimised.

### Digital Trouble

Digital trouble often shows up as jumps of the timing. The reason can sometimes be found in an improperly constructed module itself (e.g. asynchronous design not considering all conditions) or in a setup-/hold time violation, see below.

## ANALOG SICKNESSES

Figure 1 shows some examples how an analog signal (e.g. at the end of a cable) can be distorted:

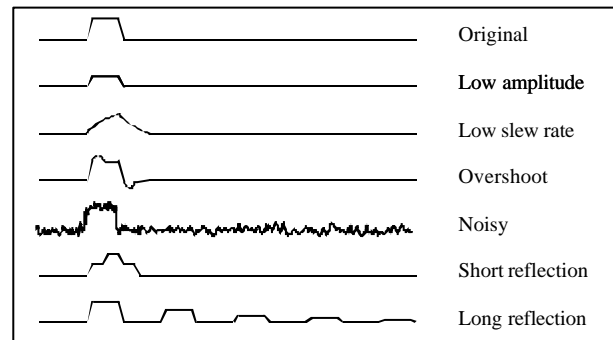


Figure 1: Analog sicknesses

## DIGITAL SICKNESSES

At a digital output, bad signals could look like this:

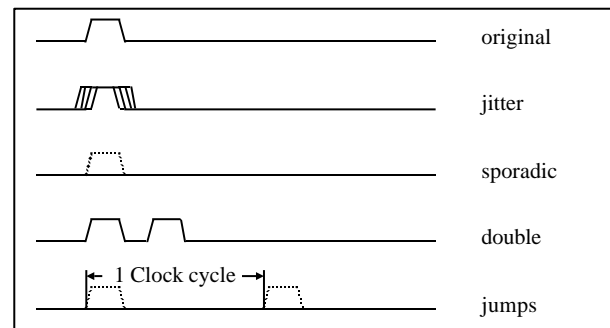


Figure 2: Digital sicknesses

## HOW TO CHECK SIGNALS

*Some poor methods to check a signal on a cable*

- Dividing the signal with a 6dB power splitter, one output going to an oscilloscope (50Ω input). This will attenuate the signal amplitude by 50%.
- Inserting a “T-piece” into the line, connecting one end by a short cable to an oscilloscope (1MΩ input). This will produce strong reflections on the main line for a fast signal.
- Looping the signal to an oscilloscope (1MΩ input). But the extra cable will give extra delay.
- Opening the destination module and checking at the input connector with an oscilloscope probe. For

## FAST DSP USING FPGAs AND DSOs FOR MACHINE DIAGNOSTICS

G.A.Naylor, ESRF Grenoble France

e-mail: [naylor@esrf.fr](mailto:naylor@esrf.fr)

### Abstract

Digital signal processing using digital signal processors is now a mature field for machine diagnostics, giving significant benefits, in particular when used to analyse BPM signals for tune measurement and fast feedback systems. We discuss here digital signal processing using Field Programmable Gate arrays (FPGAs) with large gate counts and intelligent oscilloscopes. These offer great potential for the analysis of very fast signals to maximize the information extracted from high bandwidth sensors.

i) FPGAs allow data to be filtered numerically and treated at the speed of data collection of A/D converters in the 100MHz range. Parallel, fast and continuous treatment of BPM and FCT signals is possible. Examples are given of injection efficiency, turn-by-turn injection efficiency, turn-by-turn beam position, amplitude and phase calculation with averaging over each turn or many turns.

ii) Modern oscilloscopes include much computational power. In-built DSPs can perform correlations on the traces allowing the application of FIR filters. Some oscilloscopes incorporate a PC and allow on-board manipulation of the data using MATLAB. An example is given using an FIR applied to a 5GHz oscilloscope to extend its time response to measure electron bunch lengths less than 100ps with 1ps resolution.

### PLATFORMS FOR PERFORMING DIGITAL SIGNAL PROCESSING

- Digital Signal Processor boards
- Digital Storage Oscilloscopes with processing capabilities (in-built maths operations and or PC with Matlab)
- Field Programmable Gate Arrays (FPGA)

The use of DSP boards for treating signals from diagnostic sensors is now well established (eg for feedback systems). The increase in acquisition speed of Analogue to Digital converters coupled with the large memory capacity of recent generation oscilloscopes puts a heavy demand on the network bandwidth and on post-processing. At such speeds pre-treatment of the signal with a view to extracting the useful information and reducing the bandwidth of the data to be exported becomes all the more important. The latest generation of fast intelligent oscilloscopes offer interesting possibilities for the pre-treatment of fast signals. For the ultimate in pre-treatment data bandwidth, FPGA boards may also be used.

### DIGITAL STORAGE OSCILLOSCOPES

Figure 2 shows the layout for a system using a 12GHz photo receiver [1] and a high bandwidth digital storage oscilloscope [2]. Modern digital storage oscilloscopes provide means for exporting waveform data to on board software running on the internal PC. Pre-processing of the waveform data may also be performed using standard maths library functions on the Oscilloscope DSP. Further processing on the PC part of the oscilloscope may be performed using analysis packages such as Matlab. By

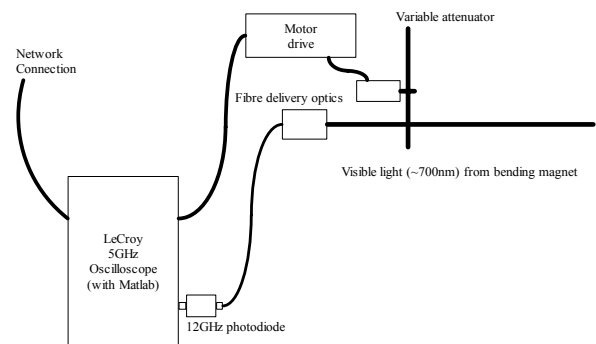


Figure 1 Optical Layout of bunch length measurement

programming custom functions using Matlab it is possible to perform tasks such as:

- i) bunch length measurement by deconvolution of the instrument response
- ii) beam phase monitoring (both fast and slow drift).

In order to perform deconvolution of the instrument response (to extend the effective bandwidth) it is important to process very clean, noise free, waveforms of high precision (10-12bits). Such waveforms should be recorded by averaging many repetitions of the waveform. A very stable trigger is required in order to maintain resolution when averaging. Using this technique, we have been able to measure pulses as short as about 95ps, see figure 2. A trend of the bunch length is shown in figure 3 during operation in a high bunch charge filling-mode, which suffers charge dependent bunch lengthening. This technique provides means of permanent monitoring of the bunch length without the continuous operation of a streak camera [3].

## Capabilities of the ELETTRA/SLS Multi Bunch Feedback Electronics

M.Dehler, R.Kramert, P.Pollet, Paul Scherrer Institut, CH-5232 Villigen PSI, Switzerland  
 M.Lonza, D.Bulfone, Sincrotrone Trieste, Trieste, Italy  
 e-mail: Micha.Dehler@psi.ch

### Abstract

Following the cessation in the production of the commercial ADC/DAC boards adopted by the ELETTRA/SLS digital multi-bunch feedback systems, a new family of 500 MS/s data conversion boards with an 8 bit resolution has been developed. The ADC and DAC circuits are separate modules containing analog and digital electronics providing a data rate of 500 MSample/sec using 250 MHz DDR clocking techniques. The following stage being a common design to both ADC and DAC reduce the data rate to 125 MS/sec, allows data recording and play back using on board RAM and allows freely programmable multiplexing/demultiplexing up to ratios of one to twelve. The digital data streams flow via Front Panel Digital Ports (FPDP). A special design criterion were low system latencies ensuring a high feedback efficiency. Apart from lab tests, we report on feedback system test and describe additional hardware applications.

### INTRODUCTION

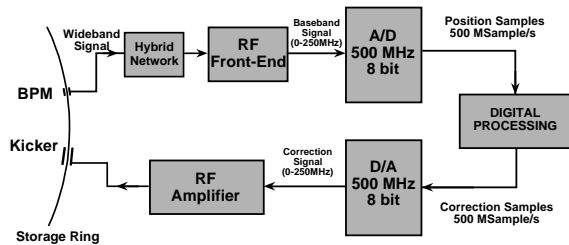


Figure 1: System Layout for the transverse multi bunch feedback

The ELETTRA/SLS Multi-Bunch Feedback System is a wide band feedback correcting the positions of individual bunches, spaced 2 ns apart (Figure 1). Wide band position signals coming from button type BPMs get converted to baseband (DC-250 MHz), followed by sampling with a fast 8 bit, 500 MS/s Analog to Digital Converters (ADC). A digital filter calculates correction kicks, which are getting reconverted via 8 bit, 500 MS/s Digital to Analog Converter (DAC). For the transverse feedback, the signals are directly fed via broad band power amplifiers and strip line kickers to the beam, in the longitudinal plane, a Lower Single Side Band (LSSB) modulator mixes the signals up to the 1.25-1.5 GHz band, where they get amplified and fed to a longitudinal kicker [1] [2].

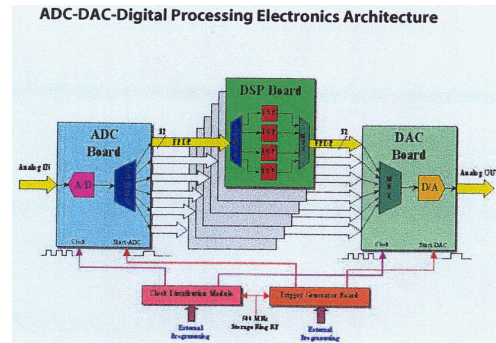


Figure 2: Digital filter structure

The digital filter (Fig. 2) consists of the ADC itself, which is followed by a first one to four demultiplexing stages. A second one to six demultiplexing reduces the data rate to approximately 20 MS/s, The six Front Panel Data Ports (FPDP) each feed a quad processor board containing TI-TMS320C6201 Digital Signal Processors (DSP). Three processors per board concurrently calculate the correction kicks, whereas one DSP takes all the data from the FPDP port and is used for on-line beam diagnostics.

The system described has been shown to work (e.g. [1]) and two systems are in routine operation on the vertical and horizontal planes at ELETTRA. A show stopper in setting up a feedback for all planes proved to be the cessation of production of the ADC and DAC boards, which were planned to be used. Following that, it was decided to launch our own development of ADC and DAC boards, at the same time trying to improve on the suitability for feedback and other accelerator applications. The main specifications of the boards are given in table 1.

### ELECTRONICS

The similarities in the functionalities of ADC and DAC boards shows up also in the layouts in figures 3 and 4 and was exploited to simplify the development process. Both boards consist of three functional blocks, the first being a dedicated mezzanine in 50  $\Omega$  matched technology and containing the pure ADC or DAC circuitry. Common to both layouts is the main board containing the VME interface, a Xilinx Virtex II FPGA and (as of now) eight MBytes of ZBT RAM. The third block, also common in terms of hardware to both ADC and DAC, is the FPDP connector card. For both main board and FPDP board, only the FPGA firmware and the mezzanine card (ADC or DAC) attached determine the difference in the functionality.

## SLIM (Sem for Low Interception Monitoring) AN INNOVATIVE NON-DESTRUCTIVE BEAM MONITOR FOR THE EXTRACTION LINES OF A HADRONTHERAPY CENTRE

L. Badano<sup>\*</sup>, O. Ferrando, M. Pezzetta, Fondazione TERA, Milan, Italy  
G. Molinari, CERN, Geneva, Switzerland

### Abstract

Real time monitoring of hadrontherapy beam intensity and profile is a critical issue for the optimisation of the dose delivery to the patient carcinogenic tissue, the patient safety and the operation of the accelerator complex. For this purpose an innovative beam monitor, based on the secondary emission of electrons by a non-perturbative, sub-micron thick Al target placed directly in the extracted beam path, is being proposed. The secondary electrons, accelerated by an electrostatics focusing system, are detected by a monolithic Silicon position sensitive sensor, which provides the beam intensity and its position with a granularity of 1 mm at 10 kHz frame rate. The conceptual design and the engineering study optimised for hadrontherapy, together with the results of the preliminary tests of the first system prototype, will be presented.

### INTRODUCTION

#### *The rationale for the SLIM project*

Hadrontherapy is the use of hadron beams to irradiate tumours. In its most advanced form, the intense end-of-track Bragg ionization peak, together with variations in beam profile and energy, are used to deliver an optimum, shaped dose to the tumour that minimizes the damage to nearby normal tissues [1]. Patient safety, accelerator operation, and that optimum dose delivery would all benefit if the beam intensity and profile could be continuously monitored during treatment, rather than just during the set-up. This has not been previously possible, since existing interceptive monitors interfere with the beam, considered that the therapeutic beam kinetic energies varies in the range (60 – 250) MeV for protons and (120 - 400 MeV/u) for carbon ions and that non-interceptive instrumentation is not sensitive enough to detect average beam intensities from few pA to few nA, with spill duration ~ 1 s. For this purpose an innovative beam monitor, named SLIM (Sem for Low Interception Monitoring), capable of providing beam intensity and profile during the treatment, has been conceived and developed in the framework of the SUCIMA (Silicon Ultra fast Cameras for electron and gamma sources In Medical Application) project. SUCIMA has been funded by the European Commission with the primary goal of developing a real time dosimeter based on direct detection in a Silicon substrate.

<sup>\*</sup> laura.badano@cern.ch; the authors research is supported by the European Commission under the contract GIRD-CT-2001-00561

#### *SLIM beam monitor principle and requirements*

A thin Al - Al<sub>2</sub>O<sub>3</sub> - Al foil set at an angle to the beam serves both as a source of secondary electrons (SE) and as an electrode with electric field lines from the foil surface that guide the emitted electrons to a pixel/pad detector beyond the beam volume. A schematic layout of the beam monitor is shown in Figure 1.

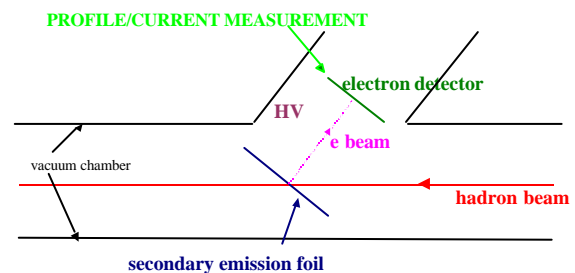


Figure 1: Schematic principle of the SLIM beam monitor.

The thin foils are produced following a technique consolidated at CERN [2] and consist of a support of 0.1 - 0.2  $\mu\text{m}$  of Al<sub>2</sub>O<sub>3</sub> coated on each side with 0.01 – 0.05  $\mu\text{m}$  of Al for a maximum diameter of about 65 - 70 mm. As secondary emission is a surface phenomenon, it will concern just the most superficial aluminium layers. The emittance blow-up induced by the foil has been evaluated with a Monte Carlo programme for plural scattering [3] and goes from 2% to 10% according to the beam divergence at the foil for a 60 MeV proton beam (worst case). Experimental validation of the model results are foreseen during the first measurements on hadron beams.

The optics for the collection of the SE, the type, size and pitch of the electron detector, the front-end electronics and the read-out system have been designed on the base of the key requirements on the performances of the SLIM beam monitor summarised below:

- real-time (during the treatment of the patient)
  - stigmatic optics (demagnifying or proximity) to preserve the information on the beam profile
  - thin foil diameter  $\Phi = 70$  mm (beam on  $10 \times 10$  mm<sup>2</sup>)
  - profile granularity 1 mm
  - vacuum compliant ( $10^6 \div 10^7$  Torr)
- and of the requirements specific for the SE detector and related electronics:
- active surface subdivided in cells (pads or pixels)
  - 5000 cells or more
  - sensitive to low-energy (~ 20 keV) electrons
  - large dynamic range ( $3 \div 9 \cdot 10^3$  e<sup>-</sup>/pixel-100  $\mu\text{s}$ )

## BEAM DIAGNOSTICS IN THE AGOR CYCLOTRON

S. Brandenburg, W.K. van Asselt, H. Post, H.W. Schreuder  
 Kernfysisch Versneller Instituut, 9747 AA Groningen, the Netherlands  
 B. Launé  
 Institut de Physique Nucléaire, 91406 Orsay CEDEX, France

### Abstract

Using the superconducting cyclotron AGOR at the KVI as an example the beam diagnostics equipment in modern multi-particle, variable energy cyclotrons for research in nuclear physics is reviewed. The experience obtained with the extensive set of diagnostics tools integrated in the design since the start of operation in 1996 is discussed.

### INTRODUCTION

The AGOR cyclotron at the KVI is a multi-particle, variable energy AVF-cyclotron [1, 2]. It accelerates ions with charge-to-mass ratio  $Q/A$  in the range  $0.1 \leq Q/A \leq 1$ . The maximum energy per nucleon is, depending on  $Q/A$ , determined by either the bending limit  $E/A = 600 (Q/A)^2$  MeV or the vertical focusing limit  $E/A = 200 Q/A$  MeV. The magnetic field, in the range 1.7 to 4T, is produced by two superconducting maincoils, fifteen trimcoils and three fully saturated iron polesectors. The beams from the external ion sources (ECR for heavy ions, multi-cusp source for light ions and atomic beam source for polarised protons and deuterons) are axially injected. The extraction system consists of an electrostatic deflector, two electromagnetic deflectors with dipole and quadrupole windings and a quadrupole channel.

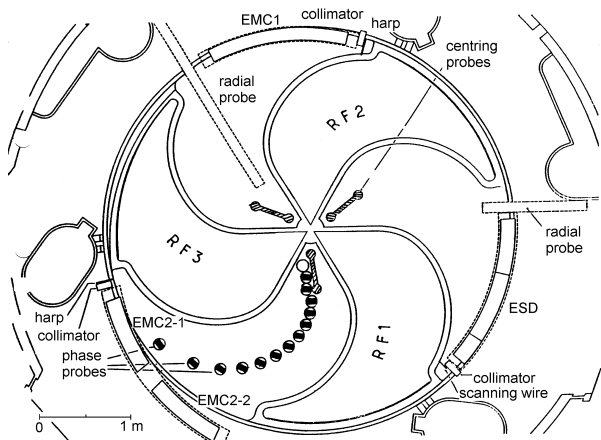


Figure 1: Layout of the AGOR median plane, showing various diagnostic tools and the position of the different extraction elements.

ESD: electrostatic deflector, EMC: electromagnetic channel

Besides the radial probe, the basic diagnostic tool in almost any cyclotron, an extensive set of diagnostics has

been integrated in the design (see figure 1) to allow a proper optimisation of beam centring, isochronism and alignment of the beam along the extraction path [4].

### BEAM CENTRING

Because of the high magnetic field along the injection path the beam has to be injected exactly on axis. This implies that the orbit of the injected beam is off axis by about 15 mm. The major part of the centring error is corrected by the geometry of the acceleration electrodes in the central region of the cyclotron. The remaining centring error (1 – 2 mm) is corrected with a first harmonic of the magnetic field produced with two of the inner trimcoils [4].

Minimising the centring error is essential to obtain high extraction efficiency and to minimise the radial emittance of the extracted beam. Because of the large phase acceptance (around  $30^\circ$ ) the number of turns needed to reach extraction radius varies by about 20, corresponding to several precession periods of the coherent radial betatron motion associated with the centring error. The resulting precession mixing causes a significant increase of the emittance of the beam at the entrance of the extraction system. This leads to reduced extraction efficiency and increased emittance of the extracted beam.

To verify the centring three probes have been installed at azimuths  $120^\circ$  apart to measure the radial turn pattern just beyond the central region of the cyclotron. The use of these probes to optimise the beam centring has turned out to be complicated:

- The observation of the individual turns requires the magnetic field to be tuned such that “turn” focusing is achieved: the number of turns required to reach a given radius has to be independent of the injection phase of the particles. The large phase acceptance allows this to be achieved only approximately, resulting in a small radial intensity modulation rather than separated turns.
- The centring error to be corrected can be as large as the radius gain per turn due to acceleration. Together with the weak turnseparation this makes it difficult to link the turn patterns from the three probes and extract the centring error from the data.

These complications preclude automatic calculation of the centring error from the measurement and thereby its use for the routine operation of the accelerator.

# BEAM BASED HOM ANALYSIS OF ACCELERATING STRUCTURES AT THE TESLA TEST FACILITY LINAC

M. Wendt, S. Schreiber, P. Castro, A. Gössel

Deutsches Elektronen Synchrotron (DESY), Hamburg, Germany

M. Hüning, Fermi National Accelerator Laboratory (FNAL), Batavia IL, U.S.A.

G. Devanz, M. Jablonka, C. Magne, O. Napoly, CEA, Saclay, France

N. Baboi\*, Stanford Linear Accelerator Center (SLAC), Stanford, U.S.A.

## Abstract

The beam emittance in future linear accelerators for high energy physics and SASE-FEL applications depends highly on the field performance in the accelerating structures, i.e. the damping of higher order modes (HOM). Besides theoretical and laboratory analysis, a beam based analysis technique was established [1] at the TESLA Test Facility (TTF) linac. It uses a charge modulated beam of variable modulation frequency to excite dipole modes. This causes a modulation of the transverse beam displacement, which is observed at a downstream BPM and associated with a direct analysis of the modes at the HOM-couplers. A brief introduction of eigenmodes of a resonator and the concept of the wakepotential is given. Emphasis is put on beam instrumentation and signal analysis aspects, required for this beam based HOM measurement technique.

## INTRODUCTION

Well controlled electron beam parameters are essential in future linear accelerators, like linear colliders for high energy physics or SASE-FEL driver linacs for applied science. The transport of very low emittance beams through the entire accelerator requires low transverse *wakepotentials* and therefore well damped *higher order modes* (HOM) in the accelerating structures. At the TESLA Test Facility (TTF) linac a series of beam based HOM measurement experiments has been performed [1, 2, 3]. Beam instrumentation, in terms of a broadband beam position monitor (BPM) and HOM-couplers, was used to characterize beam excited dipole modes of the accelerating structures.

An intensity modulated bunched beam was used, which causes tunable sideband at frequencies

$$f_{\text{side}} = n f_b \pm f_{\text{mod}} \quad (1)$$

where  $f_b$  is the bunch repetition frequency,  $f_{\text{mod}}$  is the modulation frequency and  $n$  is an integer. Resonant modes are excited if  $f_{\text{side}} = f_{\text{HOM}}$ . A beam bump offsets the beam trajectory in the accelerating structure by an amount  $\delta x$  to ensure the excitation of dipole modes. Two measurements are required to find and analyze HOM's:

1. On a downstream located broadband BPM an automatic

\* On leave from NILPRP, Bucharest, Romania

routine searches for beam excited dipole modes by analyzing it's transverse kick proportional to  $(R/Q) \delta x$ .

2. A measurement on the HOM-couplers of the accelerating structures is required to identify mode frequency and Q-value.

## HIGHER ORDER MODES

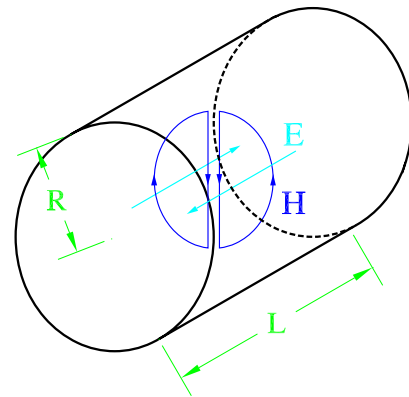


Figure 1: Cylindrical “pill-box” cavity, shown with the field lines of the  $\text{TM}_{110}$  dipole mode (horizontal polarized).

A cylindrical cavity (“pill-box” cavity) forms a simple single-cell accelerating structure (Fig. 1). By neglecting the vacuum chamber ports the resonant behavior in terms of the eigenmodes can be derived analytically, which results in a infinite number of eigenfrequencies at:

$$f_{npq}^{\text{TM(TE)}} = \frac{1}{2\pi R \sqrt{\epsilon\mu}} \sqrt{x_{np}^{(r)2} + \left(\frac{q\pi R}{L}\right)^2}$$

where  $x_{np}$  and  $x'_{np}$  are the zeros of the  $n^{\text{th}}$ -order Bessel-function respectively its derivative.

Each mode behaves equivalent to a parallel resonant circuit, driven by a current source. The fundamental  $\text{TM}_{010}$  mode is used for particle acceleration and driven by the rf-transmitter. All other *higher order modes* (HOM) are unwanted, but may be excited by the beam itself. Due to the finite conductivity of the cavity walls, power  $P_d$  is dissipated which limits Q-value of the resonances:

$$Q_0 = \frac{2\pi f_0 U}{P_d} = \frac{f_0}{\Delta f} \quad R_0 = \frac{V^2}{2 P_d}$$

## USE OF OPTICAL TRANSITION RADIATION INTERFEROMETRY FOR ENERGY SPREAD AND DIVERGENCE MEASUREMENTS

R. B. Fiorito and A.G. Shkvarunets, Institute for Research in Electronics and Applied Physics, University of Maryland, College Park, MD 20742, USA

### Abstract

OTR interferometry (OTRI) has been shown to be an excellent diagnostic for measuring the rms divergence and emittance of relativistic electron beams when the fractional energy spread  $\Delta\gamma/\gamma$  is less than the normalized rms divergence  $\sigma = \gamma\theta_{\text{rms}}$ . This is the case for most beams previously diagnosed with OTRI. To extend this diagnostic capability to beams with larger energy spreads, we have calculated the effects of all the parameters effecting the visibility of OTR interferences,  $V$ ; i.e. energy spread, angular divergence, the ratio of foil separation to wavelength ratio,  $d/\lambda$  and filter band pass. We have shown that: 1) for a given  $\Delta\gamma/\gamma$ , the sensitivity of  $V$  to  $\sigma$  is proportional to the observation angle  $\theta_0$ , the fringe order  $n$  and the ratio  $d/\lambda$ ; 2) the sensitivity of  $V$  to  $\Delta\gamma/\gamma$  is independent of  $\theta_0$  and  $n$  but is proportional to  $d/\lambda$ . Thus, by adjusting  $d/\lambda$ , and choosing the appropriate fringe order, one can separate out and measure *both* the energy spread and divergence. However, the filter band pass must decrease with  $\theta_0$  and  $n$ . Results of our calculations will be given for various beams of interest.

### INTRODUCTION

A conventional optical transition radiation interferometer [1] consists of two parallel thin foils, oriented at 45 degrees with respect to the electron beam. A charged particle or particle beam produces forward directed OTR from the first foil and backward directed OTR from the second foil, which is usually a mirror. Interferences between the two radiations will be seen near the direction of specular reflection when the distance between the foils,  $d$  is comparable to the vacuum coherence length,  $L_V$ , the distance in which phase ( $\phi$ ) of field of the electron and the OTR photon differ by  $\pi$ .

The component of intensity of OTR interferences parallel to the plane of incidence can be written as

$$\frac{d^2 I_{\parallel}(\gamma, \lambda, \theta)}{d\omega d\Omega} = \frac{4\alpha}{\pi^2 \omega} \frac{\theta_x^2}{(\gamma^{-2} + \theta^2)} |1 - e^{i\phi}|, \quad (1)$$

where  $\phi = d/L_V$  and  $L_V(\theta, \gamma, \lambda) = (\lambda/\pi)((\gamma^{-2} + \theta^2))^{-1}$ ,

$\alpha$  is the fine structure constant,  $\gamma$  is the Lorentz factor of the beam,  $\lambda$  is the observed wavelength,  $\theta = (\theta_x^2 + \theta_y^2)^{1/2}$  is the observation angle measured with respect to the direction of specular reflection,  $\theta_x$  is the x component of  $\theta$  projected onto a plane perpendicular to the direction of specular reflection and  $\omega$  is the angular frequency of the observed photon.

We have developed a useful rms beam divergence diagnostic using OTR interferences [2]. In this method one focuses the beam to a waist. Then the visibility of the interference pattern is primarily a function of the rms beam divergence,  $\theta_{\text{rms}}$  provided that the energy spread of the beam is less than the normalized divergence,  $\sigma = \gamma\theta_{\text{rms}}$ . This is the usual case observed for high energy beams. Also, if one observes perpendicular and parallel polarized OTR interferences, i.e. by inserting a variable polarizer into the optical path, the corresponding components of the divergence can be measured.

Since the visibility is also affected by the optical bandwidth of the observation, one must take care to make this narrow enough so that the change in visibility due to the divergence can be seen. The inter foil distance and the filter band pass must be designed to produce the required number and spacing of the fringes for a given range of divergence. This is typically done with the aid of a computer code, which calculates the OTR interferences, for example, Eq. (1) convolved with a Gaussian distribution of particle trajectory angles and a given filter transmission function. The fit of measured to calculated interferences give the beam energy via the position of the fringes to about 1% precision and the rms divergence to about 10 % precision [2].

Recent theoretical studies have considered use of OTR from a stack of multiple dielectric foils as a beam energy distribution diagnostic [3]. In this study the effect of divergence is neglected. We are currently planning to measure divergence and transverse emittance of a low energy beam (8 MeV) where nonlinear space charge forces create a large energy spread on the beam (1- 10 %), and the normalized divergence  $\sigma = \gamma\theta_{\text{rms}} \sim 0.03$ , which is comparable to the energy spread. For this application a careful analysis of the effects of all beam and measurement parameters and a strategy for separating out the effects of divergence and energy spread is required.

### APPROACH

Our approach to this problem is twofold:

1. Calculate of the effect of variations of beam angle (divergence), energy spread and wavelength (filter band pass) on the difference in phase between OTR photons produce at each foil. It is this phase that determines the fringe visibility and corresponding capability of OTR interferometry (OTRI) to diagnose beam parameters with good sensitivity and precision.
2. Develop estimates and computer codes which convolve variation effects with OTRI patterns to determine and define parameter ranges needed to separate out effects of energy spread and beam divergence.

## STUDIES OF OTR ANGULAR DISTRIBUTION ON CTF2

E. Bravin and T. Lefèvre, CERN, Geneva, Switzerland

### Abstract

Optical Transition Radiation (OTR) is widely used in beam diagnostics. The most common application is the acquisition of the transverse and longitudinal beam profiles. Other beam parameters, like divergence and energy, can also be deduced from the angular distribution of the OTR emission (“Doughnut”). In order to investigate the possibilities and the limits offered by this technique we have performed a test on the 48MeV, 1nC electron beam of the CLIC Test Facility 2 (CTF2.). Beam divergences between 2 and 6mrad were measured with an accuracy of a few percent. A good agreement was also found between the energy measurements obtained with a classical spectrometer and the OTR based technique. We conclude by describing some possible applications of OTR based diagnostics for CLIC.

### 1 INTRODUCTION

Optical Transition Radiation [1] has become a familiar tool in accelerator diagnostics for beam imaging [2]. Its success resides in its simplicity, only requiring a conducting foil and an adequate optical system, providing thus a robust and cheap instrument. The perfect linearity of the light intensity versus the number of particles is a significant advantage compared to scintillating screens, which are subjected to saturation. Its femtosecond time resolution [3] allows accurate bunch length measurement, limited in most cases by the performance of the camera. Using the so-called ‘quadrupole scan method’, beam emittances are routinely extrapolated from OTR beam profile measurements. As already pointed out in the ‘70s, much more information than the beam profiles can be extracted from the OTR emission [4]. The beam energy and divergence are accessible in the angular distribution of the OTR. In this case, the camera must be located in the focal plane of the optical system, which is focused at infinity. A lot of experiments have been done in this direction during the past years, demonstrating the strong potential of transition radiation for single shot emittance measurement [5] or beam energy and energy-spread determination [6]. OTR interferometry using a two-foil assembly has been also developed [7] and has shown its capability to enhance the performance of the OTR angular techniques.

In this paper, we report on the OTR study performed at the CLIC Test Facility 2 (CTF2) [8] using a 48MeV, 1nC electron bunch. Our effort has been concentrated on the angular distribution observation. Beam divergences were measured with a good accuracy and OTR based energy measurements have been compared with success to the classical energy measurements performed with a spectrometer line. We finally give some perspectives for its utilization in the CLIC context [9].

### 2 OTR FOR RELATIVISTIC PARTICLES

Let us consider the interface between vacuum and a material with a relative permittivity  $\epsilon$ . Let us also assume that this interface is tilted with respect to the beam trajectory by an angle  $\psi$ , as shown in figure 1. Using the formalism developed in [4], the backward OTR spectral and angular distribution emitted with polarizations parallel and perpendicular to the observation plane can be expressed by:

$$\frac{\partial^2 I_{\parallel}}{\partial \omega \partial \Omega} = \frac{\alpha \cdot \hbar \beta_z^2 \cos^2(\theta)}{4\pi^2 \sin^2(\theta)} \left| \frac{(1-\epsilon)(A \cdot \sin^2(\theta) - B)}{C \cdot D \cdot E} \right|^2$$

$$\frac{\partial^2 I_{\perp}}{\partial \omega \partial \Omega} = \frac{\alpha \cdot \hbar (\beta_x^2 \beta_z^4 \sin^2(\phi) \cos^2(\theta))}{4\pi^2} \left| \frac{(1-\epsilon)}{C \cdot D \cdot F} \right|^2$$

with  $\beta_z = \beta \cos(\psi)$ ,  $\beta_x = \beta \sin(\psi)$ ,  $\alpha$  the fine structure constant,  $\hbar$  the reduced Planck constant and the following functions defined by:

$$A = 1 + \beta_z \sigma - \beta_z^2 - \beta_x \sin(\theta) \cos(\phi), \quad B = \beta_x \beta_z \sigma \sin(\theta) \cos(\phi)$$

$$C = (1 - \beta_x \sin(\theta) \cos(\phi))^2 - \beta_z^2 \cos^2(\theta), \quad D = 1 - \beta_x \sin(\theta) \cos(\phi) + \beta_z \sigma$$

$$E = \sigma + \epsilon \cos(\theta), \quad F = \sigma + \cos(\theta), \quad \sigma = \sqrt{\epsilon - \sin^2(\theta)}$$

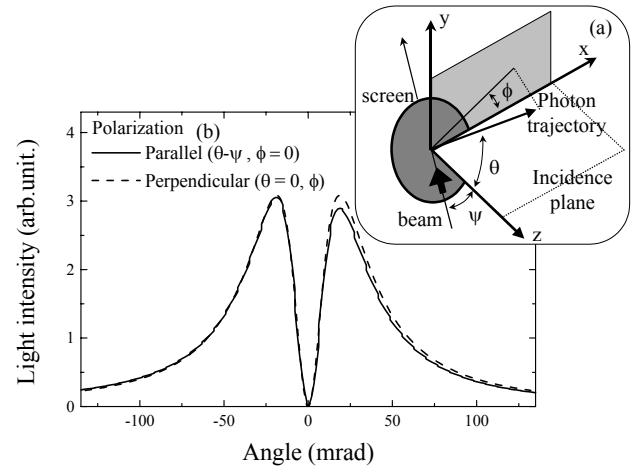


Figure 1: (a) Geometrical configuration: The incident plane contains both the normal to the screen and the beam velocity (b) OTR angular distribution,  $I_{\parallel}$  and  $I_{\perp}$  for a 50MeV electron. The tilt of the screen introduced an asymmetry of the lobes pattern, only visible in the  $I_{\parallel}$  signal. The relative position of the maximums with respect to the centre of the distribution gives a measurement of the beam energy ( $=1/\gamma$ ).

Assuming that the electron beam has a Gaussian angular distribution defined as follow:

$$D_{\parallel, \perp}(s) = \frac{e^{-\frac{s^2}{2\sigma_{\parallel, \perp}^2}}}{\sqrt{2\pi} \cdot \sigma_{\parallel, \perp}}$$

The angular distribution of the OTR light is obtained by the convolution of  $I_{\parallel, \perp}$  and  $D_{\parallel, \perp}$ . Some examples are given

## OTR FROM NON-RELATIVISTIC ELECTRONS

C.Bal, E.Bravin, E. Chevallay, T. Lefèvre and G. Suberlucq, CERN, Geneva, Switzerland

### Abstract

The CLIC Test Facility 3 (CTF3) injector will provide pulsed beams of high average current; 5A over 1.56 $\mu$ s at 140keV. For transverse beam sizes of the order of 1mm, as foreseen, this implies serious damage to the commonly used scintillating screens. Optical Transition Radiation from thermally resistant radiators represents a possible alternative. In this context, the backward OTR radiation emitted from an aluminium screen by a 80keV, 60nC, 4ns electron pulse has been investigated. The experimental results are in good agreement with the theoretical expectations, indicating a feeble light intensity distributed over a large solid angle. Our conclusions for the design of the CTF3 injector profile monitor are also given.

### 1 INTRODUCTION

The injector of the CTF3 facility in the nominal phase will produce intense beams [1]. The pulse will be 1.56 $\mu$ s long at a repetition rate of 50Hz, the nominal average current will be 5.4A, the electron energy 140keV and the beam size of the order of 1mm ( $\sigma_{x,y}$ ). These values render the use of standard scintillating screens impossible since they will not stand the corresponding thermal load [2]. Reducing the beam current or the pulse length during the measurement can circumvent this problem. But for the optimum machine operation the observation of the beam profile in the transverse plane up to full intensity is required. For this reason alternative techniques must be developed. One solution consists of using Optical Transition Radiation (OTR) [3] with a graphite or carbide-based radiator. At the beginning of the '60s a lot of work was done on the OTR theory [4], together with experiments with electrons of energies between 1-100keV[5]. With the development of accelerators, OTR from relativistic particles [6] was studied and its application as a beam diagnostic tool has been widely developed. In the case of non-relativistic particles, OTR radiation, which is less efficient than scintillation in terms of light intensity, was never used, to our knowledge, for beam profile monitoring.

In order to investigate the feasibility of using an OTR screen for the CTF3 injector, we have been carried out some measurements on the 80keV electron beam available in the photocathode test stand at CERN [7]. Our paper is organised as follows. First, the OTR light characteristics are calculated for low energy electrons, in particular the angular distribution of the radiation. The beam line arrangement of the photocathode laboratory is described including the detection system added for this test. Experimental results are compared to our theoretical expectations and some perspectives for the CTF3 injector profile monitor are finally expressed.

### 2 OTR EMISSION FROM NON RELATIVISTIC ELECTRONS

We consider the transition between the vacuum and a material with a relative permittivity  $\epsilon$ . The screen is tilted with respect to the beam trajectory ( $\vec{z}$ ) by an angle  $\psi$ , as shown in figure 1. The OTR emission results from the contribution of the direct ( $\vec{n}$ ), the reflected ( $\vec{n}'$ ) and the refracted ( $\vec{n}''$ ) radiations emitted by the particle. Using the formalism developed by Wartski in [6], the backward OTR spectral and angular distribution emitted with polarizations parallel and perpendicular to the observation plane<sup>†</sup> can be expressed by:

$$\frac{\partial^2 I_{\parallel}}{\partial \omega \partial \Omega} = \frac{\alpha \cdot \hbar}{4\pi^2} \left| \frac{\vec{\beta}_{\parallel} \wedge \vec{n}}{1 + \vec{\beta} \cdot \vec{n}} + r_{\parallel} \frac{\vec{\beta}_{\parallel} \wedge \vec{n}'}{1 + \vec{\beta} \cdot \vec{n}'} - \frac{f_{\parallel}}{\epsilon} \frac{\vec{\beta}_{\parallel} \wedge \vec{n}''}{1 + \sqrt{\epsilon} \vec{\beta} \cdot \vec{n}''} \right|^2$$

$$\frac{\partial^2 I_{\perp}}{\partial \omega \partial \Omega} = \frac{\alpha \cdot \hbar}{4\pi^2} \left\| \vec{\beta}_{\perp} \right\|^2 \left| \frac{1}{1 + \vec{\beta} \cdot \vec{n}} + r_{\perp} \frac{1}{1 + \vec{\beta} \cdot \vec{n}'} - \left( \frac{f_{\perp}}{\sqrt{\epsilon}} \right) \frac{1}{1 + \sqrt{\epsilon} \vec{\beta} \cdot \vec{n}''} \right|^2$$

with  $\hbar$  the reduced Planck constant,  $\alpha$  the finite-structure constant ( $=1/137$ ),  $\vec{\beta}_{\parallel}$  and  $\vec{\beta}_{\perp}$  the projection of electron velocity in the planes parallel and perpendicular to the observation plane and the corresponding Fresnel coefficients defined by:

$$f_{\parallel} = \frac{2\sqrt{\epsilon} \cos \theta}{\sqrt{\epsilon} \cos \theta + \sqrt{1 - \sqrt{\epsilon} - \sin^2 \theta}} \quad f_{\perp} = \frac{2\sqrt{\epsilon} \cos \theta}{\cos \theta + \sqrt{\epsilon - \sin^2 \theta}}$$

$$r_{\parallel} = f_{\parallel} - 1 \quad r_{\perp} = \sqrt{\frac{1}{\epsilon}} f_{\perp} - 1$$

and  $\theta$  the angle between the normal of the screen and the direction of the OTR photons. The characteristic of the forward OTR emission can be obtained from the previous formula replacing  $\beta_z$  by  $-\beta_z$  ( $\beta_z = \beta \cos(\psi)$ ).

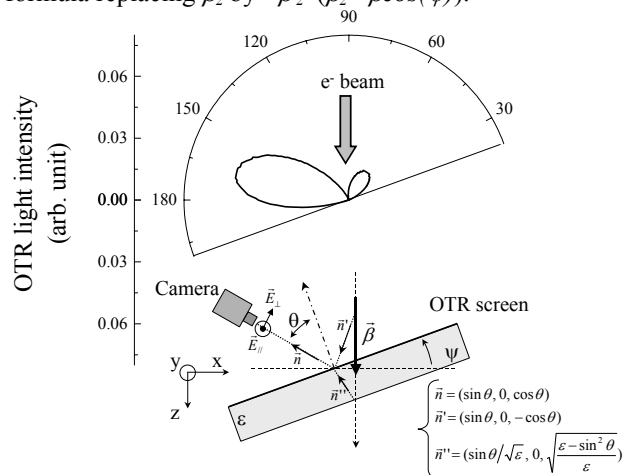


Figure 1: The angular distribution of the backward OTR emitted by 80keV electrons

<sup>†</sup> The observation plane is the plane that contains the photon's direction and the normal of the radiator

## OPTICAL TRANSMISSION LINE FOR STREAK CAMERA MEASUREMENTS AT PITZ

J. Bähr, D. Lipka, H. Lüdecke, DESY Zeuthen, Zeuthen, Germany

### *Abstract*

The photoinjector test facility at DESY Zeuthen (PITZ) produces electrons with a momentum of about 4–5 MeV/c. It is the aim to measure the temporal characteristics of the electron bunch train and single bunches with high accuracy of the order of 1 ps and better. Two types of streak cameras will be used in combination with different radiators which transform particle energy in light. The problem to be solved is the light transport over a distance of about 27 m. Basic demands to the optical system and design principles will be explained. The optical and technical solutions will be presented. The strategy of adjustment and commissioning of the optical system will be described. The system contains switchable optics for the use of different radiators (OTR, Cherenkov radiators). Diagnostic tools are foreseen at different positions along the optical axis. The results of different measurements in the laboratory will be presented. The problems on the minimalization of time dispersion in the system will be discussed.

### INTRODUCTION

The photoinjector PITZ [1] at DESY Zeuthen is a dedicated facility for the investigation of rf-guns for future FELs and linear colliders. Different diagnostics methods are used to investigate the characteristics of the produced electron beam. One important goal is the measurement of the bunch length and longitudinal phase space [2] with a temporal resolution of 2ps and 0.2ps respectively limited by the streak camera to be used as basic tool.

A large fraction of the light created by the electron beam hitting or penetrating different radiators has to be transported by the optical transmission line onto the entrance slit of the streak camera. The light transport has to be performed creating minimum time dispersion and minimum light losses.

### *Radiators*

Different radiators are foreseen to be applied basing on the effect of optical transition radiation (OTR) or the Cherenkov-effect. At a maximum beam momentum of currently about 4.7 MeV/c OTR results in a rather weak signal with a wide emission cone. Therefore the application of the Cherenkov effect will be the main method. A thin quartz plate and silica aerogel of a refractive index of  $n = 1.03$  will be the first radiators to be investigated.

### *Streak Camera Data*

Two types of streak cameras both from Hamamatsu are foreseen to be applied in the measurements.

The time resolution of the device C5680 is about 2 ps. The device is sensitive in the visible range and near UV and has a fiber-optical output by which the image is transmitted to the CCD. It has a synchroscan option and an internal gain of about  $3 \cdot 10^3$ .

The second streak camera available is FESCA-200 with a time resolution of 200 fs working in the single shot mode.

### *Principle of Optical Transmission line*

The principle of the optical transmission line consists in an optical transport of a part of the light created in the radiators by imaging the created light distribution onto the entrance slit of the streak camera. The optical system consists mainly on a chain of telescopes.

### *Design Principles*

A few basic design principles for the optical transmission line are listed below.

- Collect a maximum of created light (depending on the optical input scheme)
- Transmit the light over large distance (27 m) using telescopes
- Project the transported light onto the entrance slit of the streak camera
- Match between the collecting optics and the transmitting optics on one hand and between the transmitting optics and the demagnifying optics before the slit otherwise
- Make an aperture match between the optical sub-system before the entrance slit and the streak camera internal optics
- Minimize the number of optical elements, maximize transmission
- Optimize optical resolution
- Fix wavelength range
- Fix maximum object distribution

### INPUT OPTICAL SCHEMES

Two different optical schemes are used to match different emission characteristics. A high aperture lens system is used to collect a moderate part of the emission cone of the OTR light and of the cone of low refracting silica aerogel (see Fig.1). Subsequent imaging by telescopes takes place.

**AN IMPROVED PLL FOR TUNE MEASUREMENTS**

O.Berrig

CERN AT/MTM, Geneva, Switzerland

*Abstract*

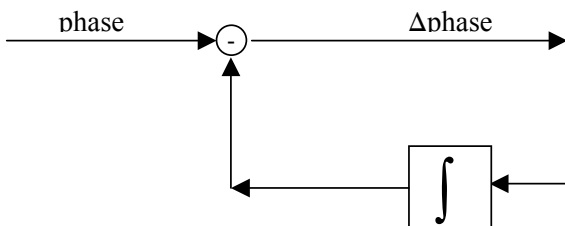
Phase locked loop (PLL) systems are being used on several machines for continuous tune measurements. All these implementations are based on a continuous sinusoidal beam excitation and a monitoring of the resulting beam oscillation.

The key element determining the dynamic performance of such a PLL is the phase detector between the beam oscillation and the internal oscillation. Most circuits use a quadrature phase detector, for which the high frequency carrier at twice the excitation frequency is attenuated by a low-pass circuit. The remaining ripple of this component contributes to the bandwidth/noise performance of the PLL.

In this paper we propose an alternative solution for the filter, notably an adaptive notch filter. We explain in detail design considerations and the resulting improvements in PLL bandwidth and/or noise figure.

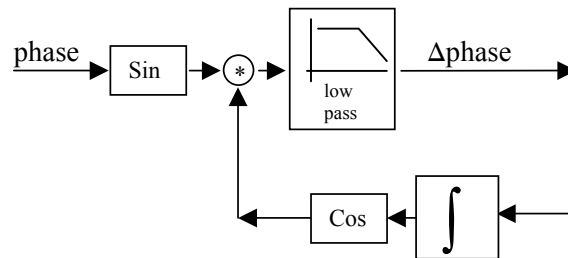
**1 PLL BASICS**

The following diagram shows the “raw” PLL:

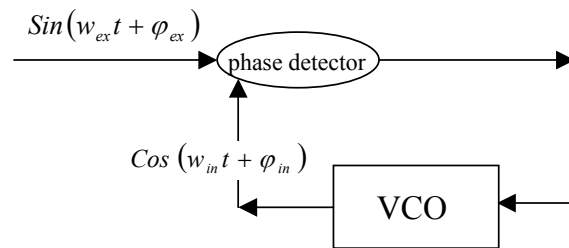


The definition of phase only has meaning when linked to a sine function. Since the sine function, which the PLL is locking on, is normally embedded within many other sine functions, only that phase should be extracted and the phases from the other sine function must be suppressed.

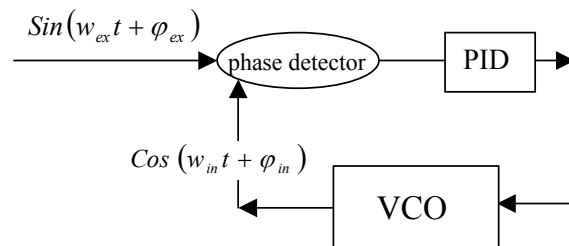
The phase difference could be extracted from the input sine function in a way similar to a Fourier integral, which is a very good filter. Assuming that the amplitude of the external sine has been normalized to 1 ( e.g. by an amplitude regulation loop ), the PLL becomes:



We can now introduce the concept of “phase detector” and VCO (Voltage controlled Oscillator):



Often a PID regulation is added ( or in some cases, combined with the phase detector filter ), which allows locking on widely varying input frequencies:



When the PLL is locked, the two inputs of the phase detector are 90 ° out of phase or “in quadrature”.

# REAL TIME MANAGEMENT OF THE AD SCHOTTKY/BTF BEAM MEASUREMENT SYSTEM

M. Ludwig, M. E. Angoletta, CERN, Geneva, Switzerland

## Abstract

The AD Schottky and BTF system relies on rapid acquisition and analysis of beam quantisation noise during the AD cycle which is based on an embedded receiver and digital signal processing board hosted in a VME system. The software running in the VME sets up the embedded system and amplifiers, interfaces to the RF and control system, manages the execution speed and sequence constraints with respect to the various operating modes, schedules measurements during the AD cycle and performs post processing taking into account the beam conditions in an autonomous way. The operating modes of the instrument dynamically depend on a detailed configuration, the beam parameters during the AD cycle and optional user interaction. Various subsets of the processed data are available on line and in quasi real time for beam intensity, momentum spread and several spectrum types, which form an important part of AD operation today.

## INTRODUCTION AND OVERVIEW

### Functional Overview

Beam diagnostics based on measurement of beam quantisation noise are principally nondestructive and therefore have always played an important role for antiproton machines at CERN. The Antiproton Decelerator's (AD) beam consists of a few  $10^7$  particles which have to be measured with sufficient precision at all frequencies on the flat tops and the ramps during an AD cycle (Fig. 1), with either bunched or randomly coasting beam.

The system hardware consists of longitudinal pick ups (measurement of beam intensity  $N$  and momentum spread  $dp/p$ ), controllable signal amplifiers, an ADC and eight digital receivers controlled by a digital signal processing stage (DSP) hosted in a dedicated VME board (DRX) [1] and synchronised real-time software (RTT) running in the DSC (see [2] for in-depth description). For optional beam transfer function measurements (BTF) (measurement of transversal tune) which can be scheduled independently anywhere during an AD cycle a transversal Pick up and a controllable coloured noise generator for beam stimulation [3] are used. The RTT continuously

schedules measurements, sets up the system hardware, post-processes the data and communicates up-stream. The system is expected to always run, auto-adapt itself to the beam parameters and conditions, be highly configurable for machine development sessions and permanently produce on-line results which must be available for at least three AD cycles.

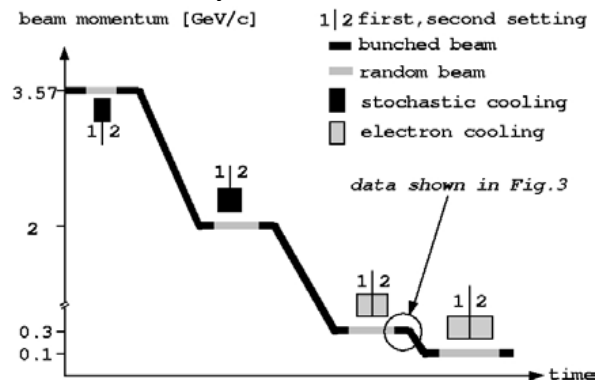


Fig.1: the beam momentum (black/grey trace) during an AD cycle, where the beam is bunched (black) or de-bunched (grey). Stochastic (black square) and electron cooling (grey square) on the flat tops all require different instrument settings. BTF measurements can be made on any ramp or flat top.

### Structural Overview

The main logical components of the system with respect to the front-end software are shown in Fig. 2 together with directed and synchronised information flows. Analogue signals generated by three pick ups in each beam-plane enter the amplifier and signal mapping hardware. This hardware receives configuration for gain, filter, input and mapping of pick ups to amplifier channels organised in a table of settings which is stepped through depending on the revolution frequency ( $f$  tables, Fig. 2). It receives this configuration at times which are determined by the conditional clock and beam logic unit (CBL) as indicated by a many dimensional data flow arrow. The CBL is an eight-dimensional looping counter which steps down each 20ms clock tick ( $T_x$ , interrupts received from an external source) and is realized as software structure. It maps to the eight receivers and inhibits (according counter  $> 0$ ) or releases (according counter = 0) the many

# RECENT ADVANCES IN THE MEASUREMENT OF CHROMATICITY VIA HEAD-TAIL PHASE SHIFT ANALYSIS

N. Catalan-Lasheras, S. Fartoukh, R. Jones<sup>#</sup>, CERN, Geneva, Switzerland

## Abstract

A so-called "Head-Tail" monitor has been operational in the CERN-SPS for a few years. The measurement of chromaticity using such a monitor relies on the periodic dephasing and rephasing that occurs between the head and tail of a single bunch for non-zero chromaticity. By measuring the turn-by-turn position data from two longitudinal positions in a bunch it is possible to extract the relative dephasing of the head and the tail, and so to determine the chromaticity. Until recently this technique had suffered from an unexplained "missing factor" when compared to conventional chromaticity measurements. This paper explains the source of this factor and also reports on the considerable experimental, simulation and analysis effort that has qualified the technique for use in the LHC.

## INTRODUCTION

The determination of chromaticity by following the evolution of head-tail phase shifts after a transverse dipole excitation is a technique which does not rely on an accurate knowledge of the fractional part of the betatron tune and, for a machine operating well above transition, is virtually independent of beam energy.

Early experiments in the CERN-SPS [1] and at HERA-p (DESY) [2] have shown the feasibility of the technique for high-energy proton beams. More recent experiments [3] have highlighted several questions concerning the use of this technique for accurate chromaticity determination. The most important of these concerned a constant factor that appeared between the calculation of chromaticity via traditional techniques and that which was calculated from head-tail phase shift measurements. Here the source of this "missing factor" is explained and a method of correction is outlined. In addition this paper seeks to summarise the extensive theoretical work carried out on this technique [4] aimed at validating the robustness of the method for the LHC.

## EXPLAINING THE "MISSING FACTOR"

A complete description of the detection and acquisition system can be found in [3]. A schematic of the layout can be seen in Fig. 1. All the results to date have shown discrepancies between the value of chromaticity measured via head-tail phase shifts and the traditional technique of tune tracking during energy modulation (referred to in the SPS as radial steering chromaticity measurements). A typical plot from such a comparison performed at the SPS is shown in Fig. 2. It can be seen that the head-tail results are consistently lower than the actual value, requiring a

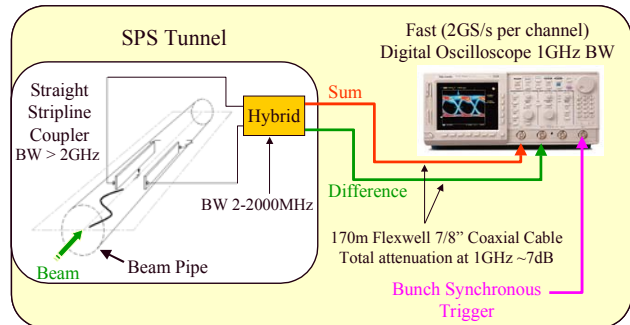


Figure 1. Schematic layout of the head-tail monitor in the CERN-SPS showing the various bandwidth limitations.

correction factor of 1.4, which remains essentially constant with chromaticity. The dotted line shows the trend of the head-tail measurements when corrected for this error, which is now seen to be in very good agreement with that measured using energy modulation.

In order to understand the origin of this correction factor, a more detailed study of both the underlying physics of the head-tail phase shift and the acquisition hardware associated with the head-tail monitor was initiated the results of which are presented in detail in [4].

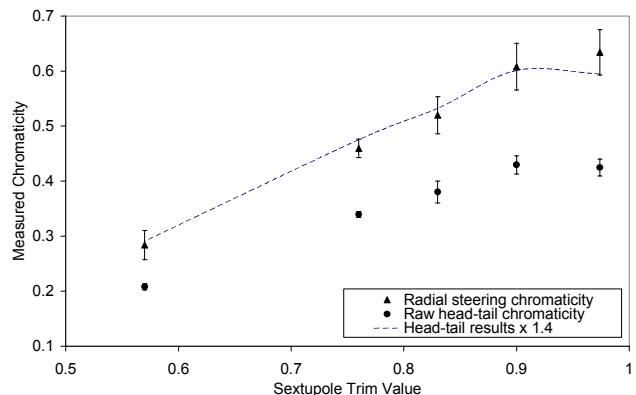


Figure 2. A comparison of head-tail and radial steering chromaticity, measured at 303GeV on the CERN-SPS.

These investigations showed that the source of the correction factor was the bandwidth limitations in the experimental set-up (indicated in Fig. 1). The main analogue contribution came from the 170m of cable connecting the hybrid in the SPS tunnel with the acquisition electronics. In addition, the 2 GS/s sampling rate of the oscilloscope reduces the upper frequencies that can be resolved without aliasing after digitisation to around 500 MHz. To see the effect that such bandwidth

<sup>#</sup>Rhodri.Jones@cern.ch

## DIAGNOSTICS FOR ELECTRON COOLED BEAMS

G. Tranquille, CERN, Geneva, Switzerland

### Abstract

Nearly all modern storage rings use an electron cooling device to increase the phase space density of the circulating beam before its transfer to another accelerator or the experiments. For fast and efficient cooling, the properties of the electron and hadron beams need to be monitored before, during and after the cooling process.

In this paper we review the various techniques, both destructive and non-destructive, used to measure and optimise the different parameters that determine the quality of the cooling.

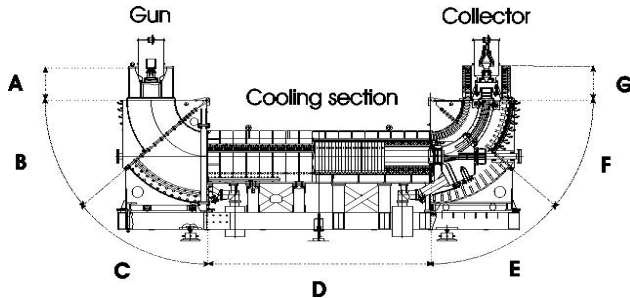


Figure 1: Electron cooler layout.

### DIAGNOSTICS FOR THE ELECTRON BEAM

A typical electron cooling device (fig. 1) consists of three parts: i) the electron gun, where an intense and mono-energetic electron beam is generated, ii) the interaction region, where the cooling of the circulating beam takes place through Coulomb interaction between the electrons and the ions, and iii) the collector, where the electron beam is decelerated and the beam power recuperated. The whole system is immersed in a strong longitudinal magnetic field, which is needed to counteract the space-charge force of the electron beam [1].

The cooling time  $\tau$  can be approximated by the following formula:

$$\tau = \frac{0.6\pi r^2 A \beta^4 \gamma^5 \theta^3}{\eta I_e Z^2},$$

where  $\eta$  is the fraction of the ring occupied by the cooler,  $I_e$  the electron current,  $\theta$  is the relative difference in angle between the electrons and ions ( $\theta = \theta_i - \theta_e$ , where  $\theta_i$  is the ion beam angle,  $\theta_e$  the electron beam transverse temperature  $v_t/v_{||}$ ),  $A$  the atomic mass,  $Z$  the charge state of the ions and  $\beta\gamma$  the relativistic factors. From the above formula the following parameters of the electron beam should be known: i) the electron current, ii) the beam position, iii) the velocity (both in magnitude and direction), iv) the longitudinal energy spread and v) the transverse energy. It is worthwhile to note that these parameters vary with radial position and also in the axial direction.

### Beam destructive methods

Probes inserted into the electron beam will in most cases immediately melt or evaporate. The power-density load is such that the absolute limit in the energy of the electron beam is 20 keV when one considers such methods. In fact 10 keV seems more realistic unless the electron beam is pulsed.

Such devices also change the space-charge fields and self-fields of the electron beam resulting in measurements that may not necessarily reflect the real beam distribution. The current intersected by the probe is also an additional load on the high voltage power supply and hence can only be used at low electron beam currents.

### Faraday cups, scintillation screens and pinhole collimators

The beam position and current density can be measured as a function of radial position and axial distance by the use of a water-cooled Faraday cup [2]. If a phosphor screen coupled to a camera is used, then one obtains a direct image of the current density distribution of the electron beam (fig. 2).

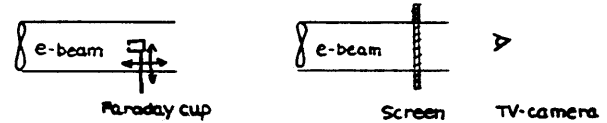


Figure 2: Electron beam measurement with a Faraday cup or scintillation screen.

By inserting a moveable pinhole collimator in the measurement system, a ‘pencil beam’ is generated and one obtains information on the divergence of the electron beam. This parameter is of the utmost importance for electron cooling as it gives a measure of the straightness of the guiding magnetic field.

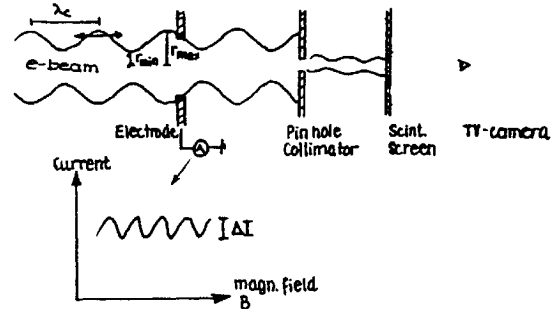


Figure 3: Measurement of the electron beam ripple.

### Measurement of the beam ripple

The cyclotron motion of the electron is superimposed on a slow drift rotational motion caused by the crossed space-charge electric field and the longitudinal magnetic field. These two motions cause the electron beam radius

## CHARACTERISATION OF FAST FARADAY CUPS AT THE ELETTRA LINAC

M. Ferianis, S. Bassanese, G. D'Auria, Sincrotrone Trieste, I-34012 Trieste, Italy

C. Deibele, SNS, Oak Ridge, TN, USA

M. Poggi, INFN-LNL, I-35020 Legnaro (PD), Italy

### Abstract

Since several years, the Diagnostic Group at Laboratori Nazionali di Legnaro (LNL) has been designing Fast Faraday Cups (FFC) to be used on their Heavy Ion Accelerators. Latest developments in this field include a Stripline FFC, jointly developed with the Spallation Neutron Source (SNS). A collaborative partnership has been set-up between LNL and the ELETTRA Laboratory to fully characterize new FFCs, using the 1GeV electron Linac in operation at the ELETTRA Synchrotron Light Source. Two FFCs, the stripline FFC, built at SNS, and a coaxial FFC, made at LNL, have been installed at ELETTRA who provided the wideband data acquisition and the remote control of the measurement. The first measurements, carried out using a 1GHz oscilloscope, have allowed the proper set-up of the instrument remote control as well as a low jitter triggering system, synchronous with the injected electrons. Wideband measurements were performed using oscilloscopes with bandwidths up to 20GHz, whereas the bandwidth of the Stripline FFC has been estimated to be roughly 20GHz.

A complete set of tests was carried out both on the coaxial FFC and on the stripline FFC. Moreover, thanks to the information provided by these wideband measurements, the Linac working point has been further optimized as well as the injection process into the ELETTRA Storage Ring.

### INTRODUCTION

The ELETTRA Linac [1] is in operation since 1992 as injector of the ELETTRA Storage Ring, providing a 1.0GeV electron beam. Since 1996 [2] the Linac has also been used parasitically as a "test facility" both for material irradiation experiments and for testing diagnostic equipments [3]. The characterization of the new Fast Faraday Cups was carried out in the frame of this second activity.

The FFCs, designed to have information on beam temporal structure, have been developed at LNL for several years to measure the bunch length of ion beams. The experience gained in that field also yielded a collaboration with the SNS project at Oak Ridge, where a strip line FFC has been developed to measure the bunch length out of the low energy ( $E=2.5\text{MeV}$  of  $H^-$ ) section of the machine.

#### The ELETTRA Linac bunching structure

The bunching section of the ELETTRA Linac, shown in Fig. 1, includes:

- a 500MHz Sub Harmonic Chopper ( $TM_{110}$  deflecting cavity)
- a 500MHz Buncher ( $TM_{101}$  pill box cavity)
- 3GHz Pre-Buncher ( $TM_{101}$  pill box cavity)
- 3GHz Buncher (0.4m long  $2/3\pi$  SW accelerating section)

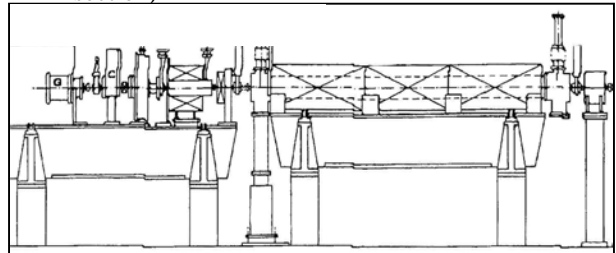


Figure 1: drawing of the ELETTRA Linac pre-injector: G=Gun, C=Chopper, PB5=Pre-buncher @500MHz, PB3=Pre-buncher @3GHz, B=Buncher @3GHz

With a proper setting of the parameters (amplitude and phase of the cavities) this configuration allows to select and fill a pure 500 MHz bucket of the Storage ring, in single bunch mode. This means that at the Linac exit all the charge is compressed in less than 1 nsec with a 3 GHz fine structure of the beam (2 or 3 S-Band micro-bunches, spaced by 330 ps). As we have observed with those measurements, changing the relative phases between the 500MHz cavities and the 3GHz ones, it is possible to change the number and the relative amplitude of the S-Band micro bunches.

### THE FAST FARADAY CUPS

The FFC station, built at LNL and holding the two FFCs, has been installed on the Linac User port at 1GeV (fig. 2). An already available fluorescent screen located upstream the station has been used for alignment purposes and for checking the electron beam focusing.



Figure 2: view of the FFC station installed on the Linac User port at 1GeV. The cable of the coaxial FFC is visible in the foreground. On the right hand side, there is the linear translation stage of the Stripline FFC.

## BEAM STUDIES MADE WITH THE SPS IONIZATION PROFILE MONITOR

G. Ferioli, C. Fischer, J. Koopman, F. Roncarolo  
 CERN, Geneva, Switzerland

### Abstract

During the last two years of SPS operation, investigations were pursued on the ability of the SPS ionization profile monitor prototype to fulfill different tasks. It is now established that the instrument can be used for injection matching tuning, by turn to turn recording of the beam size after the injection. Other applications concern beam size measurements on beams ranging from an individual bunch to a nominal SPS batch foreseen for injection into the LHC (288 bunches). By continuously tracking throughout the SPS acceleration cycle from 26 GeV to 450 GeV the evolution of parameters associated to the beam size, it is possible to explain certain beam behaviour. Comparisons are also made at different beam currents and monitor gains with measurements made with the wire scanners. Data are presented and discussed, and the possible implementation of new features is suggested in order to further improve the consistency of the measurements.

### 1 INTRODUCTION

Data obtained with a gas ionisation beam profile (IPM) monitor under test in the SPS were already reported on several occasions, [1][2]. This type of monitor is one of the instruments considered to measure transverse beam distributions in the SPS and in the LHC. The device can be used in “high resolution mode”, using an optical detection bench with a CCD camera, and integrating the signal on several hundreds of beam passages (typically 20 milliseconds). For rms beam dimensions at the monitor much lower than 1 mm, a reproducibility better than 1% is possible, with a resolution lower than 0.1 mm. Moreover, data are in agreement within a few per cents with corresponding ones taken with wire scanners.

Tests were also performed in “high speed mode”, sampling the beam at the SPS revolution frequency. This is achieved by replacing the CCD camera by a Photo Multiplier Tube (PMT) associated to a high speed acquisition electronics. It was shown in [2] that using 16 anode strips and a resolution of 3mm per strip, was a bit marginal to detect turn to turn injection oscillations.

In the past two years new features occurred. Beams could be injected and accelerated to 450 GeV in the SPS with a structure fulfilling the nominal conditions required for injection into the LHC. The instrument was used to probe them in “high resolution mode”. Comparisons were made with the same data recorded with wire scanners.

Concerning the “high speed mode”, the spatial resolution was improved down to 1.2 mm per strip, by doubling the number of anode strips (32 instead of 16) and re-tuning the optics.

The paper analyses the results of measurements made under these new conditions.

### 2 TURN BY TURN MODE – INJECTION MATCHING STUDIES

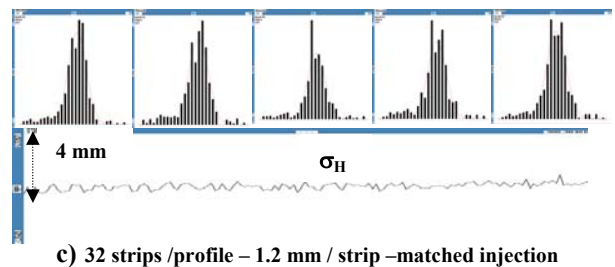
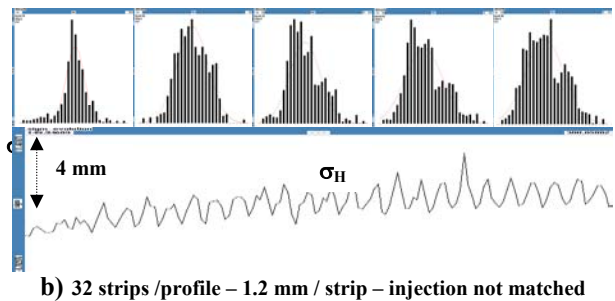
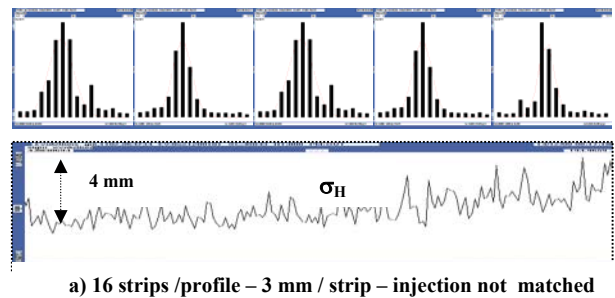


Figure 1: Beam profiles measured on one passage at injection into the SPS and associated evolution of the horizontal beam rms dimension on the first 200 turns when – a) and b): the injection conditions are not matched – and c): matching is tuned.

The results of investigations made with the IPM in fast acquisition mode using 32 anodes strips with a resolution of 1.2 mm per strip are displayed in Figure 1 case b) and c) when the injection conditions are respectively not matched and matched. Compared to the same data acquired under noisy conditions with a

# CAVITY MODE RELATED WIRE BREAKING OF THE SPS WIRE SCANNERS AND LOSS MEASUREMENTS OF WIRE MATERIALS

F. Caspers, B. Dehning, E. Jensen, J. Koopman, J.F. Malo, CERN, Geneva, Switzerland  
 F. Roncarolo, CERN/University of Lausanne, Switzerland

## Abstract

During the SPS high intensity run 2002 with LHC type beam, the breaking of several of the carbon wires in the wire scanners has been observed in their parking position. The observation of large changes in the wire resistivity and thermionic electron emission clearly indicated strong RF heating that was depending on the bunch length. A subsequent analysis in the laboratory, simulating the beam by two probe antennas or by a powered stretched wire, showed two main problems:

- i) the housing of the wire scanner acts as a cavity with a mode spectrum starting around 350 MHz and high impedance values around 700 MHz;
- ii) the carbon wire used so far appears to be an excellent RF absorber and thus dissipates a significant part of the beam-induced power.

Different wire materials are compared with the classical cavity mode technique for the determination of the complex permittivity in the range of 2–4 GHz. As a resonator a rectangular  $TE_{01n}$  type device is utilized.

## WIRES HEATING IN THE SPS TUNNEL

During the two last Machine Development periods in the SPS 2002 run, several wires were found broken. Such breaking can be typically related to the wire heating due to some energy deposition by the traversing protons on the wire. Dedicated electronics has been installed in order to have an indication of the wires heating during the LHC type beam injection and ramp in the SPS. In particular a constant current was supplied to the wire and the voltage drop across it was fed to a digital scope together with the difference between the input and output currents. The differential current ( $I_{out} - I_{in}$ ) grow up is due to the wire heating and consequent emission of electrons for thermionic effect. Fig. 1 shows such voltage and differential current evolutions during the SPS cycle with LHC type beam. No scans were performed along this cycle. It is thus evident that the wire heating does not depend on the direct wire-beam interaction. In particular it is possible to relate the wire heating to the beam intensity (two batches of 72 bunches with  $1.1 \cdot 10^{11}$  p/bunch injected in this case) and to the bunch length which is decreasing along the beam ramp to 450 GeV.

The measurements described in the previous section clearly revealed that the bunch length shortening causes a larger wire heating than the beam intensity. Such observations lead the study of possible RF coupling effects between the wire scanner wires and the proton beam travel-

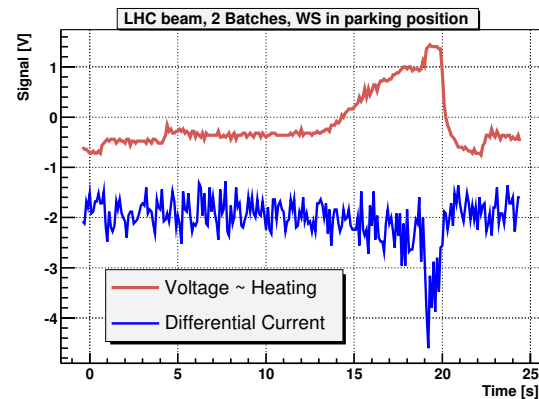


Figure 1: Wire heating due to the LHC beam injection in the SPS (No scan, wire in parking position). The beam energy ramp/bunch length decreasing begin  $t=11$  s.

ling inside the wire scanner tank which is acting as a cavity.

The proton beam circulating in the ring has a frequency spectrum which mainly depends on the bunching structure (bunch length, bunch spacing). The build up of standing waves resonating inside the tank depends on the geometry and the tank materials. If one or more of the modes matches a beam spectral line, a rather large amount of RF power can be transmitted from the beam to the wires. These hypotheses have been investigated through dedicated laboratory measurements.

## LABORATORY MEASUREMENTS

A spare SPS wire scanner tank has been equipped in the laboratory with two probe antennas connected to a Vector Network Analyzer (VNA) in order to simulate the RF modes in the beam spectrum frequency.

### Beam-Wire coupling

Two connections to the ends of the wires of the wire scanner are used during normal operation to check the wire integrity (measuring the resistance) or to detect the secondary emission signal. In the laboratory they were applied to estimate the proton beam-wire coupling while simulating the beam with a stretched wire. A  $0^\circ/180^\circ$  RF signal combiner circuit has been used to measure the differential signal at the wire ends. One port of the VNA has been connected to one end of the stretched wire, the other one at the combiner output giving the differential signal. Fig. 2 is well describing the effect. The plot gives the  $S_{21}$  signal together with the differential signal on the wire scanner wire. Where the frequency peak of the transmitted signal matches a peak of the differential signal, the power present

## THE PS BOOSTER FAST WIRE SCANNER

S.Burger, C. Carli, M. Ludwig, K Priestnall, U. Raich, CERN, Geneva, Switzerland

### Abstract

The very tight emittance budget for LHC type beams makes precise emittance measurements in the injector complex a necessity. The PS machine uses 2 fast wire scanners per transverse plane for emittance measurements of the circulating beams. In order to ease comparison the same type of wire scanners have been newly installed in the upstream machine, the PS Booster, where each of the 4 rings is equipped with 2 wire scanners measuring the horizontal and the vertical profiles.

The Booster wire scanners use new and more modern control and readout electronics featuring dedicated intelligent motor movement controllers, which relieve the system from the very stringent real time constraints imposed by the very high wire speed of up to 20m/s. In order to be able to measure beams at the very low injection energy of the PS Booster (50 MeV) secondary emission currents from the wire can be measured as well as secondary particle flows at higher primary particle energies during and after acceleration[1].

The solution adopted for the control of the devices as well as preliminary results obtained during measurements in 2002 are reported.

### SYSTEM OVERVIEW

The new control of the PS Booster (PSB) fast wire scanner is subdivided into a data acquisition part controlled by the VME CPU and a motor control unit (MCU) provided by a VME slave processor board. The MCU is an independent embedded VME board featuring a 68332 CPU, an ADC, DAC and TTL

parallel I/O piggyback module. A complementary interface card is used for signal conditioning.

The acquisition part uses sampling ADCs for position and analogue signals measurements. The VME CPU communicates with the slave processor exclusively through parallel I/O signals making motor control entirely independent from the VME bus. Fig 1a) shows an overview of the complete system.

Due to the very high acceleration and speed needed, a 400W DC motor and an associated servo amplifier with velocity feedback are employed. The complex wire scanner mechanism is depicted in Fig 2.

### MOVEMENT CONTROL

The software in the motor controller waits for triggers on its parallel input lines to power up the system and to step through speed tables defining the motor current function  $V(t)$  through its DAC module. Currently 3 selectable wire speeds of 10m/s, 15ms, 20m/s are available. A resolver whose outputs are connected to the ADC determines the motor position. I/O channels see the end position switches (HOME and OUT). The speed tables are calculated by an offline program taking into account the geometry of the mechanism. They are linked to the embedded software, which is cross-compiled using gcc on a Linux workstation and downloaded into the MCU's flash memory.

The following constraints are taken into account:

1. The last crankshaft position  $x(t_1)$  in [rad] given by the integration over the speed-table:

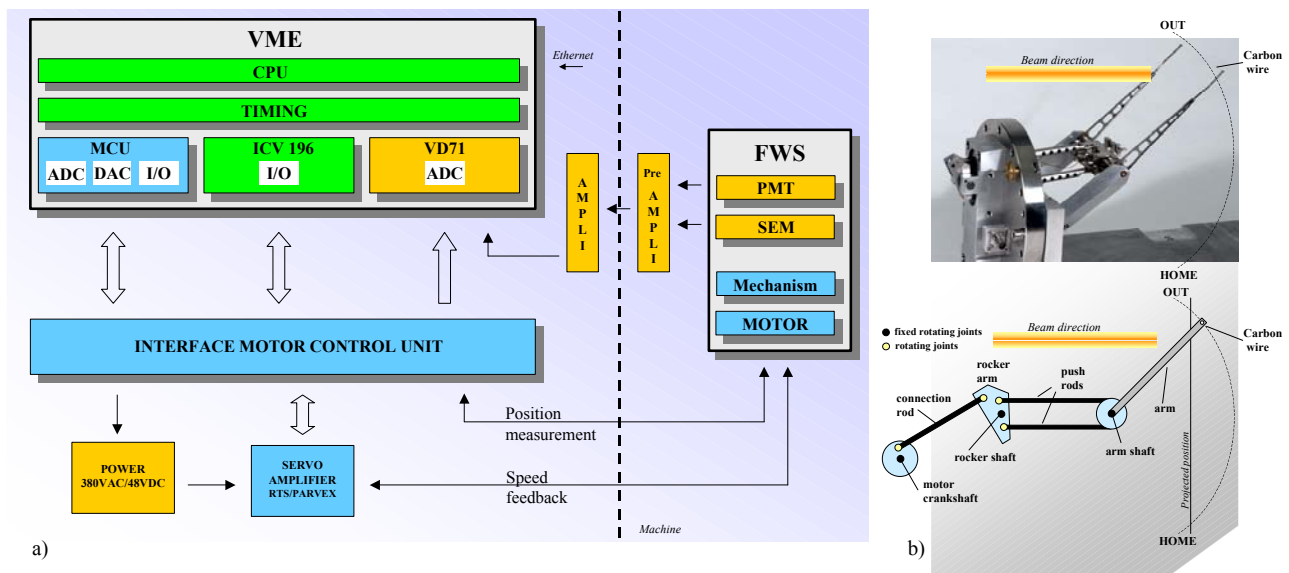


Figure 1: a) System overview of the fast wire scanner installed in the PS Booster. b) Picture and schematic of the mechanism of a fast wire scanner. Its complexity is due to stringent mechanical and physics constraints.

## UPGRADE OF THE ESRF FLUORESCENT SCREEN MONITORS

B.K.Scheidt, ESRF, Grenoble, France

e-mail: scheidt@esrf.fr

### Abstract

The ESRF injector system contains 23 Fluorescent Screen monitors: 4 in the TL-1 transferline (200MeV), 8 in the Booster, and 11 in the TL-2 transferline (6GeV). They are based on Chromium doped Alumina screens that are pneumatically inserted in the beam path with an optical system collecting and focusing the emitted light onto a low-cost CCD camera with standard 75ohm video output. Serving mainly alignment purposes in the past 10 years, the upgrade now aims at a 200um fwhm resolution for beam-size and profile measurements. This while preserving the main existing design components, notably the mechanics and the video & timing network.

The particularity of the Alumina screen not in vacuum but in atmosphere will be explained. Details of the mechanics, the optic system and the way of light flux adjustment will be given. An analysis of the factors determining the spatial resolution as well as the results obtained with different screen material will be presented.

### BASIC PRINCIPLE

The fluorescent screen is mounted on a support that itself slides into a steel tube of 40mm inside diameter. With a simple steel finger this support is pushed against the very end of the tube, at the other end this finger is attached by a screw to a cf-63 flange. By means of a bellows and a pneumatic drive the assembly can be translated over 50mm at 90° angle to the electron beam path. When inserted the centre of the screen, at 45° angle to the beam path, is at the theoretical centre of the beam.

Light emitted from the screen surface is collected with an effective opening angle of only 1° determined by the lens opening of about 7mm at 400mm distance from the screen. A simple mirror deflects the light 90° at the tube's end towards the camera. The latter is so kept outside the direct view of the screen for better and long lasting protection against radiation damage. (see fig.1)

The camera and lens are housed in an immobile 2mm lead case with a lead-glass window. Only the mirror that is attached to assembly with tube and cf-63 flange moves when inserting & extracting the screen.

### SCREEN OUTSIDE BEAM VACUUM

The screen is in ambient atmosphere and not in the UH Vacuum environment of the beam. The electron beam will first traverse the steel tube before hitting the screen surface about 20mm further down. At the beam energies of the ESRF of 200MeV and 6GeV the electrons will completely traverse the device and not cause any problem of excessive activation at this point. However, at 200MeV the scattering induced by the presently 0.5mm thick steel tube limits the spatial resolution, this is discussed further below. For practical reasons and limited costs of the upgrade, the old mechanics is maintained but may be

modified for a small number of TL-1 stations where the high resolution is essential.

A paper mask with 10lines/mm targets in the four corners is stuck directly to the screen, leaving a +/-10mm region free in the centre. It allows precise calibration and easy focussing adjustment at time of installation.

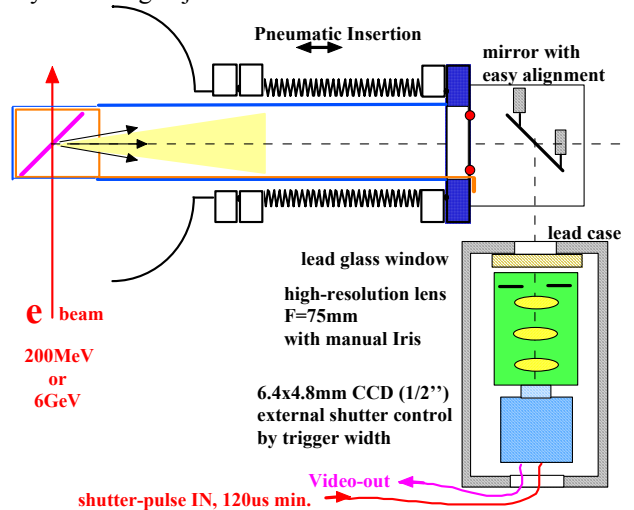


Fig. 1: Set-Up: screen in air and light collection optics.

### CHOICE OF COMPONENTS

For the screen material a Chromium doped Alumina with reference AF-995R is used [1,2]. This product offers a strong resistance to radiation induced damage, was specifically developed for particle's viewing screen applications and is available at a price of 50Euros for a 50x50x1mm plate. This material has good luminosity properties and for our applications the amount of light flux is abundant and needs reduction. This is obtained with an electronic shutter in the Sony ST-50CE CCD [3]. With a few millisecc luminosity decay time of AF-995R and the shortest shutter time of 130us the right amount of beamspot intensity is obtained by adjustment of timing between the two as illustrated below in figure 2. The 75mm macro imaging lens offering >20lp/mm resolution in object space is from Edmund Optics [4].

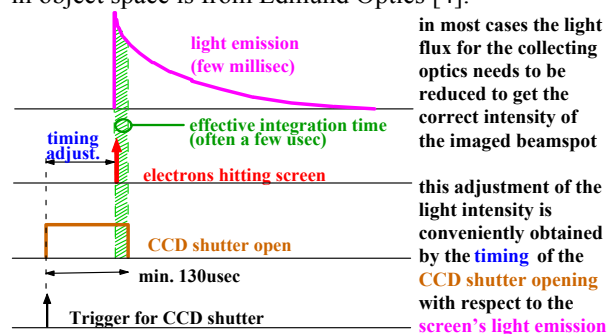


Fig.2: adjustment of light intensity with CCD shutter.

## FIRST EXPERIMENTAL RESULTS AND IMPROVEMENTS ON PROFILE MEASUREMENTS WITH THE VIBRATING WIRE SCANNER

Arutunian<sup>#</sup> S.G., Bakshetyan K.H., Dobrovolski N.M., Mailian M.R., Soghoian H.E., Vasiniuk I.E.  
Yerevan Physics Institute; K.Wittenburg, DESY

### Abstract

The paper presents the first experimental results of transverse profile scans using a wire scanner based on a vibrating wire (vibrating wire scanner - VWS). The measurements were performed at the injector electron beam (10 nA) of the Yerevan synchrotron. The beam profile information is obtained by measuring the wire natural oscillations that depend on the wire temperature. This first experiments on weak electron beam proved this new method as a very sensitive tool, even suitable for very sensitive tail measurements.

Additional, improvements were tested to overcome problems connected with signal conditioning and signal transfer in the presence of electromagnetic noise. As a result the noises were clearly separated and reduced. A mathematical method for rejection of distorted data was developed. Experiments with the scanner at the PETRA accelerator at DESY are planned for measurements of beam tails.

### INTRODUCTION

First experiment on scanning of weak electron beam of the injector of Yerevan synchrotron proved the possibility of beam profiling by the vibrating wire scanner (VWS) [1]. The profile of a low intensity electron beam (average current of the beam was few nA) was measured by using the vibrating wire scanner technique. The experimental results show that the sensitivity of vibrating wire scanners is optimal for extended measurements of beam tails.

The experiments have also shown, that the scanner was sensitive to external electromagnetic noise. It was observed that the level of distortion of frequency from the wire correlates with turn-on of high frequency accelerating klystrons independent of whether the electron beam fell on the wire. Analysing the noises allowed marking out the most sensitive parts of the readout system. The improvements were tested during the autumn 2002 experimental session. As a result the noises could be clearly separated and reduced. A mathematical method for rejection of distorted data was developed. Taking into account this experience a special board is developed for planned experiment with the scanner on the PETRA accelerator at DESY.

### SCANNING EXPERIMENTS

The principle of operation of the vibrating wire scanner is based on the dependence of the wire natural frequency  $f_0$  on the beam intensity at the given location. The energy deposition of the beam particles in the wire causes heating of the wire. Hence the stretched wire temperature can be

obtained by measuring its natural oscillations frequency by an autogenerator electronic circuit with a positive feedback loop.

Initial experiments on profiling were done using laser beams [2, 3]. The effective temperature precision was estimated to be about  $10^{-4}$  degrees C (without noise).

In this experiment the profile of the low intensity (after collimation to about 10 nA) electron beam of the injector of the Yerevan synchrotron was scanned (bunches with RF of 2797.3 MHz with pulse duration of 2  $\mu$ s). The repetition rate of pulses was 50 Hz. A beryllium-bronze wire of 90  $\mu$ m diameter as vibrating wire was used. Fig. 1 represents the result of the reconstruction of the beam profile for the first scanning. Fig. 1 also presents the profile of the beam approximated by a normal distribution with  $\sigma = 1.48$  mm and beam central position at 30.87 mm. The overall current of the beam was set to  $I_0 \sim 10$  nA. Only half of the beam could be scanned because of the short throw of the scanner.

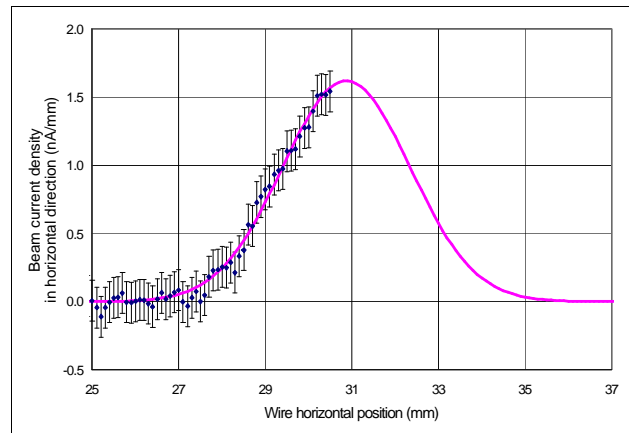


Fig. 1 Reconstructed horizontal profile of an electron beam with a current of about 10 nA. The reconstruction was done after a detailed noise analysis (see "noise studies").

### Calculations of "tail sensitivity"

Let's estimate the sensitivity of VWS with respect to the lower limit of beam intensity. In this case radiational losses of wire temperature are negligible and the balance of temperature is determined by the thermal conduction along the wire. Let the temperature of the wire near its fixation points be  $T_0$  and at the middle  $T_0+T_m$  (triangular profile of the temperature along the wire). Thermoconductive losses  $P = 4\pi\lambda r_w^2 T_m/l$ , where  $\lambda$  is the thermoconductivity of the wire with the radius  $r_w$  and length  $l$ . Total power deposited on the wire  $Q = (\pi/2)^{0.5} (r_w^2/\sigma_x) \exp(-x^2/2\sigma_x^2) (I_0 k dE/dy/e)$ , where  $\sigma_x$  is the beam size,  $x$  is the wire location with respect to the

## Wire Scanner Beam Profile Measurement for ESRF

A. B. El-Sisi, Atomic Energy Authority, NRC, Plasma and Nuclear Fusion Dept.,  
P.O.Box 13759, Cairo, Egypt

### Abstract

The wire scanner is used in beam transfer lines of European Synchrotron Radiation Facility (ESRF) to provide data for beam profiles, which is being used in emittance measurements. The beam energy in the first transfer line is 200 MeV and the peak current is 25 mA. This work will discuss the operation of the wire scanner, and the first results of the scanner in ESRF. We get the emittance value for the vertical plane and the horizontal plane ( $1.5 \times 10^{-6}$  m.rad,  $2 \times 10^{-7}$  mrad) respectively. When we used these values to simulate our result we find that, the simulation gives good fitting with real values.

### 1 INTRODUCTION

Method of beam transverse profile measurement in accelerators by wire scanner is wide spread in accelerator field [1,2,3]. The wire scanner beam profile measurement has been used extensively in the commissioning of many accelerators. It has been utilized to verify the focusing lattice, verify the functionality of the steering magnets, provide data for quad scan style emittance measurements, and helped to verify beam position diagnostics. The basic principle is based on secondary electrons generated by the interaction of the beam and the wire. The wire scanner in ESRF is controlled through TACO control system [4], accelerator control system. TACO is an object oriented control system developed at the European Synchrotron Radiation Facility.

### 2 EXPERIMENTAL FACILITY

ESRF is located at Grenoble – France. ESRF is essentially a complex of three accelerators, the preinjector, the booster synchrotron, and the storage ring. The later being equipped with insertion devices and beam-line front ends. The pre injector is 16-m long linear accelerator, which produce the electrons and accelerates them up to 200 MeV with peak current 25 mA in long pulse mode [5]. The booster is a 10 Hz cycling synchrotron 300 m in circumference, which increases the energy of the electrons up to 6 GeV before injection into the storage ring. Storage ring circumference is 844 m, 64 beam ports are spread around the storage ring to give access to beam lines on insertion device or alternatively on bending magnets. The beam of electrons is circulating at 6 GeV which make it capable for producing X-rays at each passage inside the bending magnets or insertion devices. Wire scanner is a diagnostic tool located in the transfer lines between the three accelerators TL1 and TL2, one for each line. The purpose of the wire scanner is

to provide horizontal and vertical beam profiles in transfer lines. The transverse beam emittance ( $\epsilon$ ) is deduced by the product of beam width ( $r$ ) and beam divergence ( $\dot{r}$ ) where  $\epsilon = (r \dot{r})/\pi$ . The wires are made from tungsten and gold (diameter is 40  $\mu\text{m}$ ) and are attached to an actuator driven by a stepping motor. The principle of providing profiles is based on the amount of secondary electrons generated by the interactions of the beam and the wire and measured in incremental steps. From these measurement steps the beam profile is constructed. This paper will discuss the operation of the scanner (Hardware and Software), testing the scanner during operation, obtain the profiles and finally calculating the emittance of beam in TL1. Figure (1) show a drawing of wire scanner, The basic parts of the hardware are the stepper motor and its controller, and the two ADC cards, one for each plane. The motion of wires must be continuous to avoid the wire vibration. The user of wire scanner has the ability to set the scanning parameters for profile (start position, number of measurements, and end position) using application program interface. Scanning is done under the angle  $45^\circ$  with the beam direction. Therefore, the position value obtained from the scanning is multiplied by  $\cos 45^\circ$ . Each step equals 0.1 mm in case the frequency equals 1 Hz. An external trigger must be adjusting to read the two ADC cards synchronized with the electron beam.

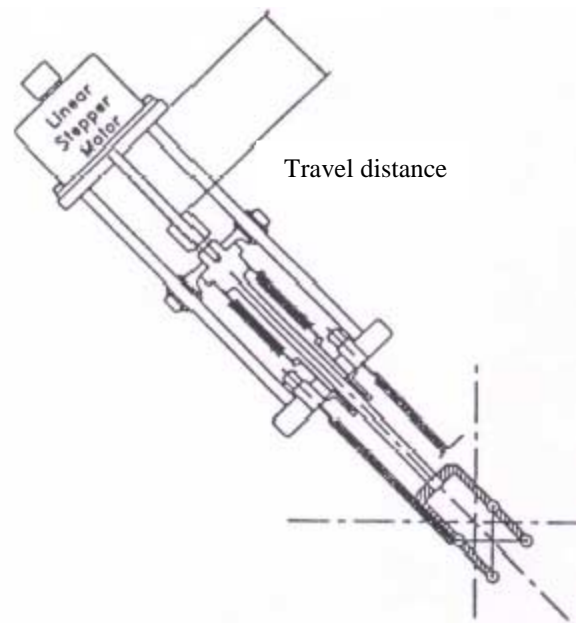


Figure (1) Schematic view of the wire scanner.

# ADVANCED RESIDUAL GAS PROFILE MONITOR FOR HIGH CURRENT SYNCHROTRONS AND COOLER RINGS

P. Forck<sup>1</sup>, T. Giacomini<sup>1</sup>, A. Golubev<sup>2</sup>, D. Liakin<sup>2</sup>, V. Skachkov<sup>2</sup>, A. Vetrov<sup>3</sup>

<sup>1</sup> Gesellschaft für Schwerionenforschung - GSI, Darmstadt

<sup>2</sup> Institute for Theoretical and Experimental Physics - ITEP, Moscow

<sup>3</sup> Moscow State University - MSU, Moscow

## Abstract

The modern ion accelerators and storage rings require faster beam profile measurement with higher resolution. We propose a new residual gas monitor, which will operate on secondary electrons whose trajectories are localized within  $\varnothing$  0.1 mm filaments along uniform magnetic field lines excited by a permanent magnet. To adopt this resolution into the data acquisition system a CCD camera with upstream MCP-phosphor screen is used. To realize a fast turn-by-turn readout a photodiode array of 100-channel with amplifier and digitizer is foreseen.

## DESIGN CRITERIA

Non-destructive profile measurement systems are needed to yield the beam emittance and its evolution during the storage in a synchrotron. An advanced high performance residual gas monitor (RGM) system seen in Fig. 1 is under development. The main features are an applied magnetic field by permanent magnets and a fast turn-by-turn as well as a high-resolution read-out mode. It will be constructed to operate in numerous wide current and energy range synchrotrons as well as low current cold beams in cooling rings.

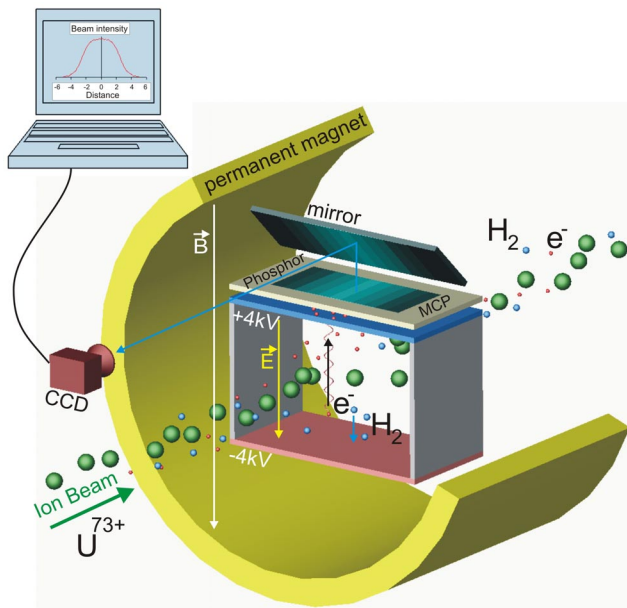


Figure 1: RGM operational principle.

It will serve as a prototype for the various existing and planned ring accelerators at the GSI facility [1].

In RGMs an electrostatic field accelerates the ionization products by the beam and residual gas towards a Micro Channel Plate (MCP). When these particles reach the MCP secondary electrons are produced and accelerated against a phosphor screen, where they produce light spots. These can be observed by a CCD camera or by a photo-diode array.

**True beam profile:** Beside the applied external electric field, the beam space charge field accelerates the ionized particles. To obtain an undistorted beam profile the particles are guided to the MCP surface by an external magnetic field parallel to the external electric field. Only when a magnetic field of about 0.1 T and an electric field of about 0.5 kV/cm are applied, the primary electrons are guided straightforward to the MCP as calculated for Fig. 2. The parameters are typical for a high current operation of the SIS synchrotron at GSI. To achieve 0.1 mm resolution limited by the MCP resolution, the applied magnetic field has to provide a cyclotron radius of the same size respective a field uniformity of 5% from starting point to the MCP. In general the cyclotron radius is given by the initial electron velocity after ionization.

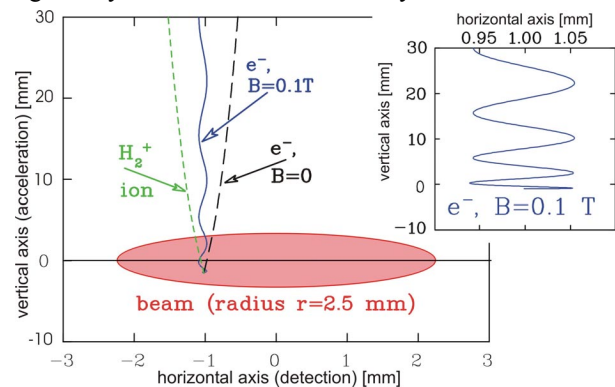


Figure 2: Trajectories of residual gas particles with and without magnetic field ( $10^9$   $U^{73+}$  per 10 m long bunch).

In different synchrotrons and storage rings various operating modes and different demands exist. We intend to provide a high-resolution (HRes) mode and a fast read-out mode (FRout).

**HRes:** For precise beam observations during the acceleration or cooling, a high spatial resolution down to

<sup>1</sup> Corresponding author: T.Giacomini@gsi.de

## RESIDUAL GAS FLUORESCENCE FOR PROFILE MEASUREMENTS AT THE GSI UNILAC

A. Bank, P. Forck, GSI, Darmstadt, Germany, email: p.forck@gsi.de

### Abstract

The high beam currents, delivered at the LINAC at GSI (UNILAC) can destroy intercepting diagnostics within one macro pulse. As an alternative for a non-destructive profile measurement the method for residual-gas-fluorescence is investigated. The fluorescence light emitted by the  $N_2$  molecules of the residual gas at the blue wavelength range can be monitored with a modern CCD camera. The images are transferred via digital bus and after analysis of the images with a modern software the profiles are generated. Due to the short beam pulses the light intensities emitted by the residual gas are low and require a high amplification which is realized with an image intensifier with double MCP, connected with a fiber taper to the CCD-chip. The design and measurements are discussed.

### Residual Gas Fluorescence

The profile of an ion beam can be determined by observing the fluorescence emitted by the residual gas molecules using a CCD camera. This method was previously applied e.g. at cw proton LINAC at Los Alamos [1] and the CERN SPS synchrotron [2]. The GSI UNILAC is a pulsed heavy ion LINAC with macro pulse lengths of several 100  $\mu$ s and is e.g. used to fill the proceeding synchrotron. The beam profile should be monitored within one macro pulse, therefore the use of a long integration time for an improved signal-to-noise ratio is impossible. Because of that short integration time and the pressure of the residual gas (typically:  $10^{-7}$  –  $10^{-8}$  mbar) the emitted light has to be amplified drastically, in this case by using a double MCP image intensifier.

Due to the large energy release in intersecting material (maximum of 1 MW beam power) at high current operation (up to 20 mA beam current) the traditional determination of transverse beam profile by using secondary emission grids (SEM-grids) can not be applied. To prevent melting, the macro pulse length has to be shorted. A non-intersecting residual gas monitor can be installed or the fluorescence of the residual gas can be used to detect the profiles in case of a full pulse length. The latter has the advantage that no mechanical parts have to be installed in the vacuum pipe, leading to a compact and cost-efficient design. In addition the spatial resolution of a SEM-grid is limited by the wire-spacing of about 1 mm. Using the fluorescence method up to 0.1 mm can be achieved. Another advantage is the compact commercial 'data acquisition system' incorporated in the CCD camera.

At GSI UNILAC the ions kinetic energy varies from 0.12 up to 15 MeV/u. Depending on ion type and charge

state this is close to the maximum of the electronic stopping power.

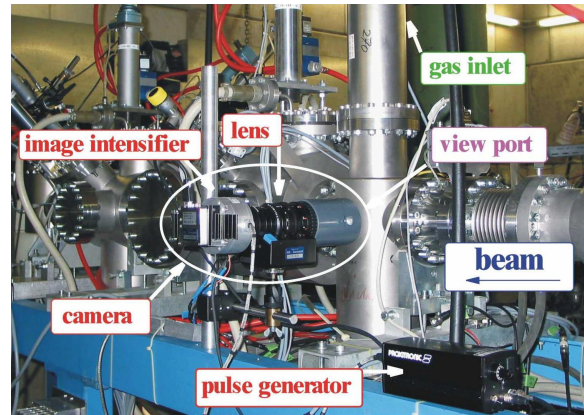


Fig. 1: The installation of the intensified CCD-camera at the target location

The residual gas at the UNILAC contains mainly Nitrogen which has a large cross section for the excitation into the ionized  $N_2^+$  molecular state, as measured in [3] by 200 keV proton collisions and at several GeV in [4]. The fluorescence light is emitted in the wave length range of 300 to 500 nm. A scaling proportional to the electronic stopping power of the beam ions is expected.

### Components

**Vacuum Chamber:** The beam is viewed through a Suprasil window (wavelength transmission between 20 nm and 2  $\mu$ m) mounted on a  $\varnothing$  35 mm flange. To suppress reflections, the tube is blackened by a vacuum suitable graphite lacquer (graphite grains solved in isopropanol).

**Zoom lens:** A remote controlled c-mount zoom lens (Fujinon D14x7.5A-R11/12) with 7.5 – 105 mm focal length and a macro setting is installed. A short distance between the beam and the lens increases the yield of captured photons, but reduces the relative depths of focus. A small focal length increases the depth of focus (i.e. with the same relative iris setting a larger depth can be imaged) but reduces the spatial resolution. A suitable setting was found with a focal length of 15 mm, a distance between lens and center of beampipe of 39 cm resulting in an minimum F-number of 2 (~55 mm depth of focus needed) and an observation length of ~5 cm.

**Image intensifier:** The installed  $\varnothing$ 25 mm image intensifier has a double (chevron) MCP setting with a maximum gain of  $\sim 10^6$ . The captured photons are converted to electrons by a photo-cathode made of S20 UV-enhanced [5], having a quantum efficiency of 25-30

## IONISATION BEAM PROFILE MONITOR AT THE COOLER SYNCHROTRON COSY-JÜLICH

V. Kamerzhiev, J. Dietrich, Forschungszentrum Jülich GmbH, Germany

### Abstract

For beam profile measurements, a residual-gas ionisation beam profile monitor using a position sensitive micro channel plate (MCP) detector was developed and installed at the cooler synchrotron and storage ring COSY.

Since COSY operates with beam intensities up to  $10^{11}$  protons/deuterons and a vacuum of  $10^{-11}$  -  $10^{-9}$  mbar, there is a high risk of detector damage. The aging of the channel plates was investigated by means of scanning electron microscope and energy dispersive x-ray microanalysis. Different implemented detector protection mechanisms are discussed. Profile measurements with electron cooled beams are reported.

### INTRODUCTION

To optimise the performance of an accelerator precise measurements of many beam parameters are required. To determine the actual charge distribution inside the beam and to find the value of beam emittance non destructive beam profile measurements are needed. One of the known techniques [1] relies on the ionisation of residual gas by the beam particles. A device utilising this principle was installed in the COSY ring [2,3].

### DESIGN

Between two electrodes a parallel ion drift field is maintained. Residual gas ions are drifted onto MCP chevron assembly that provides an electron multiplication factor up to  $10^7$  [4]. The secondary charge produced from each ion is collected by a wedge and strip anode (see Fig. 1) [5].

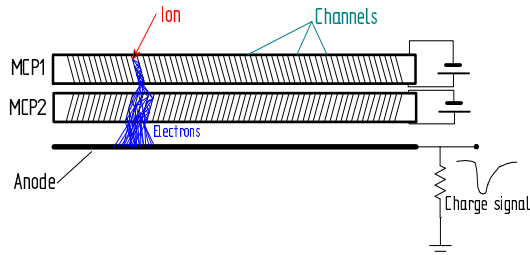


Figure 1: Position sensitive detector.

The charge signals from each electrode are first converted into time signals which are then digitised. A PC running CoboldPC software [6] is used for data readout, analysis and visualisation. The detector and the readout method used allow the measurement of position of separate residual gas ions and are especially suitable for low and medium intensity beams. The images of higher contrast compared to the phosphor screen approach are achievable [6].

### Position sensitive anode

A position sensitive wedge-and-strip anode is placed on a 2 mm thick ceramic substrate of 65 mm outer diameter with germanium layer on the opposite side (see Fig. 2). The anode consists of three electrodes called by their geometry wedge, strip and meander.

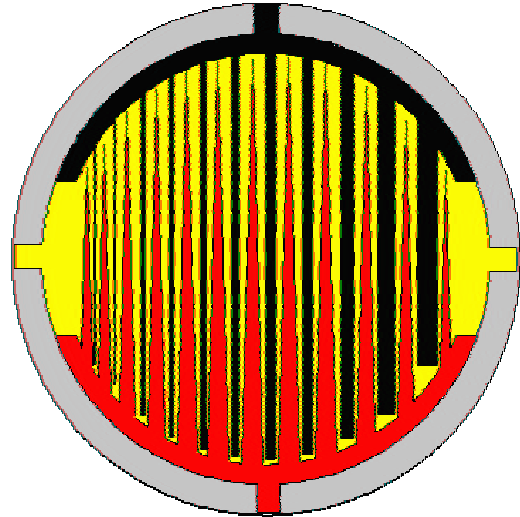


Figure 2: Wedge-and-Strip Anode.

Since this is a charge coupled device, secondary electrons leaving the MCP assembly hit the germanium layer and induce a signal on the anode structure (see Fig. 1) [7]. The charge of secondary electron cloud is distributed over all electrodes. To determine the position of cloud's centre of mass i.e. the residual gas ion coordinates one should measure the charge on each electrode independently and compute  $x$  and  $y$  values using the formulae:

$$x = \frac{Q_s}{Q_s + Q_w + Q_m};$$

$$y = \frac{Q_w}{Q_s + Q_w + Q_m}$$

where  $Q_s$ ,  $Q_w$  and  $Q_m$  are measured charges on strip, wedge and meander respectively. As one can see in Fig. 2 the equations are derived just from the geometry of the anode structure.

### Electronics

The charge-to-time converter is based on the LeCroy's MQT 300AL chip [3,8] which utilises a Wilkinson dual slope converter. The time signals are transported to control room where a time-to-digital converter (TDC)

## RECENT DEVELOPMENTS OF THE EXCYT RADIOACTIVE BEAM DIAGNOSTICS

L.Cosentino, P.Finocchiaro

INFN-LNS, via S.Sofia 44, 95125 Catania, Italy

### Abstract

The EXCYT radioactive beam facility at LNS, based on the ISOL technique, will start producing its first radioactive beams during 2004. We have set up a suitable high sensitivity diagnostics, in order to guarantee a real time monitoring of the beam parameters (transversal profiles, ion composition and current), also for very low intensity values (well below  $10^5$  particles per second). By making use of a simple technique based on a thin CsI(Tl), we can also efficiently image beams of very low kinetic energy (50 keV).

### 1 INTRODUCTION

At INFN-LNS Catania the EXotics with CYclotron and Tandem (EXCYT) facility, based on the Isotope Separator On-Line (ISOL) technique, is going to start the production of radioactive ion beams. The beam energy will range from 0.2 MeV up to 8 MeV/A, its emittance is expected below  $1\pi$  mm·mrad, with an energy spread of  $10^{-4}$  [1]. The ISOL technique consists of stopping a stable primary beam, in our case  $A < 48$   $E < 80$  MeV/A produced by a superconducting cyclotron, inside a thick target. There nuclear reactions give rise to a wide variety of radioactive species, which are extracted and transported to a high resolution magnetic isobaric separator, in order to pick out the ions of interest. The EXCYT isobaric separator consists of two main stages, each one composed of two magnetic dipoles. The first stage is placed on a 250 kV platform, while the second is grounded. The beam is finally accelerated by means of a Tandem accelerator ( $V \leq 15$  MV). The typical particle rate will fall in the range between  $10^3$  and  $10^8$  pps, depending on the intensity of the primary beam ( $< 1$  pA), on the production cross section in the target and on the overall efficiency from the ion source to the experimental area.

The beam diagnostics is an important issue of the facility, since it allows to check on-line the beam properties along the transport line, in order to perform the tuning operations. To this purpose we have developed suitable easy-to-use devices, capable of fulfilling the requirements of sensitivity and reliability [2, 3].

LEBI (Low Energy Beam Imager / Identifier) is a compact device used for stable and radioactive low energy beams (50 – 300 KeV), capable of beam imaging, particle rate measurement and identification of nuclei.

GFIBBS is a scintillating-fibre based system, operating with both stable and unstable beams, which can reconstruct with remarkable sensitivity the transverse X and Y profiles after the final acceleration. The identification of the accelerated nuclear species is performed by means of a high resolution silicon telescope.

### 2 PREACCELERATION, BEAM IMAGING AND IDENTIFICATION

#### 2.1 The LEBI device

LEBI exploits the radioactivity of the beam particles, which are implanted onto a thin Mylar tape placed in contact with a CsI(Tl) plate [4]. The emitted radiation (mainly  $\beta$  and  $\gamma$  rays) crosses the plate, thus producing a light spot representing the transverse profile of the beam, that is watched by a high sensitivity CCD camera ( $\sim 10^{-4}$  lux). LEBI can also be employed with stable beams, in order to set up the transport elements along the beam line (quadrupoles, magnetic dipoles of the isobaric separator, etc). In this latter case LEBI is positioned a little bit lower, in order to allow the beam to hit directly the scintillating plate (Fig. 1).

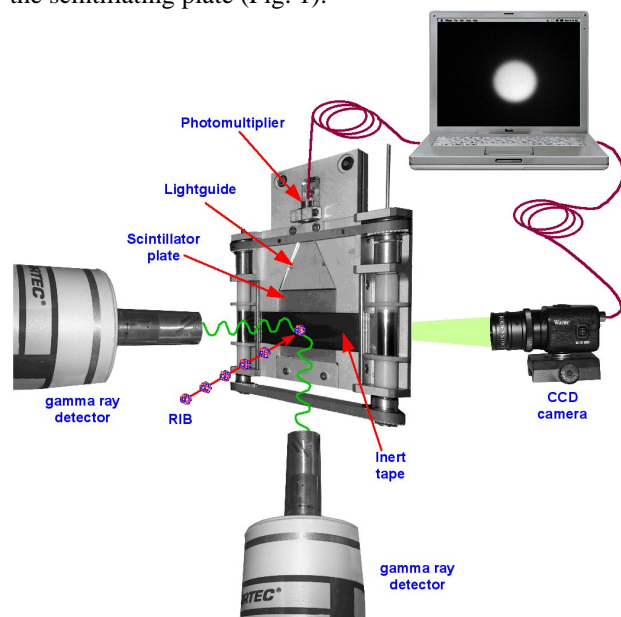


Figure 1: Sketch of the LEBI device for low energy beam imaging and identification.

## NETWORK ATTACHED DEVICES AT SNS\*

W. Blokland and T. Shea, ORNL, Oak Ridge, TN, USA  
 M. Stettler, LANL, Los Alamos, NM, USA

### Abstract

The Spallation Neutron Source (SNS) diagnostic instruments at Oak Ridge National Laboratory are based on the Network Attached Device (NAD) concept. Each pickup or sensor has its own resources, such as networking, timing, data acquisition, and processing. NADs function independently thus reducing the brittleness inherent in tightly coupled systems.

This paper describes our implementation of the nearly 400 NADs to be deployed. The hardware consists of rack-mounted PCs with standard motherboards and PCI data-acquisition boards. The software suite is based on LabVIEW and EPICS, communicating through a shared memory interface. LabVIEW supports the agile development demanded by modern diagnostic systems. EPICS is the control system standard for the entire SNS facility. Program templates and documentation tools are available to the programmer. SNS diagnostics are developed by a multi-laboratory partnership, including ORNL, BNL, LANL, and LBNL. The NAD concept proved successful during the commissioning of the SNS front-end both at LBNL and ORNL.

### INTRODUCTION

The basic idea behind a Network Attached Device is to implement an instrument as a single networked device with its own resources [1].

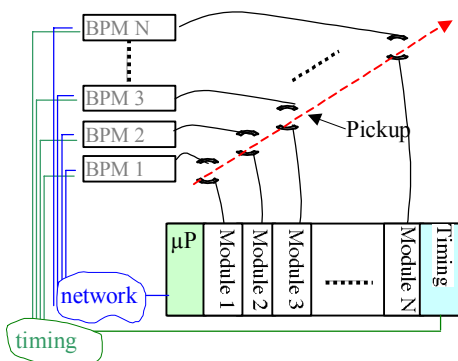


Figure 1. The NAD versus VME configuration.

For example, a typical VME implementation of a Beam Position Monitor (BPM) handles many pickups per crate, while the NAD implementation assigns each pickup its

own resources such as a processor, a timing decoder, and a network interface, to make one independent device, see Figure 1. To create a set of BPMs, the NAD implementation makes copies of a single device. This leads to simpler software and reduces failure interaction. The VME implementation has to deal with managing shared resources among the multiple BPMs. If a system is expanded, a separate integration test is needed to check the interaction of the larger set of modules with each other and the shared resources. The NAD devices don't interact and no new testing is needed when adding NADs. A failure or required maintenance in one component of a VME implementation would most likely bring down all BPMs within the crate. In the NAD implementation each device is independent and any failure in or maintenance to a component would only affect that one device, thus limiting the scope of the outage. In most cases that means that the accelerator can continue to operate.

### IMPLEMENTATION

The NAD can be implemented in many ways. In its ultimate form it would likely resemble a system-on-a-chip with a sensor. However, to make use of the wide variety of development and management software and low cost computer and data-acquisition hardware, we have chosen to base the NAD on a PC-based system. The PC-based systems consist of standard motherboards, rack-mounted for easy installation in the field, see Figure 2.



Figure 2. A rack mount PC.

LabVIEW is chosen as the main software development environment operating under Windows 2000 or XP. LabVIEW has a very well integrated visual development environment for data-acquisition and signal processing. Many vendors supply LabVIEW drivers with their hardware. Combined with the SNS software suite, described below, the SNS collaboration can efficiently implement the NADs.

\* The Spallation Neutron Source (SNS) project is a partnership of six U.S. Department of Energy Laboratories: Argonne National Laboratory, Brookhaven National Laboratory, Thomas Jefferson National Accelerator Facility, Los Alamos National Laboratory, Lawrence Berkeley National Laboratory, and Oak Ridge National Laboratory. SNS is managed by UT-Battelle, LLC, under contract DE-AC05-00OR22725 for the U.S. Department of Energy.

## PARASITIC BUNCH MEASUREMENT IN $e^+/e^-$ STORAGE RINGS

H. Franz (HASYLAB\*), M. Seebach (MDI<sup>#</sup>), A. Ehnes (HASYLAB), M. Werner (MDI)  
 Deutsches Elektronen-Synchrotron DESY, Hamburg, Germany  
 e-mail: [hermann.franz@desy.de](mailto:hermann.franz@desy.de) [michael.seebach@desy.de](mailto:michael.seebach@desy.de)

### ABSTRACT

The lepton storage rings DORIS and PETRA at DESY are used as sources for synchrotron radiation experiments. In normal operation the distance between bunches should be 96 ns in PETRA and in DORIS. The adjacent buckets must not have any stored particles or, in reality, as few as possible. This is particularly important for time-triggered photon measuring experiments. The principle of the 'parasitic bunch' measurement down to a fraction of  $10^{-6}$  of the main bunch within 20 seconds is described. Additionally, the sources of the 'parasitic bunches' and the actions to minimize them are discussed.

### INTRODUCTION

Fast time resolved X-ray measurements make use of the inherent time structure of a storage ring (SR). Depending on the size of the ring and the filling pattern (the distance between bunches) the active time window may be in the range of few ns to few  $\mu$ s. This allows studying kinetics in pump-probe experiments or dynamics using resonant scattering processes [1]. In particular the latter is very sensitive to spurious charge in the machine, which is usually accumulated in buckets adjacent to the intentionally filled bunch. For this reason most SRs used to produce synchrotron radiation have installed a system to detect the time structure of the machine with high sensitivity [2, 3]. In the following we describe a system, which has been installed at PETRA allowing us to detect spurious charge already during the injection process.

### SOURCES OF PARASITIC BUNCHES - THE IDEAL MACHINE

All lepton SRs at DESY (DORIS, PETRA and HERA) have a 500 MHz RF-system, i.e. buckets are separated by 2 ns. All storage rings and the pre-accelerators are synchronized via a common bunch-marker system. However, not all buckets are filled with  $e^+/e^-$ . The normal bunch distance in PETRA is an integer multiple of 48 buckets (96ns). This means a maximum of 80 bunches may be injected. However, also other patterns are possible. The situation at DORIS is similar. In an ideal storage-ring only the addressed buckets contain  $e^+/e^-$ . All other buckets must not have any stored particles. In any real machine some particles are stored in other buckets, in particular in the adjacent buckets, the so-called 'parasitic bunches'.

### THE 'PARASITIC BUNCH' SITUATION

In principle any SR with non-uniform filling patterns should have parasitic bunches. This is due to the fact that in the initial stages of the pre-accelerator system

bunches are rather elongated. In particular at DESY the situation is as follows [4, 5]:

Right after the electron gun and a focusing lens the 'ante-linac-chopper' (a vertical electrostatic kicker combined with an upstream collimator) leads to a first bunching of the beam. This results in 10 to 60 ns long pulses at a repetition rate of 20 ms (50 Hz). In order to use the linac (running at 3 GHz) most efficiently those pulses are too long. Thus after further lenses and collimators the 3 GHz-prebuncher (a cavity with 20 kV gap-amplitude and a power of 1.5 kW) concentrates most particles in 50 ps long bunches. After being accelerated to 450 MeV in 12 linac modules particles are accumulated in PIA, a 28.9 m ring running at constant beam energy with a 10.4 MHz HF-system. In PIA several shots from the electron gun are accumulated in one bunch, which may then be several ns long. To reduce the bunch length further the accumulated beam is shortened in the last 40 ms before ejection to DESY-2 by a 125 MHz-system. This treatment reduces the bunch length to a rms value below 0.2 ns at a bunch distance of 8 ns. On the way to DESY-2 the beam extracted from PIA is again filtered by a 'post-linac-chopper' to suppress 8 ns-parasitic bunches. However, during the transfer from the 125 MHz-system at PIA to the 500 MHz-system DESY-2 2 ns parasitic bunches are created by any non-ideal behaviour in the transfer. This may be for example a deviation from the optimum setting of the DESY-2 injection energy due to jitter in the magnet currents or a wrong setting of the DESY-2 injection phase. The latter must be optimized for minimal longitudinal oscillations during injection. The same holds for the transfer from DESY-2 to PETRA and DORIS, respectively.

Further on we have learnt from first measurements that high PIA current causes post-bunches up to 6 ns. The reason for this behaviour is not clear yet, but it could be a longitudinal instability at high bunch charge.

### THE PRINCIPLE OF THE 'PARASITIC BUNCH' MEASUREMENT

The parasitic bunch measurement is achieved by an avalanche-photo diode (APD) (EG&G, C30703F) [6] detecting scattered X-rays from a 1 mm thick graphite foil. It is located in the PETRA undulator beamline 31.3 m downstream of the dipole separating the lepton from the undulator beam. This dipole is used as source for the parasitic bunch measurements. The detector signals are amplified close to the diode by a fast three-stage amplifier. The overall time resolution is approximately 0.8 ns. The amplified signal is analyzed using a time-to-digital-converter (TDC) and a multi-channel-analyzer (MCA). To reduce the influence of the so-called "walk" and to reduce the background due

# DIAGNOSTICS OF THE PROSCAN PROTON-THERAPY BEAM LINES

R. Dölling, PSI, Villigen, Switzerland

## Abstract

PROSCAN, an extended medical facility using proton beams for the treatment of deep seated tumours and eye melanoma, is in preparation at PSI [1]. An overview is given on the beam line diagnostics now under development, with emphasis on beam profile measurement.

## INTRODUCTION

In the PROSCAN facility (Fig. 1) a 250 MeV proton beam of 1 to 500 nA will be extracted from the COMET cyclotron. After degradation to the range of 230 to 70 MeV it can be delivered (at a maximum current of 10 nA) into one of four areas: Two gantries, an eye treatment room and a material irradiation area. Fast changes of beam energy are foreseen for the spot-scanning treatment of deep-seated tumours in the new gantry 2. Several diagnostics will be used to control the beam parameters in different modes of operation. At present most of the components are under development and prototypes will be tested in the next half year.

the vertical and horizontal beam profiles (Fig. 2). The pitch of the metallized strips varies from 0.5 to 1 and 2 mm (plus one broader strip at each side). 2x 68 strips are fed to the outside by flexible-printed-circuit cables.

With two exchangeable printed circuit boards placed in an electrically shielded box at the top of the profile-monitor feed-through the signals are routed to the 2x 16 channels of the electronics. With this arrangement, a strip pitch of 0.5, 1, 1.5, 2, 3 or 4 mm can be chosen for a "1 broader + 14 regular + 1 broader"-strip arrangement in each plane. This variability allows for the adaptation of the strip pitch to the expected range of beam profile width. This is required due to the limited number of only 16 channels per plane that is foreseen for most of the monitors. Simulations [3] indicate that for 16 channels beam position and width can be measured accurately if the FWHM beam width is in the range 1x to 10x strip pitch and the profile is of conventional shape. A pattern with varying strip pitch can also be chosen to further enlarge the range of possible beam profile width of a fixed configuration.

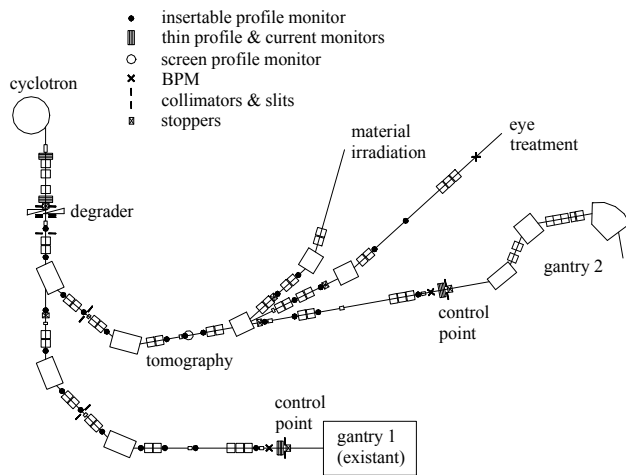


Figure 1: Overview of beam lines.

## INSERTABLE PROFILE MONITORS

Insertable monitors, successively introduced into the beam, yield the input information for the calculation of a beam envelope with the "Transport" code [2]. Each single monitor allows the measurement of the temporal development of a beam profile. Since these monitors are not thin, only a measurement at one location at a time is possible.

Multi-strip ionisation chambers (MSIC) are used to obtain enough signal from the small beam current (0.1 to 40 nA). All ionisation chambers are filled with ambient air. Metallized ceramic 0.63 mm thick boards separated by 4 mm wide air gaps provide the strip pattern and high-voltage electrodes in order to measure (the projections of)

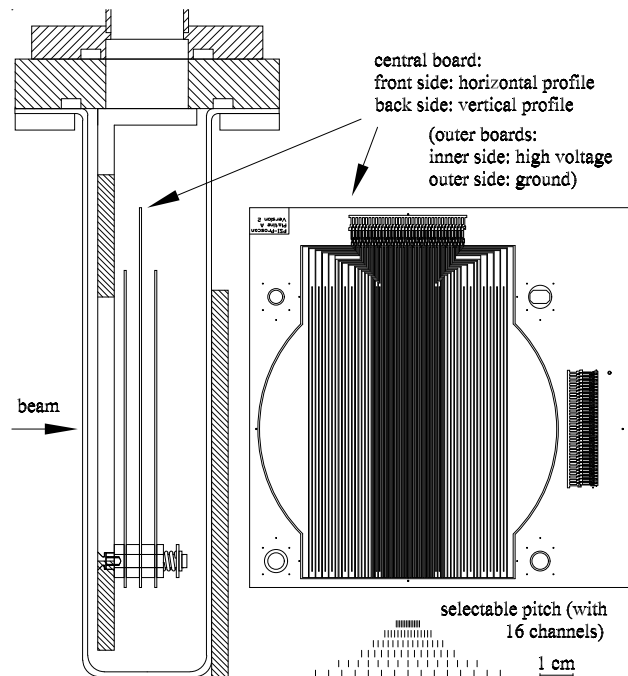


Figure 2: Insertable profile monitor.

At three successive locations, a higher resolution is foreseen for beam tomography. A "1 broader + 30 regular + 1 broader"-strip arrangement in each plane will be realised by doubling the number of cables and electronic modules. At these locations, the available strip pitch is 0.5, 1 or 2 mm. For the tomography measurements also an additional insertable screen monitor is also foreseen. It

## A SYSTEM FOR BEAM DIAGNOSTICS IN THE EXTERNAL BEAM TRANSPORTATION LINES OF THE DC-72 CYCLOTRON

G.G. Gulbekian, B.N. Gikal, I.V. Kalagin, V.I. Kazacha, FLNR JINR, Dubna, Russia  
A. Gall, DNPT FEI STU, Bratislava, Slovakia, e-mail: gall@nrsun.jinr.ru

### Abstract

The isochronous four-sector Cyclotron DC-72 will be the basic facility of the Cyclotron Center of the Slovak Republic in Bratislava. It will be used for accelerating ion beams with mass-to-charge ratio  $A/Z$  from 1 ( $H^+$ ) to 7.2 ( $^{129}Xe^{18+}$ ) with energy from 2.7 MeV/amu ( $A/Z=7.2$ ) to 72 MeV ( $A/Z=1$ ).

In the paper a system for external beam diagnostics is presented. It is intended for on-line data acquisition of the accelerated beam main parameters (current, position, profile, emittance and energy of the ion beams). The system allows one to provide effective tuning the acceleration regime as well as adjusting the ion beam transport lines with the ion optical systems to effective transportation the ions from the cyclotron exit to physical targets and set-ups.

### INTRODUCTION

Cyclotron DC-72 represents an isochronous four-sector cyclotron. The ion beam extraction from the cyclotron will be made by means of electron stripping on a graphite foil. The ions will be extracted in two directions: A and B. Main parameters of the DC-72 cyclotron are given in Table 1, and the design parameters of ion beams are given in Table 2.

Table 1: Main parameters of the DC-72 cyclotron [1]

Pole diameter	2.6 m
Extraction radius	1.118 m
$B_{\text{average}}$ at extraction radius	1.12 – 1.51 T
Number of sectors	4
Sector angle	45°
Number of Dees	2
Dee angle	42°
Frequency range	18.5÷32 MHz
Harmonic numbers	2, 3, 4, 5, 6
Ion source for $H^+$ , $D^+$ , $^2H^{1+}$	Multicusp
Ion source for heavy ions	ECR
Extraction	stripping foil
Emittance on the target	$< 20 \pi$ mm-mrad

The main areas of using DC-72 cyclotron ion beams will be the following [1]:

- Nuclear medicine and oncology;
- Production of radioisotopes for oncology ( $^{123}I$ ,  $^{81}Rb$ / $^{81m}Kr$ ,  $^{67}Ga$ ,  $^{111}In$ ,  $^{201}Tl$ );
- Production of very short living radioisotopes for positron emission tomography ( $^{11}C$ ,  $^{13}N$ ,  $^{15}O$ ,  $^{18}F$ );
- Proton therapy of eye;

- Fast neutron therapy (FNT) and boron neutron capture therapy (BNCT);
- Metrology of ionizing radiation;
- Fundamental research;
- Applied research and development programs, surface treatment of metallic and other materials;
- Nuclear physics and techniques;
- Nuclear structure and reaction kinematics studies;
- Educational programs for students of nuclear physics and related fields.

Table 2: The design parameters of DC-72 ion beams [1]

Ch.	Technology and set-ups	Ion beam	Energy [MeV/u]	Intensity [ $\mu A$ ]
1	$^{123}I$ production	p	30	50
2	$^{87}Rb$ production	p	30	30
3	$^{67}Ga$ , $^{201}Tl$ , $^{111}In$ prod.	p	30	100
4	Proton therapy	p	72	0.05
5	Fast neutron therapy	p	66–72	30–35
6	Applied research	Li–Xe	2.8–2.7	5–1
7	Mass-spectrometry	C–Kr	8.6–2.8	20–2
8	Physical research	Li–Xe	2.8–2.7	5–1

### EXTERNAL BEAMS DIAGNOSTICS

#### Beam intensity measurement

The ion beam intensities at the cyclotron extraction region and in the beam transportation lines are the main parameters. The beam current measurements will be realized by special Faraday Cups (FC) (20 pieces). The sketch of FC is shown in Fig.1. At the FC design, we paid special attention to problem of FC cup radioactive activation and choice of the appropriate material. Also, we spent some time to calculate the 3D temperature distribution in the cup. From the point of view of minimal activation, the cup of FC will be made of aluminum. To satisfy the temperature condition the cup has a water-cooling system [2]. The accelerated particles are absorbed in the cup and the integrated electrical charge creates an electrical current that is measured by a current-to-voltage converter (LOG104) and than converted to a digital signal by the A/D converter (MCP3201). After all, the current value will be shown at the console in the cyclotron control room.

To eliminate the influence of secondary electrons emission on the current measurement accuracy we use a transversal magnetic field created by CoSm permanent magnets that surround the cup. The calculation results of the magnetic field distribution are presented in [2].

## MULTIFUNCTION TEST-BENCH FOR HEAVY ION SOURCES

S.Barabin, V.Batalin, A.Kozlov, T.Kulevoy, R.Kuybida, D.Liakin<sup>#</sup>, A.Orlov, V.Pershin, S.Petrenko, D.Seleznirov, Yu.Stasevich.

Institute for Theoretical and Experimental Physics, Moscow, Russia

### Abstract

The new test-bench for heavy ion sources has been created in ITEP. It is planned to equip test-bench with a set of measurement devices to cover wide range of beam widths, divergences, durations, currents etc. It will provide measurements of different heavy ion beams parameters, particularly, emittance and charge state distribution. The last parameter may be measured both by the time-of-flight method and with the magnet analyzer. Two emittance measurement devices will be installed. It will be possible to use both slit/grid and CCD based “pepperpot” methods, which will give advantages of combination of classical emittance measurements with performance of the CCD based devices. The detailed description of test-bench and its equipment is presented. The first results at MEVVA ion source and beam investigations are discussed.

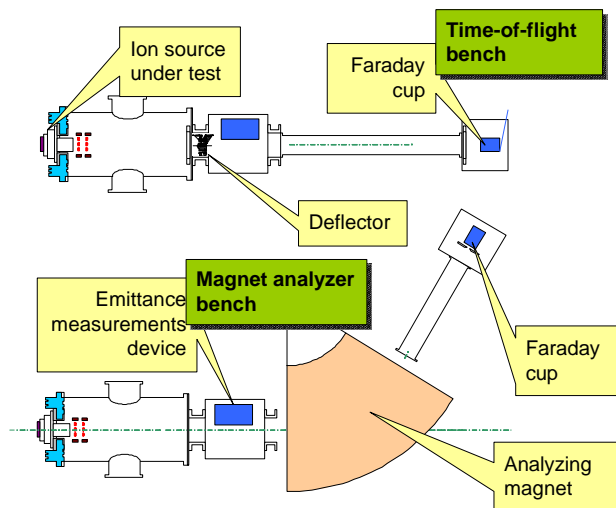


Fig. 1. Structure of the test-bench.

### TEST-BENCH STRUCTURE

The structure of heavy ion sources test-bench is shown on fig. 1. Two independent vacuum tanks are available for time-of-flight and magnet analyzer ion beam spectrum measurements. A 100 mA 20-80 kV high voltage source is shared between those chambers.

### TOF ANALYZER

Time-of-flight (TOF) method allows measuring the charge state distribution (CSD) evolution during the ion beam pulse that can be used for investigation of process into ion source plasma [ 1].

The ITEP test-bench for TOF measurements includes: cylindrical deflector, drift channel and current detector

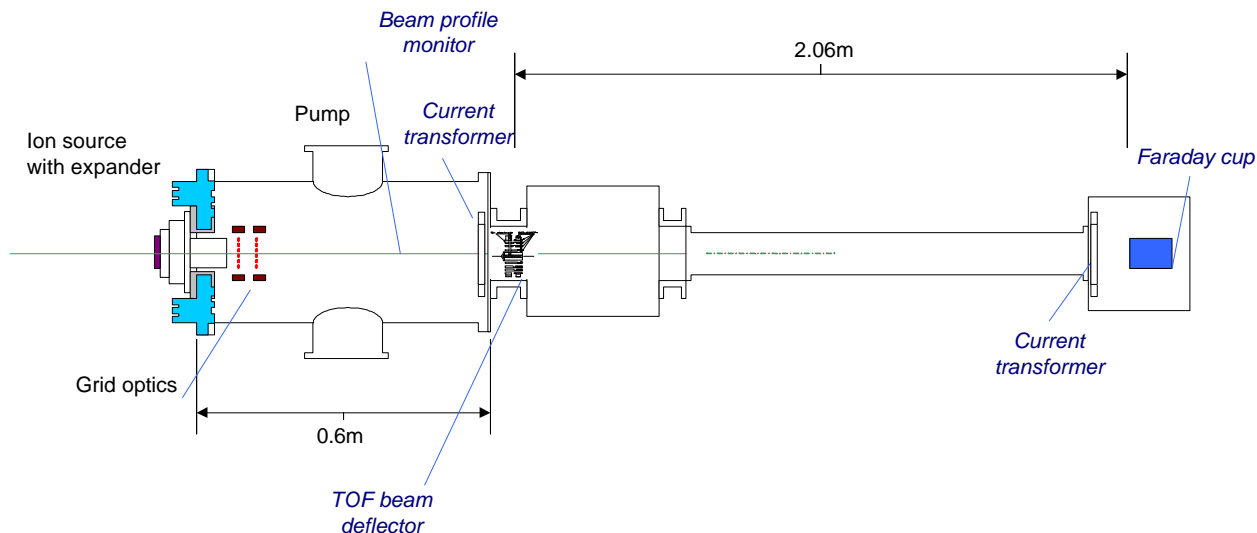


Fig. 2 Layout of TOF test-bench.

<sup>#</sup>Liakin@vitep1.itep.ru

## APPLICATION OF BEAM DIAGNOSTICS FOR INTENSE HEAVY ION BEAMS AT THE GSI UNILAC

W. Barth, L. Dahl, J. Glatz, L. Groening, S. Richter, S. Yaramishev  
 Gesellschaft für Schwerionenforschung, D-64291 Darmstadt, Germany

### Abstract

With the new High Current Injector (HSI) of the GSI UNILAC the beam pulse intensity had been increased by approximately two orders of magnitudes. The HSI was mounted and commissioned in 1999; since this time the UNILAC serves as an injector for high uranium intensities for the synchrotron SIS. Considering the high beam power of up to 1250 kW and the short stopping range for the UNILAC beam energies ( $< 12$  MeV/u), accelerator components could be destroyed, even during a single beam pulse. All diagnostic elements had to be replaced preferably by non-destructive devices. Beam transformers instead of Faraday cups mainly measure the beam current, beam positions are measured with segmented capacitive pick-ups and residual gas monitors instead of profile harps. The 24 installed phase probes are also used to measure widths and phase of the bunches, as well as beam energies by evaluating pick-ups at different positions. The residual gas ionisation monitors allow for on-line measurements of beam profiles. The knowledge of the real phase space distribution at certain position along the linac is necessary for optimising the machine tuning, for the improvement of the matching to the synchrotron, and for a better understanding of beam dynamic issues under space charge conditions. The paper reports the application of different beam diagnostic devices for the measurement of transverse beam emittances at different UNILAC beam energies and at different beam intensities. Additionally, measurements of the bunch structure after the HSI and the design of a new device for the measurement of the longitudinal emittance at the end of the UNILAC are included.

### INTRODUCTION

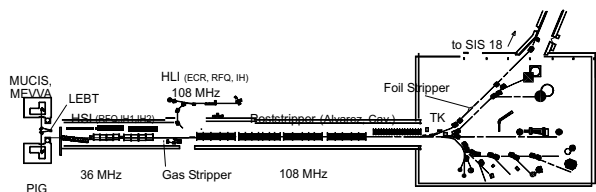


Fig. 1: Schematic overview of the GSI UNILAC.

The GSI-UNILAC is specified to deliver up to  $4 \cdot 10^{10}$   $U^{73+}$  particles to the heavy ion synchrotron (SIS) during 100  $\mu$ s, whereby the HSI accelerates 15 emA  $^{238}U^{4+}$ . The required beam parameters (for the uranium case) are summarized in Table 1. In 1999 the UNILAC (see Figure 1) underwent a renewal of its prestripper section to increase the ion beam current to  $I = 0.25$  A/q (emA) for mass over charge ratios of up to 65. The high

Table 1: Specified beam parameters along the UNILAC.

	HSI entrance	HSI exit	Alvarez entrance	SIS injection
Ion species	$^{238}U^{4+}$	$^{238}U^{4+}$	$^{238}U^{28+}$	$^{238}U^{73+}$
El. Current [mA]	16.5	15	12.5	4.6
Part. per 100 $\mu$ s pulse	$2.6 \cdot 10^{12}$	$2.3 \cdot 10^{12}$	$2.8 \cdot 10^{11}$	$4.2 \cdot 10^{10}$
Energy [MeV/u]	0.0022	1.4	1.4	11.4
$\Delta W/W$	-	$4 \cdot 10^{-3}$	$\pm 1 \cdot 10^{-2}$	$\pm 2 \cdot 10^{-3}$
$\epsilon_{n,x}$ [mm mrad]	0.3	0.5	0.75	0.8
$\epsilon_{n,y}$ [mm mrad]	0.3	0.5	0.75	2.5

current injector HSI consists of ion sources of MEVVA-, MUCIS- or Penning-type, a mass spectrometer, and a low energy beam transport system (LEBT). The 36 MHz RFQ accelerates the ion beam from 2.2 keV/u to 120 keV/u. The matching to the following IH-DTL is done with a short 11 cell adapter RFQ (Super Lens). The IH-DTL consists of two separate tanks accelerating the beam to the full HSI-energy of 1.4 MeV/u [1]. Before injection into the Alvarez accelerator the HSI-beam is stripped (gas stripper) - charge analysis is indispensable. A five stage accelerator provides seven discrete beam energies in the range of 3.6 to 11.4 MeV/u, the following 10 single gap resonators allow any energy up to 13 MeV/u. In the transfer line to the synchrotron at 11.4 MeV/u a foil stripper and another charge state separator system is in use.

### OPERATING BEAM DIAGNOSTICS

Table 2: Number of beam diagnosis devices in the UNILAC.

Element	Number	Resolution
Faraday Cups	73	100 nA (high power capable)
Current Transformers	45	100 nA (100 kHz)
Profile Grids	103	$\geq 1$ mm
Capacitive Pickups (to determine positions)	34	$\Delta W/W = 0.1\%$
Emittance Meas. Device	8	variable
Bunch Shape Monitors	2	25 ps (0.3°)

The wide spread of beam intensities – from pA up to mA demands for a very versatile set of different beam diagnostics elements. To measure the different beam properties such as position, profile, intensity, energy, transverse emittance and, bunch shape various beam diagnostic elements (listed in Table 2) are employed.

The Faraday cups serve primarily as beam stoppers, and secondarily as diagnostics devices. Current transformers and profile grids are used for beam set-up and tuning. The capacitive pick-ups measure the beam energy by a time-of-flight technique; the sampled signal of up to two pick-ups can be displayed on a video screen.

# A MODULAR VME DATA ACQUISITION SYSTEM FOR COUNTER APPLICATIONS AT THE GSI SYNCHROTRON

D. A. Liakin\*, T. Hoffmann, P. Forck  
 Ges. f. Schwerionenforschung, 64291 Darmstadt, Germany  
 \*ITEP, Moscow  
 e-mail: D.Liakin@gsi.de

## Abstract

Particle counters perform the control of beam loss and slowly extracted currents at the heavy ion synchrotron (SIS) at GSI. A new VME/Lynx – PC/Linux based data acquisition system has been developed to combine the operating purposes beam loss measurement, spill analysis, spill structure measurement and matrix switching functionality in one single assembly. A detailed PC-side software description is presented in this paper. The software has been divided into time critical networking and data deploying threads and low or normal priority interface tasks to achieve best system stability. Some new abilities in the fields of data computation and presentation are described. First experiences gained while the commissioning of the system are discussed.

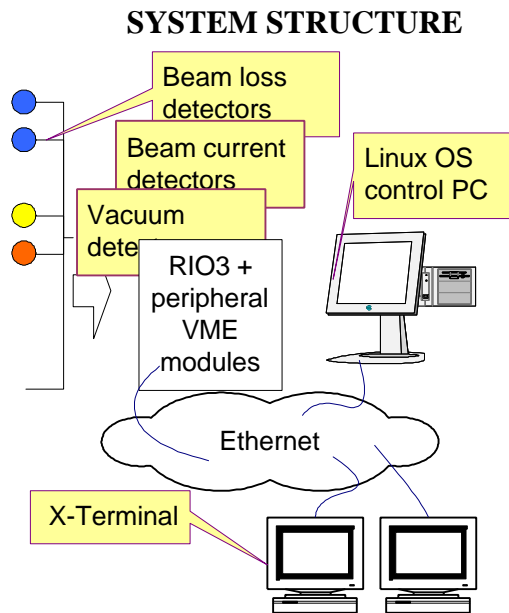


Fig. 1 Scheme of the system structure.

The structure of the new system is shown in Fig. 1. The VME data acquisition modules are controlled by a CES RIO3 processor with an installed Lynx as a real time operating system. The set of acquired data is transferred via 100MBit Ethernet connection to the control PC for being processed by different applications. Detailed description of the used hardware and LynxOS software can be found in [1].

## PRINCIPLE OF OPERATION AND DATA STRUCTURE.

All detectors which are used in this system are operating in a pulse counting mode. Even if some detectors initially deal with continuous signals like currents and voltages, finally current-to-frequency or voltage-to-frequency converters are used. A high dynamic range and linearity are advantages of using modern VME counters[2] compared to other methods of data acquisition. At the same time, high timing resolution can be obtained with matched signals, therefore a fine time structure of investigated processes is also available.

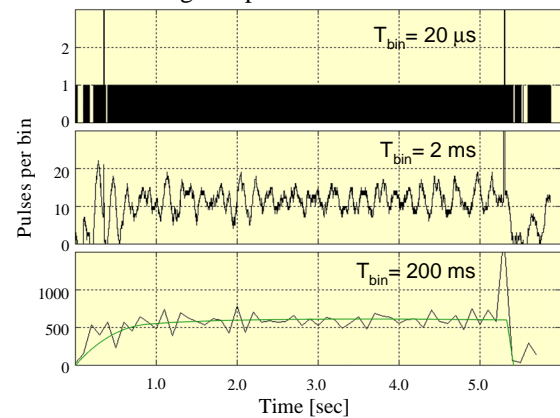


Fig. 2. The beam current in amount of pulses is shown as a function of time. The time unit is 20 $\mu s$  at the top, 2ms in the middle and 200ms at the bottom.

The sampling frequency may be changed according to the aims of different applications. As an example the beam current transformer signal is shown in Fig. 2. At the top one can see the full bandwidth case. In this situation the sampling frequency of 50 kHz is higher than the incoming pulse rate and only one pulse may be acquired within this 20 $\mu s$  interval. At the bottom the low bandwidth case is shown. Low bandwidth is acceptable for the most applications except those where special analysis is required. Spectral parameter of the Fig. 2 top signal are shown in Fig.3. A Fourier spectrum and a spectrogram[3] were prepared to investigate the fine structure of this signal. The Fourier spectrum shows a presence of a number of harmonics of a 1kHz internally generated frequency. In contrast to a simple spectrum the spectrogram illustrates the possibility to detect a more complex non-periodic system behaviour. A current-to-frequency converter is used to convert measured current

## BEAM POSITION AND PHASE MEASUREMENTS USING A FPGA FOR THE PROCESSING OF THE PICK-UPS SIGNALS

G. Naylor, E. Plouviez, G. F. Penacoba  
European Synchrotron Radiation Facility (ESRF), Grenoble, France

### Abstract

We have implemented the signal processing needed to derive the transverse beam position and the beam phase from the signals of a four electrode BPM block on a FPGA (field programmable gate array). The high processing rate of a FPGA allows taking the full benefit of the high data acquisition rate of the more recent ADC. In addition, it is possible to implement on a FPGA a processing algorithm exactly tailored to the measurement of the beam parameters. The efficiency of the signal processing has also been improved by a careful choice of the frequencies of the sampling clock and of the RF front-end local oscillator, which are derived from the storage ring RF frequency. This paper describes the BPM, the RF front-end electronics and the FPGA algorithm. It presents some of the applications of this BPM at the ESRF and gives measurement results.

### INTRODUCTION

ADC with resolution and sampling rate adequate for the acquisition of storage ring beam signals have been available for several years. The sampling rate of these ADCs is in the 20MSPS to 100MSPS. Such a high data rate cannot be efficiently processed by a regular DSP. A solution to this problem is to pre process the data in order to decimate the data flow using a specialized circuit called a Digital Down Converter (DDC)[1]. This solution gives good results but does not take full advantage of the periodicity of a beam signal. Therefore, a FPGA was used with a processing algorithm tailored to the time structure of our SR beam. The main features of this processing are:

- Synchronous I/Q demodulation

- Computation of the amplitude and phase modulation

The useful frequency range of the BPM pick-up signals usually starts well above the maximum frequency that an ADC can handle. In our case we selected a 10 MHz bandwidth around 352.2 MHz in the pick-up signals, and the maximum input frequency of the ADC that we use (AD9225) is only 100 MHz. So a RF front-end circuit must be implemented to down convert the frequency of the pick up signals in the input frequency range of the ADC. The efficiency of the digital signal processing will depend on the wise choice of the frequency shift applied to the pick-up signals. In our case, we wanted to be able to measure the bunches position and phase in case of so-called time structure mode filling of the storage ring: The ring is then filled with 1 or 16 high intensity bunches equally spaced. So we needed a sampling frequency

equal to one quarter of the bunch spacing in the 16 bunch filling mode.

### RF FREQUENCY DOWN CONVERSION

#### General Layout

The layout of the RF front-end is shown in figure 1.

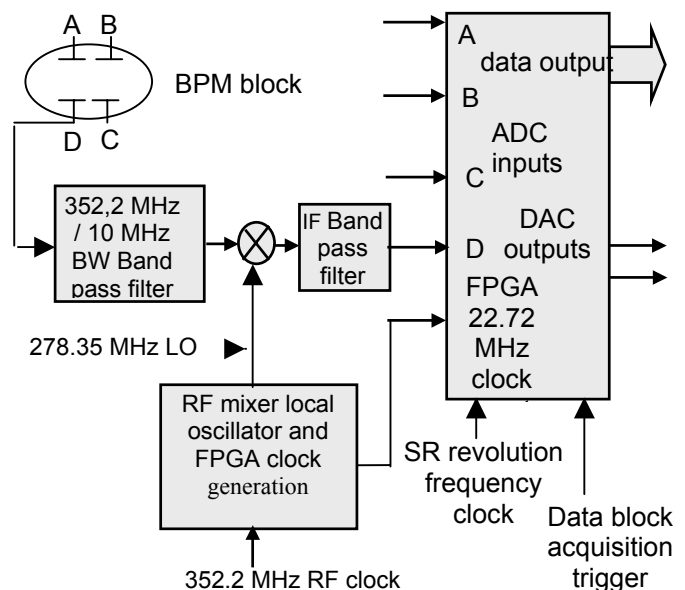


Figure 1: Layout of the BPM

The ESRF RF frequency is 352.2 MHz, the ring harmonic number is  $992=32*31$  and the revolution frequency is  $f_{rev}=355\text{KHz}$ . The choice of the clock and local oscillator frequency has been done following this line

#### ADC sampling clock frequency

The maximum sampling frequency of the 12-bit ADC AD9225 is 40MHz (definitely not the ultimate fast ADC available today...). The T delay between 2 bunches with a 16 bunch filling pattern of our storage ring is 88.018 ns;  $1/T=352.2\text{MHz}/62=5.68\text{MHz}$ . We have chosen 22.72 MHz for the ADC sampling clock frequency  $f_s$ ,  $2X\ 352.2\text{MHz}/31$ . Using such a clock, a synchronous in phase and in quadrature acquisition (I/Q) of all the harmonics of  $f_{rev}$  up to 11.36 MHz can be performed

#### Local oscillator frequency

The intermediate frequency IF can be higher than  $f_s/2$  providing the IF signal bandwidth is lower than  $f_s/2$

## Pill-box Cavity BPM for TESLA Cryomodule

V. Sargsyan, DESY-Zeuthen and TU-Berlin, Germany

### Abstract

A new cavity BPM with  $10\ \mu\text{m}$  resolution is designed and built to perform single bunch measurements at the TESLA linear collider. In order to have a low energy dissipation in the cryogenic supermodule, the inner surface of the cavity is copperplated. Cross-talk is minimized by a special polarisation design. The electronics, at 1.5 GHz, is a homodyne receiver normalized to the bunch charge. Its LO signal for down-conversion is taken from the same cavity.

### THE PICK-UP STATION

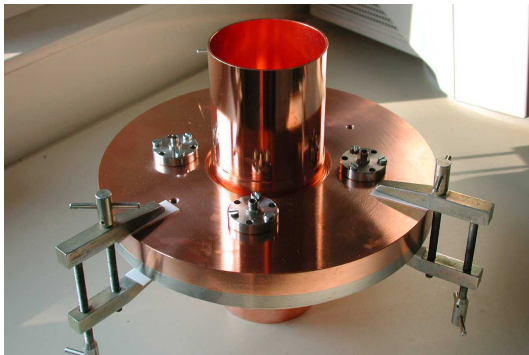


Figure 1: The pick-up station with four feed-troughs

A cylindrical pill-box cavity has been constructed as seen in figure 1. The pick-up station is fabricated from stainless steel. Dimensions and material properties of the structure are listed on table 1.

Table 1: Cavity dimensions and material parameters

type of stainless steel		1.4429
shrinkage from 293K to 2K [%]		0.3
conductivity (293K)	$[\Omega^{-1}\text{m}^{-1}]$	$1.33 \cdot 10^6$
cond. (2K)	$[\Omega^{-1}\text{m}^{-1}]$	$1.88 \cdot 10^6$
Room Resistivity Ratio (copper)		6.9
conductivity (293K)	$[\Omega^{-1}\text{m}^{-1}]$	$3.569 \cdot 10^6$
cond. (2K)	$[\Omega^{-1}\text{m}^{-1}]$	$24.84 \cdot 10^6$
Cavity diameter	[mm]	222 (221.3 at 2K)
Beam-pipe diameter	[mm]	78 (77.8 at 2K)
Cavity length	[mm]	18 (17.9 at 2K)
Coupling antenna depth	[mm]	7.6

In order to decrease energy dissipations on the walls the cavity was copper plated.

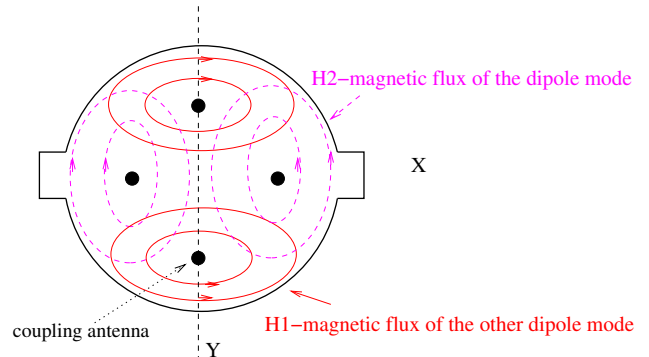


Figure 2: Cut of the cavity with two rectangular recesses

Two rectangular recesses were symmetrically eroded inside the cavity, in x-direction, see figure 2. It is done to get minimal cross-talk [2].

Fabrication tolerances result to changes in the anticipated  $\text{TM}_{110}$ -dipole mode frequency, see the following table. This results in a total error of

Table 2: Mechanical parameters sensitivity

dimension	target [mm]	sensitivity $\pm 100\ \mu\text{m}$	tolerances $[\mu\text{m}]$	shrinkage $[\mu\text{m}]$
cavity radius	111	$\mp 1.247\ \text{MHz}$	$\pm 10$	-433
cavity length	18	$\pm 0.158\ \text{MHz}$	$\pm 100$	-203
pipe radius	39	$\mp 0.305\ \text{MHz}$	$\pm 50$	-146

$$\Delta f = \sqrt{\Delta f(\delta R_{\text{res}})^2 + \Delta f(\delta l)^2 + \Delta f(\delta r)^2} \approx 252\ \text{kHz} \quad (1)$$

For simulations of the structure and resonant mode parameter computations the computer code GfdidL was used [1]. The signal which an antenna couples from the cavity on 1.512 GHz dipole mode frequency is

$$V^{\text{out}}(1.512\ \text{GHz}) = V_{110}^{\text{out}} + V_{010}^{\text{out}} + V_{020}^{\text{out}} + V_N \quad (2)$$

Where

- $V_{110}^{\text{out}}$  is the coupled voltage of the dipole mode,
- $V_{010}^{\text{out}}$  is the coupled voltage of the common mode on 1.512 GHz-dipole mode frequency,
- $V_{020}^{\text{out}}$  is the coupled voltage of the second monopole mode on 1.512 GHz-dipole mode frequency, and
- $V_N$  is the noise level, which is approximately -70 dBm (0.07 mV).

# ADVANTAGES OF IMPLEMENTING DIGITAL RECEIVERS IN FIELD PROGRAMMABLE GATE ARRAYS (FPGA)

Saša Bremec, Rok Uršič, Uroš Mavrič  
Instrumentation Technologies, Solkan, Slovenia

## Abstract

Today's state-of-the-art FPGA technology allows designers to satisfy almost any demand for high-speed data processing that is needed in digital signal processing (DSP) applications and fast data transfers. Dedicated FPGA resources are used in DSP applications to perform down conversion, filtering, and data formatting. New trends in system architecture favor serial data rather than parallel data transfer by using FPGA's internal resources, BlockRAMs (BRAMs), high-speed serial input/outputs (IO), and hard core processors.

## 1 INTRODUCTION

The latest trends show that the FPGA technology is gaining its share and becoming implementation technology of choice among digital receivers designers. This trend also reflects mature state of FPGA devices. An other appealing characteristic of FPGAs is their ability to integrate multiple functions or a complete system on a single chip. This is a generic trend in today's integrated circuit design and is referred to as system-on-chip (SoC) concept. Other features of today's high end FPGAs include embedded processors (PowerPC, ARM), which can run a variety of real time operating systems (RTOS) and powerful serial links, which support implementation of a multitude of open-standards protocols like Gigabit Ethernet, Fibre Channel, RapidIO, Infiniband and similar.

## 2 DIGITAL DOWN CONVERTER

The main advantage of implementing digital receivers on FPGAs in beam position monitors (BPM) or other similar beam instrumentation applications is that designers can tailor and optimize their designs to the

requirements of the specific applications. ASIC devices, on the other hand, where all the functional building blocks are embedded only allow the designer to change different parameters.

As an example we present a specific configuration of a digital receiver that was optimized for one of our applications. The requirement was to provide a simultaneous stream of wide-band and narrow-band measurements. Figure 1 shows the corresponding functional block diagram.

Fast analog to digital converter supplies a constant stream of data from a directly sampled IF or RF signal. The data stream is then split into two chains, which are multiplied by a stream of sine and cosine samples respectively, generated by a numerically controlled oscillator (NCO). If the frequency of the NCO corresponds to that of the input sampled frequency, then two signals following the multiplier contain the base-band component and the component at twice the NCO frequency. The cascaded integrator comb (CIC) filter followed by the finite impulse response (FIR) filter eliminate the second harmonic component and provide the required spectral shaping. The CORDIC building block calculates amplitude of the signal from the stream of I and Q samples. The data stream then splits into two branches. The top one provides additional filtering for low-bandwidth application, while the bottom one is used for wideband applications.

Another advantage of using FPGAs in digital receivers is that they allow implementing a variety of analog to digital converter configurations and architectures. Using advanced technique sampling rates up to 300 Msamples/s can be obtained, something currently not achievable with standard ASICs.

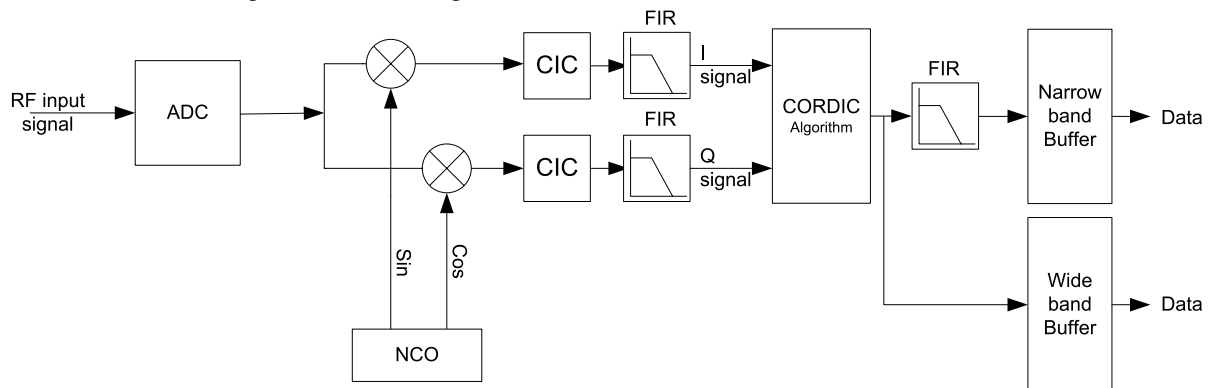


Figure 1 A specific configuration of a digital receiver that was optimized for one of our applications. The requirement was to provide a simultaneous stream of wide-band and narrow-band measurements..

# EXPERIENCE WITH SAMPLING OF 500MHz RF SIGNAL FOR DIGITAL RECEIVER APPLICATIONS

Uroš Mavrič, Saša Bremec, Rok Uršič  
Instrumentation Technologies, Solkan, Slovenia

## Abstract

This article presents test results of the prototype system that was built to evaluate feasibility of direct sampling of 500 MHz RF signal for use in digital receiver applications. The system consists of variable gain RF front-end, fast analog to digital converter (ADC) and field programmable gate array (FPGA), which provides the glue-logic between the ADC and a PC computer.

## 1 INTRODUCTION

The new trend in RF front-end design is to minimize the RF front-end complexity and to digitalize the signals as close as possible to the antenna. As a result, down-conversion can be omitted and the RF signal can be directly sampled using under-sampling technique.

The prototype was designed and constructed to investigate and evaluate the most important parameters that influence the performances of such a system.

## 2 PROTOTYPE

The prototype consists of RF amplification and filtering chain, fast analog to digital converter, and FPGA to control the outgoing data from the ADC and direct them to a serial port of the computer (PC).

### 2.1 RF amplification and filtering chain

Figure 1 shows the RF processing chain that consists of a few amplifiers (MMIC), filters, and variable attenuators. The cumulative amplification of a series of amplifiers boosts the incoming RF signal to cover the required dynamic range. Furthermore, the analog input of the ADC is set to +10dBm (full-scale) in order to give the best linear performances. Two variable attenuators provide a mechanism for keeping the output signal power constant whatever the input signal within the dynamic range is.

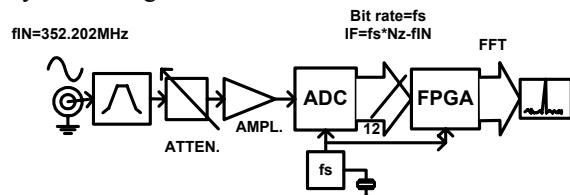


Figure 1: Prototype for direct RF sampling. It consists of amplification and filtering chain, fast analog to digital converter, FPGA, and personal computer for additional processing (FFT) and data visualization.

Relative position of variable attenuators in the RF processing chain and the switching scheme determine SNR and SFDR performance. In addition, the RF processing chain can be optimized for minimum noise figure or maximum third order intercept point, yielding high linearity. Figure 2 shows how SNR for these two cases varies with respect to the input signal. It is worth to mention that only the switching scheme changed.

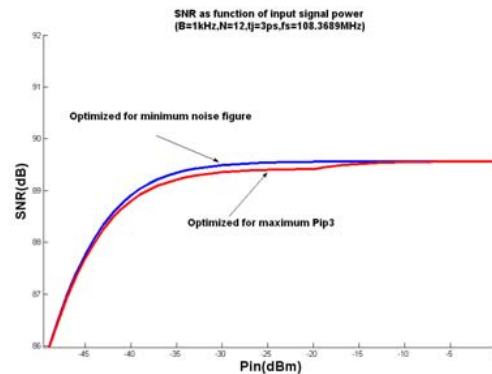


Figure 2: SNR as a function of the RF input signal. The upper curve is the SNR when attenuators are switched to keep the noise figure at its minimum. The lower curve is the SNR when attenuators are switched to give maximum  $P_{IP3}$ .

The input band-pass filter acts as an anti-aliasing filter and it covers only one Nyquist zone (Figure 4). If the input signal is a pulse and the pulse repetition frequency is much lower than the input band-pass filter bandwidth, the input signal doesn't anymore have a CW shape but the shape of the signal, which is shown in the Figure 3. It is important that pulse width is long enough to ensure enough samples to be taken by the analog to digital converter. A rule of thumb is 10 samples per pulse. At the same time we have to be aware of its amplitude, which should be well below the 1 dB compression point of the first amplifier after the band-pass filter. The pulse shown in Figure 3 gives a satisfying peak-to-average characteristic for a typical synchrotron light source operated in the single bunch mode.

### 2.2 ADC (analog to digital converter)

We use AD9433, which permits sampling of RF signals up to 750MHz with a sampling rate of maximum 125MSPS. In order to fulfill the Nyquist criteria it is necessary to use the previously mentioned under-sampling technique (Figure 4).

# Dynamic X-Y Crosstalk / Aliasing Errors of Multiplexing BPMs

Till Straumann, SLAC, Menlo Park, CA 94025, USA

## Abstract

Multiplexing Beam Position Monitors are widely used for their simplicity and inherent drift cancellation property. These systems successively feed the signals of (typically four) RF pickups through one single detector channel. The beam position is calculated from the demultiplexed base band signal. However, as shown below, transverse beam motion results in positional aliasing errors due to the finite multiplexing frequency. Fast vertical motion, for example, can alias into an apparent, slow horizontal position change.

## INTRODUCTION

Fig. 1 shows a typical arrangement of four BPM pickup electrodes or “buttons” in the cross section of a vacuum chamber. A bunched beam of charged particles travels in  $z$ -direction, inducing RF signals to the pickups. A multiplexing BPM processing system (fig. 2) sequentially samples the buttons  $A..D$  using a single receiver channel. Since only amplitude ratios are needed to determine the beam position, this approach features good drift rejection.

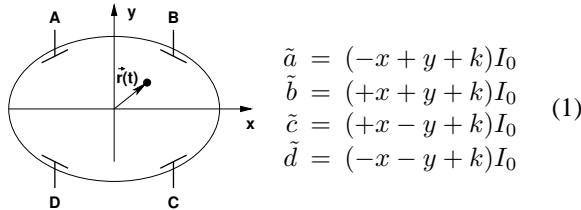


Figure 1: BPM Geometry and linear model equations

## LINEAR MODEL

To the first order, the amplitudes of the pickup signals induced by a particle beam at position  $(x, y)$  can be approximated by eqns. 1 where  $x$  and  $y$  are assumed to be properly scaled according to the beam pipe geometry, and deviations from symmetry are neglected.  $k$  is a constant offset and  $I_0$  denotes the beam current.

Note that  $\tilde{a}..d$  actually refer to RF signal amplitudes. However, for the purpose of this analysis, we neglect the fact that a practical system (fig. 2) multiplexes RF signals into a single receiver/detector. We simply assume the presence of four identical detectors upstream of the multiplexer such that the entire analysis can be performed in base-band.

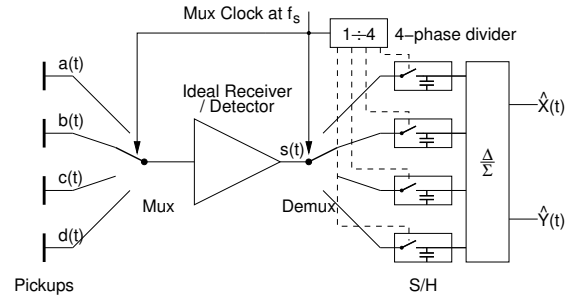


Figure 2: Multiplexing BPM system block diagram. All signals are in baseband, normalized to the beam current.

The beam position can be determined from the normalized button signals  $a..d = \tilde{a}/I_0..d/I_0$ :

$$\begin{aligned}
 \tilde{I}_0 &= (+\tilde{a} + \tilde{b} + \tilde{c} + \tilde{d})/4 \\
 \hat{x} &= (-a + b + c - d)/4 \\
 \hat{y} &= (+a + b - c - d)/4
 \end{aligned}$$

We use a “^” accent to distinguish the system response from the “true” beam position.

## DYNAMIC SYSTEM BEHAVIOR

Let’s now investigate the dynamic behavior of the multiplexed BPM system running at a multiplexing clock frequency of  $f_s$ , i.e. each button gets measured at a rate of  $f_s/4$ . Beam motion can be described by a time dependent vector in the  $x, y$  plane.

$$\vec{r}(t) = \{x(t), y(t)\}$$

For further analysis, we assume the motion to be band-limited to  $\pm f_s/2$ .

### Multiplexer Analysis

The time-multiplexed signal  $s(t)$  consists of a stream of “excerpts” of the individual pickup signals  $a(t)..d(t)$ . We introduce the abbreviated notion:

$$s^\square(t) = \{a, b, c, d\} = \begin{cases} a(t) & 0 \leq t < T_s \\ b(t) & T_s \leq t < 2T_s \\ c(t) & 2T_s \leq t < 3T_s \\ d(t) & 3T_s \leq t < 4T_s \end{cases}$$

Besides sampling the pickups in a “(counter) clockwise” ( $a, b, c, d$ ) fashion, there exists the possibility of scanning them in the “butterfly” sequence  $s^\bowtie(t) = \{a, c, b, d\}$ . (Due

# CAVITY BEAM POSITION MONITOR FOR THE TESLA ENERGY SPECTROMETER

A.Liapine, TU-Berlin, Germany

## Abstract

In order to measure the beam position with a precision of better than  $1\mu m$  in the TESLA energy spectrometer a cavity beam position monitor is proposed. A slotted cavity with a waveguide coupling is used to achieve a good common mode rejection and therefore a better precision. The paper gives a short overview of the monitor functionality and describes resolution measurements which were made on a  $1.5GHz$  cavity prototype with homodyne electronics. The estimation based on this measurements shows about  $100nm$  of spatial resolution.

## INTRODUCTION

A magnetic chicane spectrometer is foreseen for the beam energy measurements in TESLA (TeV Energy Superconducting Linear Collider) (Fig.1) [1]. This type of spectrometer realizes a simple principle - the beam is deflected from its original direction by a magnet and the deflection angle is determined measuring the beam position in a few points after the magnet. Mapping the magnetic field with high accuracy one can obtain the average beam energy as:

$$E_{beam} = \frac{ec \int Bdl}{\theta} \quad (1)$$

The problem is that the beam energy at the end of the linac is so high that the deflection angle is small and can not be increased because the synchrotron radiation rises drastically. Therefore the beam position has to be measured with a very high precision, a few  $100nm$ , in order to get the demanded accuracy of a few  $10^{-5}$ .

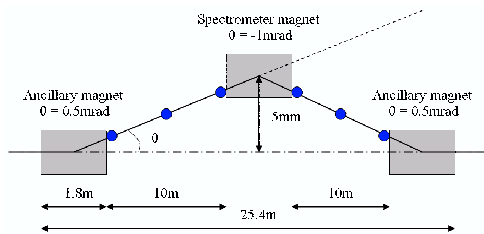


Figure 1: The foreseen spectrometer layout

## SLOTTED CAVITY BPM

A slotted cavity beam position monitor (BPM) was proposed for the application in the spectrometer [2]. The goal of the slotted cavity structure (Fig.2,4) is a strong rejection of the first monopole modes [3], which deliver strong noise signals at the frequencies close to the frequency of the dipole mode of the cavity (Fig.3).

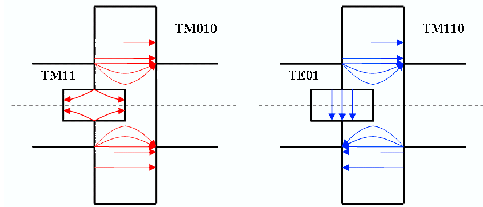


Figure 2: Mode selection in a slotted cavity

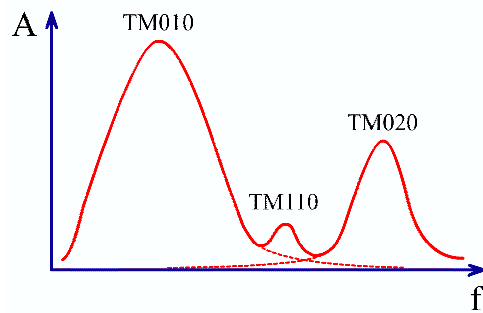


Figure 3: The influence of the monopole modes

A prototype of the slotted cavity for the laboratory measurements was designed and built for the frequency of  $1.5GHz$  (Fig.4, 5). Results of the estimations and simulations done for the prototype are listed in the Table1.



Figure 4: Cavity prototype inside

The resonance frequency of the common mode is  $1.0GHz$ . The common mode is practically uncoupled that is why the cavity was made from stainless steel in order to make the quality factor of the common mode smaller.

The common mode voltage  $V_{in}$  excited in the cavity is about  $130dB$  higher as the voltage of the dipole mode. At the cavity output this difference is already at  $45dB$  because

## THE LHC ORBIT AND TRAJECTORY SYSTEM

E. Calvo\*, C. Boccard, D. Cocq, L. Jensen, R. Jones, J.J. Savioz, CERN, Geneva, Switzerland  
 D. Bishop, G. Waters, TRIUMF, Vancouver, Canada

### Abstract

This paper describes the definitive acquisition system selected for the measurement of the closed orbit and trajectory in the CERN-LHC and its transfer lines. The system is based on a Wide Band Time Normaliser (WBTN) followed by a 10-bit ADC and a Digital Acquisition Board (DAB), the latter developed by TRIUMF, Canada. The complete chain works at 40MHz, so allowing the position of each bunch to be measured individually. In order to avoid radiation problems with the electronics in the LHC tunnel, all the digital systems will be kept on the surface and linked to the analogue front-ends via a single mode fibre-optic connection. Slow control via a WorldFIP field bus will be used in the tunnel for setting the various operational modes of the system and will also be used to check power supply statuses. As well as describing the hardware involved, some results will be shown from a complete prototype system installed on four pick-ups in the CERN-SPS using the full LHC topology.

### INTRODUCTION

The installation of the cabling structure and magnets in the LHC tunnel and its transfer lines started a few months ago in order to be ready for the commissioning in 2007. The complete Orbit and Trajectory system design is already definitive. The BPM sensors and electronics have been tested on the SPS, and the series production has started or will start by the end of the year for most equipment. This paper will review the chain of equipment involved in this system: from the beam sensors to the acquisition and processing units. The results of the tests in the SPS during 2002 will be also presented.

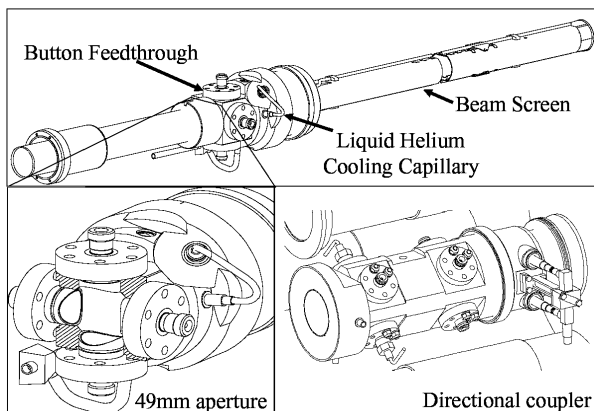


Figure 1. a) BPM body used in the LHC arcs. b) Zoom of the electrodes. c) Directional coupler used near the interaction points.

\* eva.calvo.giraldo@cern.ch

### COMPLETE SYSTEM LAYOUT

In the short straight sections of the LHC ring there is one BPM monitors per ring, per quadrupole. They are connected through a cryogenic coaxial cable to the outside of the cryostat and then to an electronic chassis, placed on the floor under the quadrupole. Each chassis contains a power supply card, 4 Wide Band Time Normaliser (WBTN) cards, an intensity measurement card and a control-communication card. The different working modes of the chassis are set and monitored through the control card, which receives and sends information via a WorldFip field bus. The measured position (or the intensity) of the beam is sent to the surface through a single mode optical fibre at 1310 nm. At each of the 8 access points, there are two racks, one per half octant. Inside each, there are 4 VME chassis, with a CPU, a TTC timing receiver card, and up to 18 Digital Acquisition Boards (DAB). Each DAB is able to handle the data from two measured planes. The calculated orbits are sent at 10 Hz through an Ethernet link up to a central processor, which calculates and sends any corrections to the orbit correctors and to the control room. Figure 2 shows the explained scheme.

### BEAM SENSORS

The sensors used to measure the position of the beam in the LHC are going to consist mainly of a BPM body with 4 button electrodes (about 1008) placed at one end of each quadrupole, as shown in Fig.1a) and b). However, near the interaction points the two beams are going to share the same vacuum pipe, making it necessary to use directional couplers (about 24 in total) in order to discriminate with the desired resolution the position of each beam. The length of the strip-line coupler has been designed in order to provide the same shape of signal as that from the button electrodes. This is a critical requirement given the "timing working mode" of the front-end electronics. The induced signals will be transmitted to the outside of the cryostat through eight semi-rigid cryogenic 50Ω coaxial cables. All this equipment will be installed inside the cryostat (in a secondary vacuum environment) at 5-25 K, with very high radiation dose levels (up to about 1000Gy/y). Moreover, through out the lifetime of the LHC, they have to withstand being cooled down and warmed up from 5K to 300K (and vice versa) tens of times without damage or deterioration to the seals or the electrical connections, since they will be extremely difficult to access after installation. As a consequence, hard requirements on the thermal conductivity, vacuum, impedance, electrical length and radiation tolerance are imposed which make their manufacturing and testing a challenge.

# CAVITY-TYPE BPMs FOR THE TESLA TEST FACILITY FREE ELECTRON LASER

H. Waldmann\*, H. J. Schreiber, DESY Zeuthen, D-15738 Zeuthen, Germany

## Abstract

For measurements of the beam position at the undulator section of the TESLA Test Facility (TTF) at DESY cavity-type beam position monitors were developed, installed and brought into operation. Apart from some theoretical aspects results of in-beam measurements at the TTF are presented and the pros and cons of this monitor concept are discussed.

## INTRODUCTION

For a successful operation of a Free Electron Laser (FEL) [1] working in a self-amplified spontaneous emission mode an overlap between the electron beam and the photon beam over the entire length of the undulator is required. Therefore a "beam based alignment" is fundamental. This requires beam position monitors (BPMs) with a resolution of a few  $\mu\text{m}$ . To meet these requirements the TTF-FEL with three undulators was equipped with high-precision BPMs [2] and correction coils within the undulators. Additionally, diagnostic stations containing a cavity-type BPM and a wirescanner at the entrance, the exit and between two adjacent undulator modules [3 - 5] were installed.

## PRINCIPLE

Because [6] gives a detailed theoretical background on cavity-type BPMs only a few relevant aspects are summarized as follows. A charged particle passing a cavity generates a superposition of an infinite sum of rf modes. In a circular cavity predominantly the common modes  $\text{TM}_{010}$  and  $\text{TM}_{020}$  and the less distinct dipole mode  $\text{TM}_{110}$  are excited. Fig. 1a shows a sketch of the field lines of the electrical field of the  $\text{TM}_{010}$  and  $\text{TM}_{110}$  modes, Fig. 1b the corresponding amplitudes as a function of the frequency.

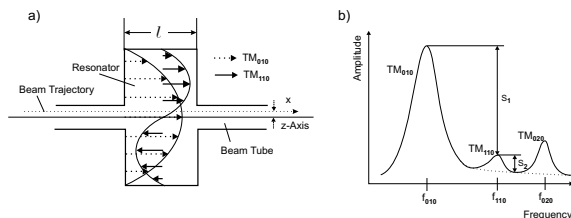


Figure 1: a) Excitation of the  $\text{TM}_{010}$  and  $\text{TM}_{110}$ -modes, b) Amplitudes of the  $\text{TM}_{010}$ ,  $\text{TM}_{110}$  and  $\text{TM}_{020}$  modes as a function of frequency

Transversal beam displacement is measured using the

\* waldmann@ifh.de

detection of the  $\text{TM}_{110}$  (12.025 GHz) mode. The amplitude of this mode scales with the bunch charge and the beam offset, i.e. it disappears for a centered beam. The common mode  $\text{TM}_{010}$  can be used for measuring the bunch charge. For small displacements its amplitude is nearly independent of the position.

## EXPERIMENTAL SETUP

The cavity-type BPM consists of a cupreous cavity body integrated into the diagnostic station, pickup antennae, cables for the output signals and electronics for signal processing.

For the horizontal and vertical beam displacements two separate circular cavities were used. "Nose cones" close to the beam pipe were integrated to reduce interferences. Each cavity was connected to the beam pipe. In order to define horizontal and vertical directions waveguides were arranged radially in opposite directions (see Fig. 2). The microwave signals are transmitted via antennae into coaxial cables. The signals from two opposite antennae were

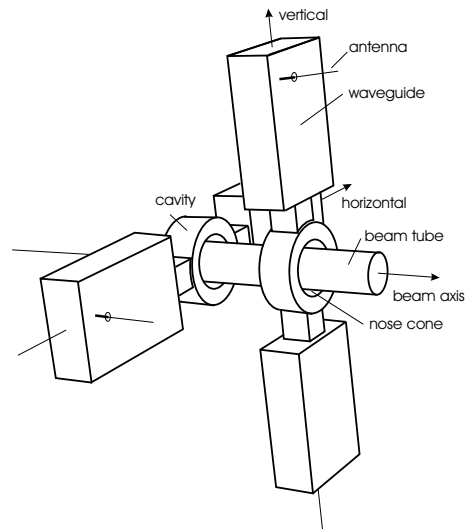


Figure 2: Sketch of the cavity BPM consisting of the beam tube, cavities with nose cones, waveguides and feedthroughs with antennae

combined in a  $180^\circ$  hybrid circuit. The resulting difference signal was mixed by an I-Q-mixer with a reference signal of 12.025 GHz. The resulting I (in-phase) and Q (in quadrature) were finally converted by a fast 14-bit ADC at a preselected sample time. The beam displacement can be detected using  $S = \sqrt{I^2 + Q^2}$ , the left-right ambiguity is resolved by the phase information  $\phi = \arctan \frac{Q}{I}$ .

## BEAM PHASE MEASUREMENT IN THE AGOR CYCLOTRON

S. Brandenburg, T.W. Nijboer, W.K. van Asselt  
 Kernfysisch Versneller Instituut (KVI), 9747 AA Groningen, the Netherlands

### Abstract

Beam phase measurement to optimize the isochronism is an essential part of the diagnostics in multi-particle, variable energy cyclotrons. In the AGOR cyclotron an array of 13 non-intercepting beam phase pick-ups is installed. To reduce the large disturbances from the RF system the measurements are traditionally performed at the 2<sup>nd</sup> harmonic of the RF frequency. To further improve the sensitivity intensity modulation of the beam has been introduced. Measurements with the different methods are presented, demonstrating that the intensity modulation strongly improves the sensitivity of the measurement. Useful beam phase measurements can now be made for beam intensities down to 10 nA.

### The AGOR facility

The AGOR cyclotron has been designed to accelerate all elements, explicitly including protons. The maximum energy per nucleon for ions is  $600(Q/A)^2$  MeV, while protons can be accelerated to a maximum energy of 200 MeV. The magnetic field is produced by two sets of superconducting coils and can vary from 1.7 to 4 T. Fifteen sets of correction windings are mounted on the

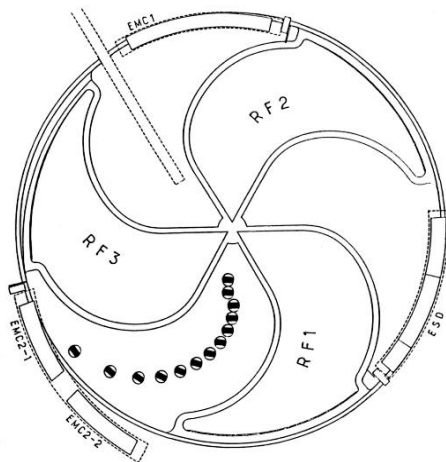


Figure 1. Cross-section through the median plane

three-fold symmetric iron hill sectors, which are located between the three RF cavities as shown in figure 1. These cavities provide the accelerating voltage for the beam and operate in the frequency range of 24 to 64 MHz, at harmonic mode 2, 3 or 4.

Extraction of the beam from the cyclotron is accomplished by successively an electrostatic channel, a room temperature electromagnetic channel, a superconducting electromagnetic channel and finally a superconducting quadrupole doublet.

### Motivation for beam phase measurements

Cyclotrons operate without longitudinal phase stability, and therefore there is no automatic feedback from the RF system on the beam, like in synchrotrons. The magnetic field and thus the beam phase is affected by different mechanisms:

- Accuracy of calculated settings for different beams. For most beams the magnetic field values have to be obtained from interpolation in field maps. These are available at 20 points in the operating diagram for the main coils. This leads to inaccuracies of the reference for the magnetic field of  $3\text{-}5 \cdot 10^{-4}$ .
- There are tight tolerances on the isochronism of the magnetic field. For protons ( $h = 2$ ) a maximum field error of  $\Delta B/B \sim 1.5 \cdot 10^{-4}$  results in a phase slip of  $90^\circ$ , when acceleration stops.
- The reproducibility of the magnetic field is adversely affected by long term variations of the temperature of the magnet iron, causing changes of the saturation magnetization of  $0.2 \text{ mT/K}$  [1].
- Accumulation of phase slip can also increase vertical beam blow-up in regions with weak vertical focusing because of the increased time spent in the region.
- The precessional extraction process is very sensitive for amplitude and phase of field perturbations. This sensitivity is strongly enhanced by large phase errors. As in the non-isochronous fringe field the phase slip rapidly builds up even with optimal tuning, reproducibility of the extraction strongly depends on control of the isochronism.

Inaccuracies in the magnetic field thus directly influence the acceleration and extraction process. Therefore precise and reproducible tuning of the magnetic field is essential. Measurement of the beam phase is the tool to achieve this. The ultimate goal for such a phase measurement system is a push-button operation with only minor impact on routine operation.

## AN X-BAND CAVITY FOR A HIGH PRECISION BEAM POSITION MONITOR\*

Ronald Johnson, Zenghai Li, Takashi Naito<sup>#</sup>, Jeffrey Rifkin<sup>†</sup>, Stephen Smith, and Vernon Smith  
Stanford Linear Accelerator Center, Menlo Park, CA, USA

### Abstract

The next generation of accelerators will require increasingly precise control of beam position. For example designs for the next linear collider require beam-position monitors (BPMs) with 300 nm resolution. The accelerator designs also place difficult requirements on accuracy and stability. To meet these requirements a cavity BPM operating at 11.424 GHz was designed. The BPM consists of two cavities: an xy-cavity tuned to the dipole mode and a phase cavity tuned to the monopole mode. The xy-cavity uses a novel-coupling scheme that (in principal) has zero coupling to the monopole mode. This report will present the mechanical design, simulations, and test results of a prototype BPM. In addition BPM designs with even higher precision will be discussed

### INTRODUCTION

Designs for the next generation of accelerators place stringent requirements on Beam Position Monitor (BPM) systems. These requirements are driven by the need to establish and maintain precise optics to prevent emittance growth. Requirements include measurement of beam position with high precision, good accuracy, and good stability. For example the Next Linear Collider (NLC) [1] will require BPMs to have precision of 300 nm, accuracy of 200  $\mu\text{m}$ , and stability of 1  $\mu\text{m}$  (over 24 hours).

A preliminary design of the NLC uses over 1900 BPMs placed at each quadrupole along the (X-band) main linacs. Each of these QBPMs is rigidly attached to the quadrupole and the whole assembly is mounted on precision movers. Beam based alignment will be used to determine and adjust the centers of the magnets. But this is an invasive procedure that is not compatible with production operation. Accelerator components must remain stable over long periods.

The two usual choices for BPM pickups are striplines or cavities. The mechanical complications of striplines makes insuring good stability a problem, especially when the beam tube has an internal diameter of only about 12 mm. In addition the position signal for striplines is the difference of two large numbers. This difference must be obtained with precision analog electronics or with digital electronics with a large number of effective bits.

On the other hand cavity BPMs can be machined out of a single block of metal with tolerances of about 0.5  $\mu\text{m}$ . Simple pillbox cavities can be fiducialized to the outside with errors of this order. Also when the beam is centered in the cavity the position signal is zero and signal is generated only as the beam moves off axis.

For these reasons a research project on development of a cavity BPM that could meet the NLC requirements was started. This report presents results on the prototype BPM that was designed and fabricated. An initial report [2] on this prototype has been published but construction of the BPM is now complete.

### DESIGN AND FABRICATION

The main linacs of the NLC operate at X-band (11.424 GHz). Although other frequencies could be selected, the cavity BPM was designed at this frequency for two reasons. First, the QBPMs are to provide a phase reference for the low-level rf control. Second, this frequency is consistent with a compact design and well established machining techniques.

A simple cylindrical cavity was designed with a thickness that would not add significant impedance to the beam. The BPM does feature a novel design for coupling the signals out [3,4]. A rectangular waveguide at right angles to the cavity intercepts the cavity only at the corner; coupling is through the magnetic field. Only the  $\text{TM}_{11}$  mode couples to the waveguide and the monopole mode ( $\text{TM}_{01}$ ) does not couple. This is illustrated in Figure 1.

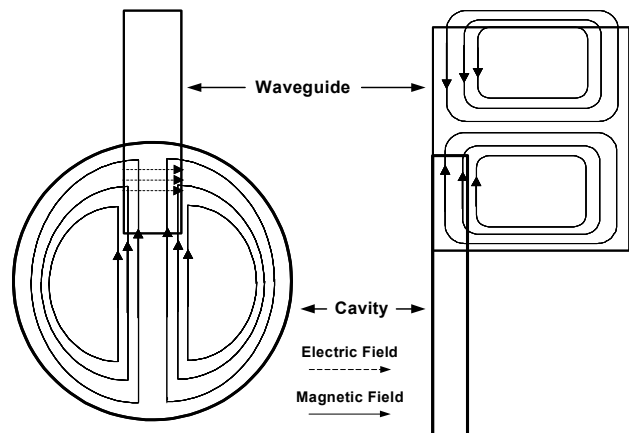


Figure 1: Coupling scheme for the cavity BPM.

Four waveguides intercept the cavity symmetrically horizontally and vertically. Signals from the vertical waveguides provide x-offsets and signals from the horizontal waveguides provide y-offsets. Extensive MAFIA simulations were performed in perfecting the design.

\*Work supported by Dept. of Energy Contract DE-AC03-76F00515

<sup>#</sup>Permanent address: KEK, 1-1Oho, Tsukuba, Ibaraki 305-0801, JAPAN

<sup>†</sup>Present address: Lyncean Technologies, Inc., Palo Alto, CA, USA

## DESIGN OF BPM PU FOR LOW-BETA PROTON BEAM USING MAGIC CODE

S. J. Park, J. H. Park, Y. S. Bae, W. H. Hwang, J. Y. Huang, and S. H. Nam,  
Pohang Accelerator Laboratory, POSTECH, Pohang, Korea  
and

Y. S. Cho, J. M. Han, S. H. Han, B. H. Choi  
Proton Engineering Frontier Project, KAERI

### Abstract

We have designed the BPM PU based on capacitive buttons for use in the KOMAC (Korea Multi-purpose Accelerator Complex), the high-intensity proton linac that are under development at the KAERI (Korea Atomic Research Institute), Korea. The KOMAC is aiming to produce CW 20-mA beam current at the 100-MeV energy. We have chosen the button-type PU since it is easier to fabricate than other type PUs including the stripline, and it could provide enough signal power because of the high beam current. The PU sensitivity was calculated by the MAGIC that is a kind of the Particle-In-Cell code that originates from the plasma science community. The utilization of the MAGIC code is especially useful for BPM PUs in the low-beta sections of the accelerator, because it is difficult to obtain the PU sensitivity experimentally due to the difficulties in simulating the low-beta beams by the electromagnetic waves in a test bench. In this presentation, we report on the design of the BPM PU based on the MAGIC calculation.

### 1 INTRODUCTION

Front-ends of modern HPPAs (High-Power Proton Accelerators), such as RFQs and DTLs are generally complex and have tight installation spaces. This is especially true for diagnostic devices, and their design and installation often become designer's "nightmare." Meanwhile, diagnostics including BPMs and CTs are very important for successful commissioning and operation of the accelerators. Hence, their implementation should be considered from the early stage of the accelerator design. Successful compromise between the two conflicting side is possible when the diagnostic devices can be made compact without sacrificing their performances. Compact devices are easy to handle, economical, and generally have better high-frequency characteristics. Modern beam diagnostic devices are far more compact than their ancestors. For example, some CTs from the Bergoz Instrumentations are now integrated with CF flanges and their total length (axial) can be made as small as 30 mm. Majority of BPM PUs (Pick-Ups) for proton accelerators are still striplines that yield well defined response even for low-intensity beams. But their sizes are still too big to be installed in the narrow front-ends the accelerator. For example, the axial length of the striplines for the SNS

(Spallation Neutron Source, USA) linac exceeds 100 mm, even if they are installed in the vacuum. Button-type capacitive PUs have been simple and reliable, but their application to the proton machines has been limited because of their insufficient response to low-intensity beams. Modern HPPAs (High-Power Proton Accelerators) such as the KOMAC are designed to have very high beam intensities, so that even the buttons could generate enough signals for precision beam position measurements. Refer to Table 1 for the major beam parameters of the KOMAC accelerator.

Table 1: Beam parameters of KOMAC accelerator

	Operation Mode		note
	CW	Pulse	
Beam Energy	3 - 20 - 100 MeV		BPM operation region
$\beta$	0.08 - 0.20 - 0.43		
V	1.003 - 1.021 - 1.107		
Average Beam Current ( $I_{av}$ )	Max 20 mA	Peak 20 mA	
Pulse Width	-	Few ms	
Bunch Length	160ps		PARMILA simulation result
Bunching Frequency	350 MHz		

In this context, we have chosen the button-type PU for use in the KOMAC accelerator. One of the disadvantages of the buttons is that, it is difficult to predict the PU sensitivity using analytic formulas. In fact, the PU sensitivity for low-beta beams can not be practically determined even by experimental methods, due to the difficulty of simulating electromagnetic fields from the low-beta beams. In this regard, we have decided to utilize the computer code for determining the sensitivity of the button-type PU. We have chosen the MAGIC code which is a kind of the PIC (Particle-In-Cell) code and can treat the particle and electromagnetic system in the full three dimensional manner.

## PERFORMANCE OF THE ELBE BPM ELECTRONICS\*

P. Evtushenko, R. Schurig, Forschungszentrum Rossendorf, Dresden, Germany

### Abstract

The radiation source ELBE is based on a superconducting LINAC. Initially it was designed to operate in CW mode with repetition rates either 13 MHz either 260 MHz. Later it was decided to operate the accelerator with reduced repetition rates for diagnostic reasons and for certain users. Now it is possible to operate with bunch frequency  $13/n$  MHz, where  $n$  can be 2,4,8,16,32,64 and 128. It is required that the BPM system supports any of these operation modes. A core element of the BPM electronics is a logarithmic detector AD8313 made by Analog Devices Inc. The logarithmic detector is a direct RF to DC converter rated up to 2.5 GHz. Initial design of the BPM electronic was sophisticated only for CW operation with repetition rate more than 10 MHz, since bandwidth of the AD8313 is about of 10 MHz. Additionally a sample and hold amplifier is built in to provide enough time for an ADC to make measurements. The sample and hold amplifier is synchronized with a bunch frequency. In the paper we present results of the modified BPM electronics test.

### THE BPM ELECTRONIC

The BPM electronics is based on the logarithmic detector AD8313 from Analog Devices [1], which is a direct RF to DC converter rated up to 2.5 GHz. Thus the BPM electronic is built without mixing down the RF signal of the BPM. The electronics operate at the fundamental frequency of the accelerator, which is 1.3 GHz. The electronics is placed in two different 19" chassis around accelerator outside the accelerator cave. An HELIAX® type RF cables connect BPMs to the RF front end. The cables have attenuation in a range 5÷6 dB at 1.3 GHz. The BPM signal goes through the bandpass filter with 3 dB bandwidth of 8 MHz. Then it is amplified with constant RF gain of about 25 dB to be matched to the linear range of the AD8313. The range goes from -65 dBm up to -5 dBm. The output of the logarithmic amplifier is matched to the ADC working range with the trim gain. The trim gain consists of adjustable gain and adjustable offset. So that four channels on one board are adjusted with difference typically 5%. Later the difference is taken in to account by software. One digit of the ADC corresponds to 8  $\mu$ m beam displacement. Principal scheme of the BPM electronics is depicted on Fig. 1.

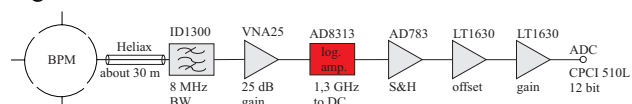


Figure 1: The electronics scheme.

Main characteristic of the BPM electronics is show on Fig. 2, where the electronics output is plotted as a function of the RF input. We decided to put four channels on a board, since the cross talk from channel to channel was measured to be less then -20 dB, which is low enough.

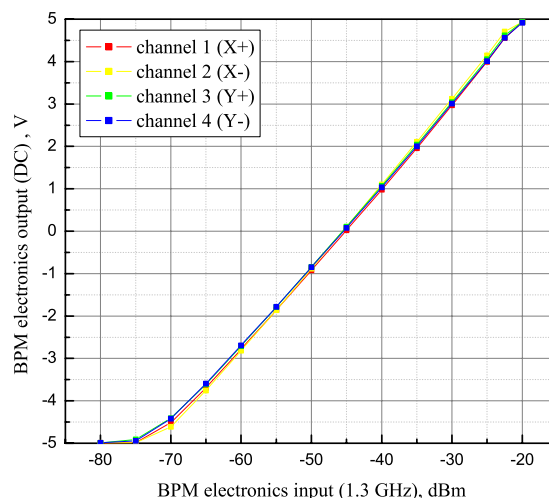


Figure 2: The electronics response curve.

### THE LOW REPETITION RATE PROBLEM

The logarithmic detector has output bandwidth of about 10 MHz. With a bunch repetition rate of 13 MHz the AD8313 provide a DC output, which can be simply amplified and sampled by an ADC. When the bunch repetition rate becomes less than certain the logarithmic detector output shows the pulsed structure as well. Such situation is demonstrated on the Fig. 3. A short pulse generator drives the logarithmic detector. The generator was connected to the channel 1 of the oscilloscope. Output of the AD8313 evaluation board is on the channel 2. On the upper oscillogram the generator frequency is high enough to make the AD8313 output just a DC signal. On the lower oscillogram the generator frequency is reduced in factor four and is less than the logarithmic detector bandwidth. As one can see in this case every pulse of the generator is transformed by AD8313 in to another more broad pulse but not in to DC signal. In a case with an electron beam and real signal from the BPM the width of the logarithmic detector pulsed output is defined by the bypass filter bandwidth or in another words by its quality factor. The real signal has 100 ns flat top. The ADC used for the data acquisition has a sampling time of 400 ns. Obviously even with proper timing the ADC does not have enough time to measure

\* P.Evtushenko@fz-rossendorf.de

## A HIGH DYNAMIC RANGE BEAM POSITION MEASUREMENT SYSTEM FOR ELSA-2

Ph.Guimbal\*, P.Balleyguier, D. Deslandes, CEA/DPTA Bruyères-le-Châtel, France  
 H. Borrión, Electrical and Electronic Engineering Dept., University College, London

### Abstract

New beam lines are presently under construction for ELSA, a 18 MeV electron linac located at Bruyères-Le-Châtel. These lines need a beam position measurement system filling the following requirements : small space occupancy, good sensitivity, wide dynamic range (more than 90 dB), high noise immunity, single-bunch/multi-bunch capability. We designed a compact 4-stripline sensor, and an electronic treatment chain based on log-amplifiers. This paper presents the design, cold and hot test results.

### INTRODUCTION

The ELSA facility [1] was designed in the late 80's as a test bench for high-power FEL physics and technology. It is now mainly used as a versatile 1-18 MeV electron source or as a picosecond hard X-ray source. In response to this shift in the user's needs, dedicated beamlines are under construction in a new experimental area [2].

In 1988, during design stage, two types of diagnostics were chosen for transverse beam monitoring :

- thin OTR screens (300 nm Al on 8  $\mu\text{m}$  kapton film)
- button-type or stripline (depending on available space) BPMs

Subsequent ELSA operation showed the limits of these diagnostics :

- OTR screens allow precise measurement of the transverse profile, but are not very sensitive. They were replaced by two-screen systems (like the one described below on fig. 1) with an OTR screen and a scintillator screen (Cr:Al<sub>2</sub>O<sub>3</sub> deposited on a thin film).
- the button BPMs (10 mm in diameter capacitive pickups) are not sensitive enough
- the BPM electronic treatment chain is not reliable enough and was specifically designed for FEL operation. Therefore, it can be used only for 14.44 MHz (and 14.44 MHz/n) rep-rate train of bunches.

### THE ELSA-2 COMBINED STATION

For these reasons, it was decided to design a new diagnostic station (fig. 1 et 2) with the following constraints:

- all-in-one OTR/scintillator/BPM station to save space and allow easy comparison of OTR and BPM data
- simple design
- high sensitivity BPM

- high dynamic range electronics, compatible with every macropulse structure of the beam, which means any sub-pattern extracted from a 144 MHz train.
- a length equal to a standart 6-way tee (164 mm)

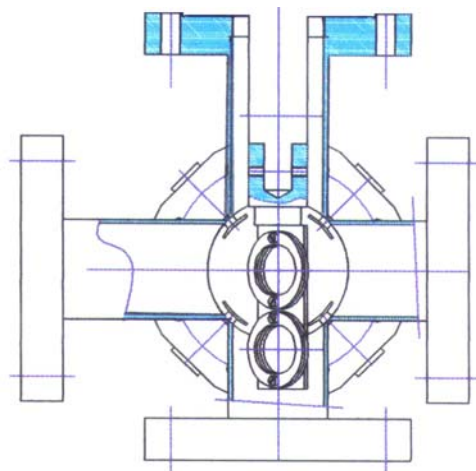


Fig. 1. Schematic drawing of the new diagnostic station combining two screens (OTR and scintillator) and a 4-stripline BPM : transverse view, showing the screens.

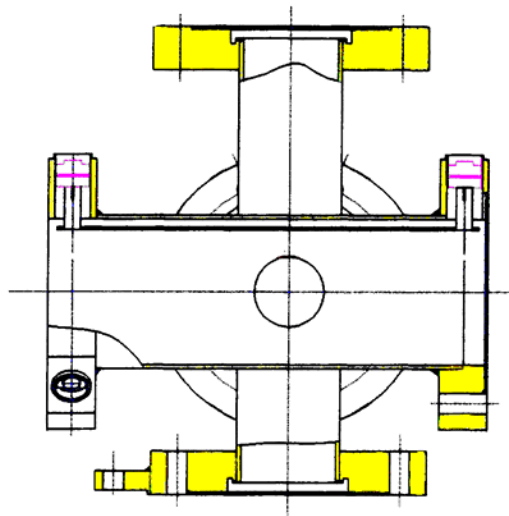


Fig. 2. Longitudinal view, showing the stripline ports.

For the BPM electronics (see details below), we chose a central frequency of 288.89 MHz. The corresponding wavelength (about 1 meter) is much longer than the stripline. In this case, the sensitivity grows with the

\*email : philippe.guimbal@cea.fr

# Impedance-Matching-Transformer for Capacitive Pick-Ups

W. Kaufmann, J. Schölles, GSI, Darmstadt, Germany

## Abstract

The transfer lines from GSI's heavy ion synchrotron (SIS) to the experimental set ups are equipped with segmented capacitive pick-ups for beam position measurement. This beam position measurement will be designed for single-bunch evaluation. Best choice for taking measurements with maximum sensitivity is a high-impedance tap at the pick-up referring to the bunch length of 50... 500 ns. Therefore the feeding of 50 Ω coaxial cables will be realized by an impedance-matching transformer located close to the pick-up. It should have an impedance > 10 kΩ on the primary side and 50 Ω matching on the secondary side with a foreseen bandwidth of 200 MHz. So it is possible to use low noise amplifiers with 50 Ω input in a radiation save environment without loading the pick-up with 50 Ω.

## INTRODUCTION

Many capacitive pick-ups at the GSI's synchrotron are used as position and phase pick-ups. Normally, high impedance head-amplifiers with an input impedance of 1 MΩ amplifies the plate signals close to the vacuum feed trough. Looking at the equivalent circuit of pick-up and amplifier explains why a high impedance signal tap is useful. This configuration behaves as a high pass filter as specified in [1]. Three different cases have to be taken into account as shown in figure 2.

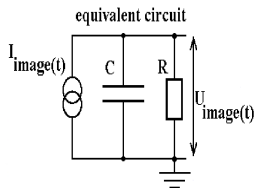


Figure 1: Equivalent circuit of one pick-up plate and amplifier

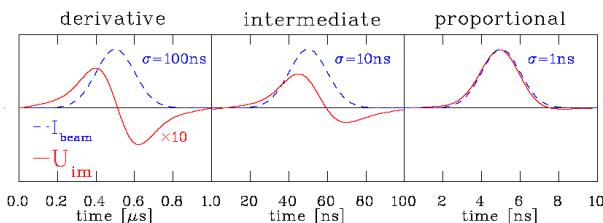


Figure 2: Theoretical bunch shaping

$$U_{\text{image}} = \frac{A}{\beta\pi c a C} \cdot \frac{j\omega RC}{(1 + j\omega RC)} I_{\text{beam}}(\omega) \quad (1)$$

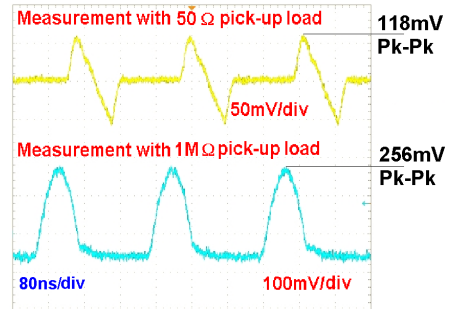


Figure 3: Measured bunch signals

Highest gain can be achieved in the proportional case. Measurements have approved the theoretical predictions (3). Figure 4 gives an information about the voltage gain of an 1 MΩ amplifier compared to a 50 Ω configuration.

It shows the calculated absolute value of the longitudinal transfer impedances ratio of a 1 MΩ and a 50 Ω amplifier.

In the range up to 1 GHz a 1 MΩ amplifier provides a higher gain. In practice, reflections will be generated due to the discontinuity of pick-up capacitance and amplifier input. But in the case of the used head amplifiers with its short cable length of a few centimeters this effect is negligible.

For beam position monitoring, at the high energy transfer lines from the SIS to the experimental area, it is necessary to use high impedance amplifiers to get a gain in position signals and a higher sensitivity. With a look to the future project of the GSI and its higher intensities it is important to make the maintenance at the beam diagnostics easier and saver. This means to get away from the beam tube into a radiation poor region of the plant.

$$U_{\text{image}} = 20000 \frac{\sqrt{1 + \omega^2 \cdot (50\Omega \cdot C_{\text{pickup}})^2}}{\sqrt{1 + \omega^2 \cdot (1M\Omega \cdot C_{\text{pickup}})^2}} \quad (2)$$

Furthermore some cryogenic regions at the new accelerator parts are provided. In this parts it is absolutely fatal to use head amplifiers with any power dissipation.

To work with 50 Ω coaxial cables is the best way to get away from the beam tube in an adequate manner. But

# DEVELOPMENT OF A BUNCH FREQUENCY MONITOR FOR THE PRELIMINARY PHASE OF THE CLIC TEST FACILITY CTF3

A. Ferrari\*, A. Rydberg, Uppsala University, Sweden  
 F. Caspers, R. Corsini, L. Rinolfi, F. Tecker, CERN, Geneva, Switzerland  
 P. Royer, Université de Lausanne, Switzerland

## Abstract

In the framework of the CLIC RF power source studies, the feasibility of the electron bunch train combination by injection with RF deflectors into an isochronous ring has been successfully demonstrated in the preliminary phase of CTF3. A new method, based on beam frequency spectrum analysis, was experimented to monitor this scheme. A coaxial pick-up and its read-out electronics were designed and mounted in the CTF3 ring to allow comparison of the amplitudes of five harmonics of the fundamental beam frequency (3 GHz) while combining the bunch trains. The commissioning of the monitor was a successful proof of principle for this new method, despite the short length of the bunch trains and the presence of parasitic signals associated to high-order waveguide modes propagating with the beam inside the pipe.

## INTRODUCTION

The Compact Linear Collider (CLIC) RF power source is based on a new scheme of bunch frequency multiplication: a 30 GHz drive beam is obtained by combining electron bunch trains in isochronous rings, using RF deflectors [1]. The preliminary phase of the CLIC Test Facility CTF3 [2] successfully demonstrated the feasibility of such a scheme at low charge [3]. A train of five pulses, produced by the source at the front-end and accelerated in a linac, was injected into an isochronous ring, using RF deflectors that create a time-dependent closed bump of the reference orbit and thereby allow the interleaving of the pulses at the injection. In this paper, we present a new method to monitor the bunch train combination, based on frequency spectrum analysis. When the first pulse is injected into the isochronous ring, the distance between two consecutive bunches is 10 cm, i.e. 333 ps. Therefore, all harmonics of 3 GHz can be found in the beam power spectrum. At the end of the bunch train combination, the distance between two consecutive bunches is reduced by a factor five. As a result, only the harmonics of 15 GHz should be found in the beam power spectrum (see Fig. 1). A coaxial pick-up and its read-out electronics were developed in order to extract the information contained in the beam. The bunch frequency monitor was installed and commissioned at CERN

during the last operating period of the CTF3 preliminary phase in 2002 [4]: a description of the measurements that were performed, as well as an analysis of the results that were obtained, are summarized in this paper.

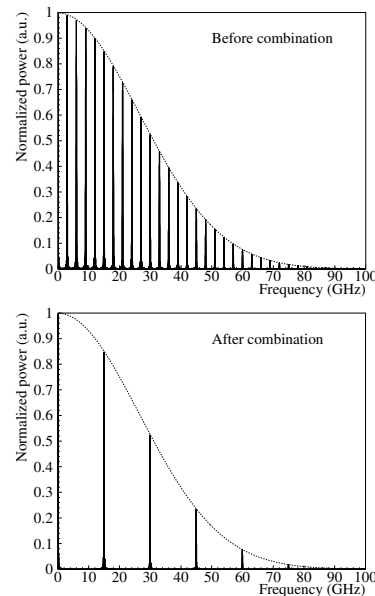


Figure 1: Calculated normalized power spectra for a train of gaussian bunches with a fwhm length of 10 ps before and after the bunch train combination with a factor five.

## DESIGN OF THE PICK-UP AND ITS READ-OUT ELECTRONICS

### Description of the coaxial RF pick-up

The geometry of the extraction coaxial pick-up was chosen in order to include a miniature ultrahigh vacuum feedthrough [5] while meeting various technical constraints (see Fig. 2). This feedthrough can be considered as a two dielectric coaxial line, with a constant inner diameter of 0.4 mm. On the vacuum side, the inner conductor is maintained in its central position by a small ceramic ring. A hole of 1.5 mm diameter was drilled in the beam pipe wall for the extraction of the signal. On the other side, the feedthrough is terminated by a K connector. The geometry of the pick-up was included in MAFIA simulations [6] and its transfer impedance was derived for the five frequencies of interest (9, 12, 15, 18 and 21 GHz).

\* The research of A. Ferrari was supported by a Marie Curie Fellowship of the European Community Programme "Improving Human Research Potential and the Socio-economic Knowledge Base" under contract number HPMF-CT-2000-00865.

## TRANSVERSE FEEDBACK SYSTEM FOR THE COOLER SYNCHROTRON COSY-JÜLICH – FIRST RESULTS

V. Kamerzhiev, J. Dietrich, I. Mohos, Forschungszentrum Jülich GmbH, Germany

### Abstract

The intensity of an electron cooled beam at COSY is limited by transverse instabilities. The major losses are due to the vertical coherent beam oscillations. To damp these instabilities a transverse feedback system is under construction. First results with a simple feedback are presented. Due to operation of the system the intensity and lifetime of an electron cooled proton beam at injection energy could be significantly increased. Measurements in frequency and time domains illustrate the performance of the system.

### INTRODUCTION

The cooler synchrotron COSY delivers unpolarized and polarized protons and deuterons in the momentum range 300 MeV/c up to 3.65 GeV/c. Electron cooling at injection level and stochastic cooling covering the range from 1.5 GeV/c up to maximum momentum are available to prepare high precision beams for internal as well as for external experiments in hadron physics. Electron cooled beam at injection energy can become unstable [1,2]. Major current losses result from the vertical coherent oscillations of the dense electron cooled beam. One of possible cures of this problem is an active feedback system which damps the instabilities [3].

### DOES COSY NEED A FEEDBACK SYSTEM

Let us look at the behaviour of an electron cooled intense proton beam at injection energy. To do this standard diagnostic equipment such as beam current transformer (BCT) and beam position monitor (BPM) have been used. BPM difference ( $\Delta$ ) signals in time and frequency domains have been simultaneously analysed.

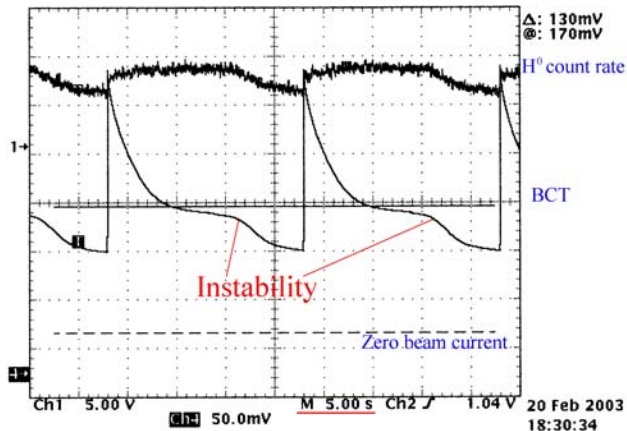


Figure 1: BCT (100 mV are equal to 1 mA beam current) and  $H^0$  count rate signals.

On Fig. 1 the beam losses due to the instability are shown. The proton beam was cooled by 170 mA electron current. Vertical and horizontal BPM difference signals together with BCT signal are demonstrated on Fig. 2. Since the vertical aperture of the vacuum chamber in the arcs is more than two times smaller than the horizontal one

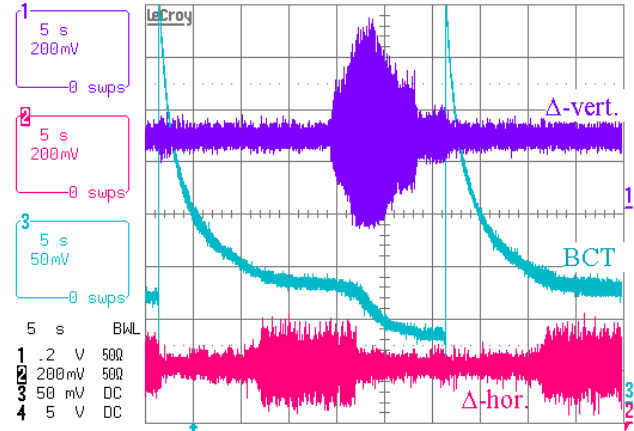


Figure 2: Vertical/horizontal BPM  $\Delta$ -signals and BCT.

the beam oscillations in vertical plane are more dangerous and result in significant losses (see Fig. 2). Due to these reasons there is a necessity of the vertical damping.

### SIMPLE FEEDBACK SYSTEM

The goal is to damp coherent vertical oscillations of the coasting proton beam at injection energy [4]. If the cavity gap is properly short-circuited the frequency spectrum of the vertical  $\Delta$ -signal contains only vertical betatron sidebands (see Fig. 3).

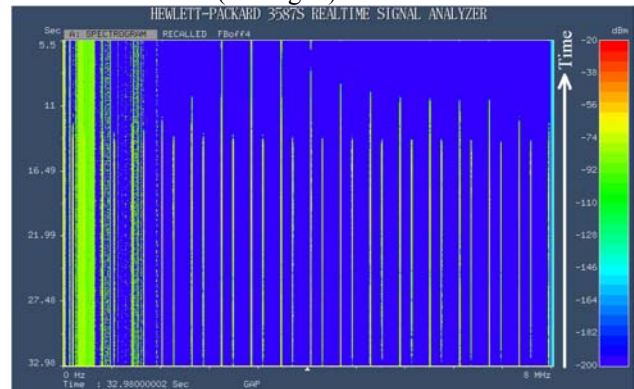


Figure 3: Frequency spectrum of the vertical  $\Delta$ -signal.

In such a case the feedback system consists of a pick-up with a hybrid, preamplifier, delay, 180°-splitter, power amplifier and a kicker. No additional signal processing is necessary.

## A NEW WIDE BAND WALL CURRENT MONITOR

P.Odier CERN, Geneva, Switzerland

### Abstract

Wall current monitors (WCM) are commonly used to observe the time profile of particle beams. In CTF3, a test facility for the CERN Linear Collider study CLIC, high current electron beams of 1.5  $\mu$ s pulse length are bunched at 3 GHz and accelerated in a Linac working in fully loaded mode, for which a detailed knowledge of the time structure along the pulse is mandatory. The WCM design is based on an earlier version developed for CTF2, a previous phase of the test facility, in which the beam duration was only 16 ns. Due to the longer pulse width the low frequency cut-off must be lowered to 10 KHz while the high frequency cut-off must remain at 10 GHz. The new WCM therefore has two outputs: a direct one for which an increase of the inductance results in a 10 GHz to 250 kHz bandwidth while the second one, using an active integrator compensating the residual droop, provides a 10 kHz to 300 MHz bandwidth. The new WCM has been installed in CTF2 late 2002 in order to test its high frequency capabilities prior to its use in CTF3. Design considerations and first results are presented.

## 1 INTRODUCTION

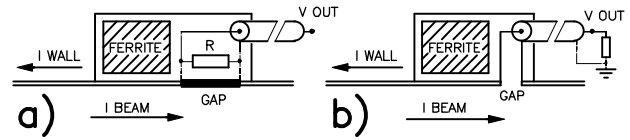
In CTF3, the test facility for the CERN Linear Collider study, high current electron beams of 1.5  $\mu$ s pulse length are bunched at 3 GHz and accelerated in a Linac working in fully loaded mode, for which a detailed knowledge of the time structure along the pulse is mandatory. The new WCM design is based on an earlier version developed for CTF2 a previous phase of the test facility[1,2], in which the beam duration was only 16 ns.

The 1.5  $\mu$ s pulse duration in CTF3, much larger than in CTF2, requires a significant decrease of the WCM low frequency cut-off, down to 10 kHz in order to limit the signal droop along the pulse. The high frequency cut-off should remain 10 GHz since the bunch repetition frequency will be 3 GHz. Owing to limited space availability, the overall length of the WCM should not exceed 260 mm. The monitor sensitivity is not a critical parameter in CTF3 since the mean beam current during the pulse is high enough, 1.5 A to 35 A.

## 2 DESCRIPTION OF THE NEW WCM

### 2.1 Principle of WCM

The general principle of resistive wall current monitor is very simple. A resistor is connected, either directly (Fig.1a) or through a vacuum feedthrough and a cable (Fig.1b) across a gap made in the wall of the vacuum pipe.



Figures 1a and 1b: principle of WCM

The image current, which accompanies the beam along the inside of the vacuum pipe develops a voltage across the resistor. A screening box filled with magnetic material, usually ferrite, is electrically connected on the two sides to force the image current to pass through the resistor. The equivalent circuit of such an arrangement is shown in Fig.2.

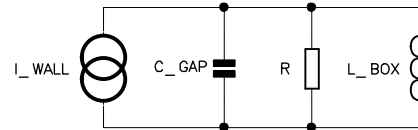


Figure 2: equivalent circuit

The dependence of the observed signal to beam radial position is minimised by collecting and summing the image current in 8 places around the gap circumference using 8 feedthroughs and an external combiner.

### 2.2 Bandwidth limitations

The high frequency cut-off depends on  $C_{\text{gap}}$  and on  $R$ . The standard connectors and coaxial cables being 50  $\Omega$  and the number of outputs being limited to 8 by the physical size of the monitor, the value of  $R$  is  $50 \Omega/8 = 6.3 \Omega$ . For a given vacuum pipe diameter, the value of  $C_{\text{gap}}$  depends on the length of the gap and on the permittivity of the insulator. In principle the gap length should be smaller than the beam length, which is 1.5 mm rms in CTF3. For practical reason the gap length has been fixed to 2 mm. It is made of a simple cut in the vacuum pipe; the capacitance of a ceramic gap would have been too high for the expected frequency bandwidth. For this reason the connections as in Fig. 1b have been chosen.

The low frequency cut-off depends on  $R$ , already mentioned, and on  $L$  the inductance of the screening box, which should be increased for CTF3 purpose.

### 2.3 Vacuum issues

The pressure required in the linac is in the region of  $10^{-7}$  mbar and lower than  $10^{-8}$  mbar in the combiner ring. With no ceramic gap in the WCM the interior of the screening box is under vacuum. This imposes a 150  $^{\circ}$ C bake-out process and determines the type of ferrite to be used. In order to avoid virtual leakages, particular care has been taken with respect to welding from inside as

## Microwave measurement of intra bunch charge distributions

M.Dehler,

Paul Scherrer Institut, CH-5232 Villigen PSI, Switzerland

e-mail: Micha.Dehler@psi.ch

### Abstract

A direct way of obtaining intra bunch charge distributions is to measure the amplitude roll off as well as the phase behavior of the spectrum of the single bunch self field. To that effect, a microwave pickup together with a microwave front end has been installed in the storage ring of the Swiss Light Source (SLS). As pickup, button type bpms are used, which have been designed for a broad band behavior in the excess of 30 GHz. Three bpms together with their individual front ends are used in order to sample the beam spectrum at frequencies of 6, 12 and 18 GHz, which compares to the standard spectrum of a 1 mA single bunch extending to approximately 12 GHz (13 ps rms bunch length). The signals are mixed to base band in loco using the multiplied RF frequency as a LO. By shifting the LO phase, simultaneously the amplitude roll off as well the complex phase of the beam spectrum can be obtained. Where using a resonator as a pickup would smear out the response over several bunches, allowing only the determination of average values, the current setup has a band width of approximately 2 GHz, so that individual bunches in the 500 MHz bunch train can easily be resolved.

### INTRODUCTION

Intra bunch properties like the bunch length or the intra bunch charge distribution is reflected in the spectral composition of the self field of the bunches.

Measuring the bunch length makes use of the following property of Fourier transforms. With  $h(t)$  as an arbitrary distribution and  $H(j\omega)$  its Fourier transform, the following holds for the relation between its n-th order moment  $m_n$  and the Fourier transform [1]:

$$(-j)^n m_n = \frac{\partial^n H(j\omega)}{\partial \omega^n} \Big|_{\omega=0}$$

An alternative representation uses cumulants,  $H(j\omega)$  is expressed via its cumulants  $k_n$

$$H(j\omega) = \exp(j\omega k_1 - \frac{\omega^2}{2} k_2 - j \frac{\omega^3}{6} k_3 \dots)$$

With  $\log(H(\omega)) = a(\omega) + j\phi(\omega)$ , odd cumulants are solely determined from the phase

$$k_{2n+1} = (-1)^n \frac{\partial^{2n+1} \phi}{\partial \omega^{2n+1}}$$

and even cumulants from:

$$k_{2n} = -(-1)^n \frac{\partial^{2n} a}{\partial \omega^{2n}}$$

Relating these to the properties of the beam,  $k_1$  is the center of gravity of the bunch,  $k_2$  its variance aka square of the rms length,  $k_3$  the unnormalized skewness and and  $k_4$  the unnormalized excess of the charge distribution in the bunch.

In comparison to other alternatives, this approach for the measurement makes the minimum amount of assumptions about the bunch, be it the shape of its distribution, be it the presence of single or multi bunch instabilities.

With an theoretical bunch length of 13 ps at a nominal single bunch current of 1 mA, the roll-off of the bunch spectrum happens at around 12 GHz, so that measurements should go up to at least 18 GHz. One cannot hope to have an integral view of the bunch spectrum from DC-18 GHz, so the interesting question is the number of frequencies, one needs to sample in order to be sure to see any feature in the bunch charge distribution. This is given by maximum bunch length, which we estimated to be 36 psec. Due to this length even a pure sinusoidal modulation of the density will give a bump in the bunch spectrum with a width of 4.5 GHz to both sides of the modulation frequency. So including some security factors it was decided to setup measurements at 6, 12 and 18 GHz.

### HARDWARE

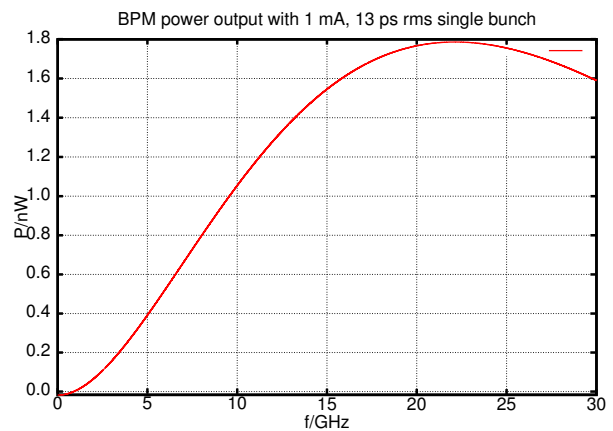


Figure 1: Power spectrum at the output of the two-button BPM assuming a 1 mA single bunch with the theoretical value for the SLS of 13 ps rms.

The hardware setup consists of three separate channels for processing the signals at the dedicated frequencies. As a signal pickups three special BPMS with two buttons sitting in the 28 mm high chamber of the SLS injection straight are used. For an optimum high frequency response, the BPM

## Measurement of the longitudinal phase space at the Photo Injector Test Facility at DESY Zeuthen

J. Bähr, I. Bohnet, J. H. Han, M. Krasilnikov, D. Lipka\*, V. Miltchev, A. Oppelt, F. Stephan, DESY Zeuthen, Zeuthen, Germany, K. Flöttmann, DESY Hamburg, Hamburg, Germany

### Abstract

A setup for the measurement of the longitudinal phase space at the photo injector test facility at DESY Zeuthen is described. The measurements of the momentum distribution, the length of an electron bunch and of their correlation are discussed. The results of the momentum distribution measurement are shown, a maximum mean momentum of 4.7 MeV/c and a RMS momentum spread of 14 keV/c is observed. The setup for the measurement of the bunch length includes a Cherenkov radiator which is used to convert the electron beam into a photon beam with a wavelength in the visible range. The Cherenkov radiation mechanism is chosen in order to measure the bunch length with good time resolution. A silica aerogel radiator with low refractive index will be used. Geant 4 simulations show that a resolution of 0.12 ps can be reached. The time dependent behaviour and the position of the photon bunch will be measured by a streak camera system. A simultaneous measurement of the bunch length and the momentum spread will provide the full information about the longitudinal phase space. The design considerations of the radiators and their properties are discussed.

### INTRODUCTION

The photo injector test facility at DESY Zeuthen (PITZ) has been developed with the aim to deliver low emittance electron beams and study their characteristics for future applications at free electron lasers and linear accelerators. The energy of the electron beam varies in the range between 4 and 5 MeV. A description of PITZ can be found in [1].

Successful optimisation and improvement of the PITZ performance requires good beam diagnostics for investigating the electron bunch properties. This paper is focused on longitudinal emittance measurements.

A spectrometer dipole and a YAG screen are used for the measurement of the momentum distribution of the electron bunch. The bunch length can be measured by using a radiation process, where a photon bunch is produced with the same time properties as the electron bunch has. The photon bunch is transported by an optical transmission line [2] to a streak camera, where the bunch length will be measured. At the electron energies available at PITZ a large amount of photons can be produced in the Cherenkov radiation process. To be able to transport the photon bunch to the streak camera small output angles from the radiator are requested.

Therefore, Cherenkov radiation in silica aerogel ( $\text{SiO}_2$ ) is suggested for the photon production mechanism.

For the measurement of the full longitudinal phase space of the electron bunch a dipole, a Cherenkov radiator in the dispersive arm and a streak camera will be used. The produced photon bunch provides the information about the time properties and the momentum spread of the electron bunch. The simultaneous measurement of the bunch length and momentum spread allows to investigate the correlation between these characteristics.

### MOMENTUM DISTRIBUTION

The mean momentum of the electron bunch as a function of the set point phase compared to a simulation with ASTRA [3] is shown in Fig. 1. In a large phase range the mean momentum is consistent with the simulation, where an appropriate phase shift is chosen. Up to now, the highest measured mean momentum at PITZ is 4.7 MeV/c, which corresponds to a gun gradient of 41.5 MV/m and a RF power of 3.15 MW.

Fig. 2 compares a measured momentum distribution with the simulation. The experimental data are obtained by using the projected image from the YAG screen in the dispersive arm, the space coordinates are recalculated into values of momentum. The simulation was done from the gun cathode to the middle of the dipole, it was not tracked through the full dipole, while the data are taken on the

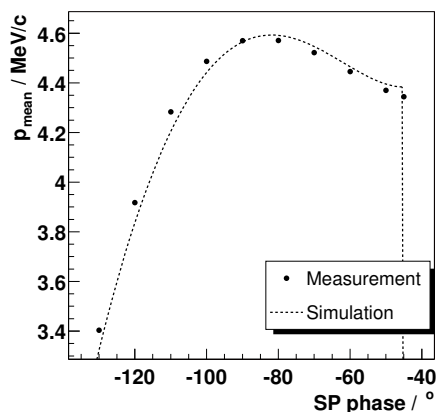


Figure 1: Mean momentum of the electron bunch as a function of set point phase for a gradient of 40.5 MV/m compared to the simulation. The errors of the measurements are of the order of 50 keV/c.

\* dlipka@ifh.de

## TRANSVERSE EMITTANCE MEASUREMENTS AT THE PHOTO INJECTOR TEST FACILITY AT DESY ZEUTHEN (PITZ)

K. Abrahamyan, J. Bähr, I. Bohnet, M. Krassilnikov, D. Lipka, V. Miltchev\*, A. Oppelt, F. Stephan, DESY Zeuthen, Zeuthen, Germany,  
 K. Flöttmann, DESY Hamburg, Hamburg, Germany,  
 Iv. Tsakov, INRNE Sofia, Sofia, Bulgaria

### Abstract

The components and functionality of the emittance measurement system at PITZ are introduced. In brief some design considerations are reviewed as well. The influence of the noise due to dark current and electronic noise in beam size measurements is discussed and estimated. Results from recent transverse emittance measurements are presented and compared with simulations. Examples of a strongly distorted trace space are also considered where the application of a single slit scanning technique is a successful alternative of the multi-slit method.

### INTRODUCTION

The main research goal of the Photo Injector Test Facility at DESY Zeuthen (PITZ) is the development of electron sources with minimized transverse emittance like they are required for the successful operation of Free Electron Lasers and future linear colliders [1]. The process of electron beam optimization requires characterization of the transverse emittance at a wide range of operation parameters. A slit/pepper-pot emittance diagnostic is designed and commissioned in order to characterize the trace space of the space charge dominated electron beam produced by PITZ.

### EMITTANCE MEASUREMENT SYSTEM (EMSY)

EMSY (Figure 1) consists of two sets of masks for sampling the trace space distribution in both transverse directions. Each set is mounted on a separate carrier (actuator). In general EMSY has four degrees of freedom: rectilinear vertical and horizontal motion and rotation around both transverse axes. All motions are remote controllable. The masks are made out of 1-mm thick tungsten\* plates. The slits have an opening of 50  $\mu\text{m}$ , the diameter of the pepper pot mask holes is of the same size. There are two variations of multi slit masks installed in EMSY: with 1mm and 0.5 mm slit to slit separation. The design of the masks meets some general requirements introduced in [2], [3]:

-The beamlets produced by a slit mask must be emittance dominated

-The distance between the slits is a compromise between obtaining a good representation of the phase space and avoiding overlapping of the beamlets

-The contribution of the initial beamlet size to the beamlet size at the observation screen should be as small as possible

-The thickness of the mask is a compromise between the need to scatter electrons to form a uniform background and the desire to minimize the slit-edge scattering.

The masks are installed on the two actuators in the following arrangement: on the vertical actuator a multi-slit mask, a pepper-pot mask and a single slit mask are mounted. On the horizontal one: multi-slit mask, single-slit mask and YAG screen for direct observation of the electron beam.

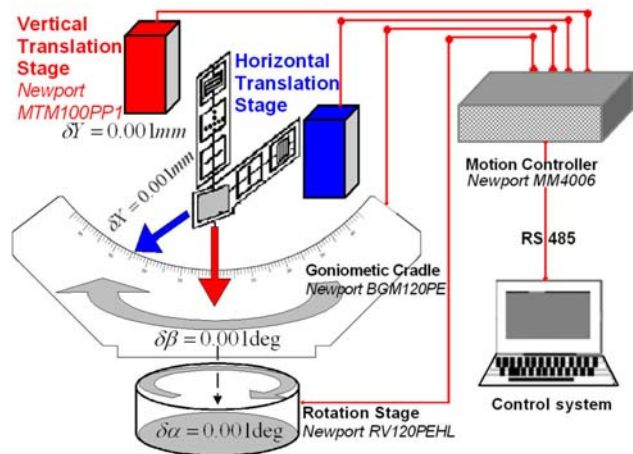


Figure 1: The emittance measurement system.

### BEAM SIZE AND TRANSVERSE EMITTANCE MEASUREMENTS

The beam position and RMS size measurements are performed by calculating first and second central moments of intensity distributions of images obtained by CCD cameras:

\* miltchev@ifh.de

## Development of a Bunch-Length Monitor with Sub-Picosecond Time Resolution and Single-Shot Capability\*

Daniel Sütterlin<sup>1</sup>, Volker Schlott<sup>1</sup>, Hans Sigg<sup>1</sup>, Heinz Jäckel<sup>2</sup>

<sup>1</sup> Paul Scherrer Institute, CH-5232 Villigen, Switzerland

<sup>2</sup> Institute of Electronics, ETHZ, CH-8092 Zürich, Switzerland

### Abstract

A bunch-length monitor with single-shot capability is under development at the 100 MeV pre-injector LINAC of the Swiss Light Source (SLS). It is based on the electro-optical (EO) effect in a ZnTe crystal induced by coherent transition radiation (CTR). A spatial auto-correlation of the CTR in the EO-crystal rotates the polarisation of a mode-locked Nd:YAG laser to produce an image on an array detector representing the Fourier components of the CTR spectrum. Up to now a theoretical model for the emission of transition radiation has been developed in order to design optics allowing efficient transport of the CTR onto the EO-crystal. The frequency dependency of the CTR due to the finite size of the target screen has been measured in the sub-THz regime at the SLS LINAC. The results strongly support the theoretical descriptions of the radiation source. By expanding the intensity pattern in higher-order Laguerre-Gaussian modes, the transmission through the optical transfer system is calculated.

### EO AUTO-CORRELATION

The electro-optical effect provides the potential to measure electron bunch lengths with sub-ps time resolution. A number of experiments have already been performed using the coincidence of fs-laser pulses with coherent radiation emitted from short electron bunches [1]. At the SLS, a novel bunch length monitor is under development, which uses an actively mode-locked Nd:YAG laser to analyse the spatial auto-correlation of CTR in an EO-crystal. A schematic set-up of the monitor is shown in fig. 1.

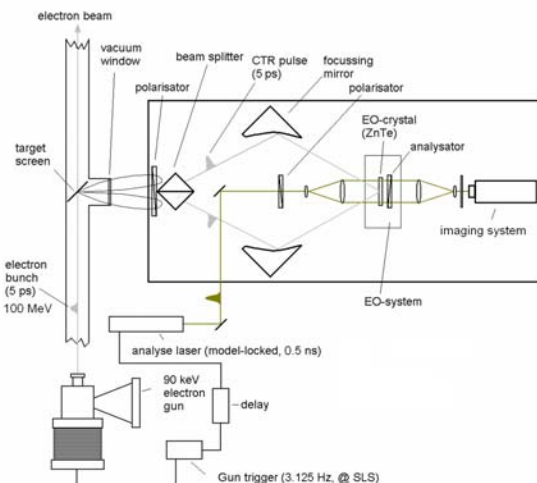


Figure 1: Schematic setup for EO-auto-correlation.

In this experiment, the synchronization of the laser with the CTR from the electron beam is not considered as critical due to the relatively long pulses of the Nd:YAG laser ( $< 500$  ps), however the signal to noise ratio needs to be addressed more carefully.

The interference pattern produced by the auto-correlation of CTR in the EO-crystal can be expressed as:

$$I(\vec{r}, \omega) = 2I(\omega) \left[ 1 + \text{Cos} \left[ 2 \text{Sin}(\theta) \frac{\omega}{c} r_1 \right] \right] \quad (1),$$

where  $\theta$  is the incident angle between the wave vector  $k$  and the normal vector  $n$  on the EO-crystal.

The power of the analyse laser is therefore modulated by the EO-crystal according to

$$I^{out} \approx I_{Laser} \left( \frac{\pi d}{V_{\lambda/2}} \right)^2 E_{CTR}^2. \quad (2)$$

$V_{\lambda/2}$  is the so-called half wave voltage necessary to rotate the laser polarisation by  $\pi/2$ :

$$V_{\lambda/2} = \frac{\lambda}{2n^3 r_{41}}. \quad (3)$$

For ZnTe the half wave voltage is 3.8 kV. Assuming a thickness of the electro-optical crystal of 0.5 mm the laser power modulated by a field of 1 kV/cm is  $2 \cdot 10^{-3} I_{Laser}$ .

Background intensity  $B_{Background}$  and noise contributions have to be considered as well. According to eq. (1), the incoherent background is in the same order of magnitude as the signal itself. The most dominant noise sources, which contribute during the entire duration of the laser pulse ( $\approx 500$  ps), are: the stray light scattered into the detector due to the limited extinction of the polarizer, the limited polarisation state of the laser beam and the strain induced birefringence of the electro-optical crystal. The weighted contributions are given by  $\epsilon_{Polariser}$ ,  $\epsilon_{Laser}$  and  $\epsilon_{Strain}$ . Although polarisers with  $\epsilon_{Polariser} < 10^{-5}$  are available, the experimentally achievable total extinction  $\epsilon_{Total} = \epsilon_{Polariser} + \epsilon_{Laser} + \epsilon_{Strain}$  may thus not be better than  $10^{-4}$ .

The resulting signal dynamic is given by

$$d_s = 10 \text{Log}_{10} \left( \frac{I_{Signal}}{I_{Signal} + B_{Background} + \epsilon_{Total}} \right) \quad (4).$$

With an assumed bunch length of 5 ps (at the SLS pre-injector LINAC) the signal dynamic is  $-8$  dB. Assuming a detection system with a dynamic range  $d_N$  of about 30 dB (commercial CCD-camera) a signal to noise ratio defined as  $d_{S/N} = d_N + d_s$  of  $> 20$  dB is achievable for electric field strengths of more than 1 kV/cm.

## FAST TUNE MEASUREMENT SYSTEM FOR THE ELETTRA BOOSTER

S. Bassanese, M. Ferianis, F. Iazzourene Sincrotrone Trieste, S.S. 14 Km163.5, 34012 Trieste, ITALY

### Abstract

A major upgrade of the ELETTRA injector is currently on going: the 1GeV Linac will be replaced with a 100MeV Linac and a 2.5GeV Booster Synchrotron, cycling at 3Hz. A new set of diagnostics is under development for these two new machines. The new Fast Tune measurement system for the Booster represents a significant improvement as compared to the present Tune measurement system.

To completely characterise the dynamics of the Booster during the energy ramp, whose duration is 160ms, a set of 25 tune values is required, corresponding to a 6.4ms interval between successive measurements. The accuracy of this measurement is  $<10^{-3}$ . Such frequency spans are achievable using a Real Time Spectrum Analyser (RTSA) from Tektronix, which is a fast sampling instrument with built-in FFT algorithm and data presentation.

In this paper, after describing the system specifications and architecture, we present the results of the preliminary tests, which have been carried out both in the laboratory and on the Storage Ring.

### INTRODUCTION

The new injector, which will replace the 1GeV Linac, is a new 100MeV Linac and a 2.5GeV Booster synchrotron. Full energy injection and top-up operation of the Storage Ring are the driving forces for this major machine upgrade. This new operating condition (constant current and energy) will greatly improve the stability of the ELETTRA light source as both the Storage Ring and the Beam lines will work under stationary conditions.

The development of the new diagnostics has started and it includes a new fast tune measurement system for the Booster synchrotron. Compared to the present Tune System [1], the performance up-grade mainly concerns the tune measurement rate, which will be shifted from the present 0.5Hz to 200Hz.

Actually for sake of reliability there will be two systems measuring the Booster Tunes, independently: the one described in this paper, based on the RTSA, and a second system, based on the Digital BPM Detector, already in use at ELETTRA [2]. The first one is believed to be useful especially during Booster commissioning, due to the convenient data presentation provided by the RTSA [3] as spectrograms. The second one will be installed as an Automatic Tune Measurement system, continuously checking the mean tunes.

In this paper we present the design of the fast tune measurement system based on the RTSA and the tests, performed on the Storage Ring, with the prototype of the new system. Full advantage has been taken from recently available new instruments, called Real Time Spectrum

Analyzers. The tests carried out confirmed our expectations on performance improvement.

### SYSTEM DESCRIPTION

The specifications for the fast tune measurement system require the real time measurement of horizontal and vertical tune and chromaticity during the energy ramp.

The time variation of the bending magnetic field during the ramping cycle of the Booster produces an eddy current in the metallic vacuum chamber of the bending magnet [4]: the main effect is an induced time-varying sextupolar component. To fully characterize the chromaticity variation and to keep it at the desired values [5], a minimum of 25 measurements per ramp is required, with a frequency resolution of  $10^{-3}$ . The nominal duration of a ramp is 160ms, but it will go up to 1s during the commissioning phase of the Booster, which calls also for the system to be flexible.

#### Tune excitation and detection

A block diagram of the system is shown in fig. 1. A white noise excitation scheme has been adopted which is band-limited around the expected tune frequencies. The limited bandwidth of the excitation signal allows a more efficient use of the power amplifier.

The output of a white noise generator is band-pass filtered and amplified by a wide-band power amplifier. During preliminary tests, carried out on the ELETTRA Storage Ring at 2GeV, 50W (in a 100 kHz bandwidth) of diagonal excitation produced tune peaks of  $-71\text{dBm}$  over a noise floor of  $-95\text{dBm}$ . Therefore, the Amplifier Research model 150A100B, a 150W amplifier with a bandwidth 10KHz-100MHz, has been selected for beam excitation. A strip-line kicker, equipped with four  $50\Omega$  electrodes, will be used for both single plane (Horizontal or Vertical) and Diagonal excitation.

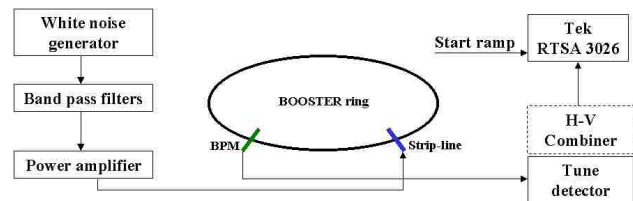


Figure 1: Fast Tune measurement system block Diagram

The transverse beam oscillations will be picked-up by a dedicated Beam Position Monitor placed at a high beta ( $\beta_v, \beta_h$ ) location; the 500MHz signals from the BPM will be down converted by the ELETTRA Tune Detector [1].

The two outputs of the Detector provide the horizontal and vertical components of the betatron oscillations in base band. These signals will be summed up and delivered to the RTSA 3026 from Tektronix.

# CRYOGENIC CURRENT COMPARATOR FOR ABSOLUTE MEASUREMENTS OF THE DARK CURRENT OF SUPERCONDUCTING CAVITIES FOR TESLA

K. Knaack, M. Wendt, K. Wittenburg, DESY Hamburg  
 R. Neubert, S. Nietzsche, W. Vodel, Friedrich Schiller Universität Jena  
 A. Peters, GSI Darmstadt

*Abstract*

A measurement system for detecting dark currents, generated by the TESLA cavities, is proposed. It is based on the cryogenic current comparator principle and senses dark currents down to the nA range. Design issues and the application for the CHECHIA cavity test stand are discussed.

## 1. INTRODUCTION

The 2x250 GeV/c TESLA linear collider project, currently under study at DESY [1], is based on the technology of superconducting L-band (1.3 GHz) cavities. The two 10.9 km long main linacs are equipped with a total of 21024 cavities. A gradient of 23.4 MV/m is required for a so-called superstructure arrangement of couples of 9-cell cavities. To meet the 2x400 GeV/c energy upgrade specifications, higher gradients of 35 MV/m are mandatory.

Dark current, due to emission of electrons in these high gradient fields, is an unwanted particle source. Two issues are of main concern, thermal load and propagating dark current [2].

Recent studies [3] show, that the second case seems to be the more critical one. It limits the acceptable dark current on the beam pipe "exit" of a TESLA 9-cell cavity to approximately 50 nA. Therefore the mass-production of high-gradient cavities with minimum field emission requires a precise, reliable measurement of the dark current in absolute values. The presented apparatus senses dark currents in the nA range. It is based on the cryogenic current comparator (CCC) principle, which includes a superconducting field sensor (SQUID). The setup contains a faraday cup and will be housed in the cryostat of the CHECHIA cavity test stand.

## 2. REQUIREMENTS OF THE DARK CURRENT INSTRUMENT

Electrons can leave the niobium cavity material, if the force of an applied external electric field is higher than the bounding forces inside the crystal structure. The highest field gradients occur at corners, spikes or other discontinuities, due to imperfections of the cavity shape. Another potential field emitter is due to any kind of imperfection on the crystal matter, like grain boundaries, inclusion of "foreign" contaminants (microparticles of e.g.

In, Fe, Cr, Si, Cu) and other material inhomogeneous. At these imperfections the bounding forces are reduced and electrons are emitted under the applied high electromagnetic fields [4]. With a series of special treatments the inner surface of the TESLA cavities are processed to minimize these effects. A reliable, absolute measurement of the dark current allows the comparison of different processing methods and a quality control in the future mass-production.

TESLA will be operated in a pulse mode with 5 Hz repetition rate. The 1.3 GHz rf pulse duration is 950  $\mu$ s. During this time the dark current is present and has to be measured. Therefore a bandwidth of 1 kHz of the dark current instrument is sufficient. As field emission is a statistical process, the electrons leave the cavity on both ends of the beam pipe. Thus, half of the dark current exits at each side, and has to be measure on one side only. With the 1.3 GHz rf applied, we expect that the dark current has a strong amplitude modulation at this frequency. This frequency has to be rejected from the instrument electronics to insure its proper operation. The dark current limits and the related energy range of the electrons are shown in Table 1.

Parameters	9-cell test cavity in CHECHIA	TESLA cavity modules (12x9-cell cavity)
Energy of dark current electrons	up to 25...40 MeV	up to 350...560 MeV
dark current limits	< 50 nA	< 1 $\mu$ A

**Table 1:** Expected dark current parameters

The use of a faraday cup as dark current detector for the TESLA cavity string will suffer from the high electron energies and low currents. The capture of all secondary electrons in the stopper are challenging. The use of a cryogenic current comparator as dark current sensor has some advantages:

- measurement of the absolute value of the dark current,
- independence of the electron trajectories,
- simple calibration with a wire loop,
- high resolution,
- the electron energies are of no concern.

The required liquid He temperature for the CCC and the cryogenic infrastructure for the whole apparatus will be provided by the CHECHIA test stand. An effective shielding to external magnetic fields has to be considered,

## A 40MHZ BUNCH BY BUNCH INTENSITY MEASUREMENT FOR THE CERN SPS AND LHC.

H. Jakob, L. Jensen, R. Jones<sup>#</sup>, J.J. Savioz, CERN, Geneva, Switzerland

### Abstract

A new acquisition system has been developed to allow the measurement of the individual intensity of each bunch in a 40MHz bunch train. Such a system will be used for the measurement of LHC type beams after extraction from the CERN-PS right through to the dump lines of the CERN-LHC. The method is based on integrating the analogue signal supplied by a Fast Beam Current Transformer at a frequency of 40MHz. This has been made possible with the use of a fast integration ASIC developed by the University of Clermont-Ferrand, France, for the LHC-b pre-shower detector. The output of the integrator is digitised using a 12-bit ADC and fed into a Digital Acquisition Board (DAB) that was originally developed by TRIUMF, Canada, for use in the LHC orbit system. A full system set-up was commissioned during 2002 in the CERN-SPS, and following its success will now be extended in 2003 to cover the PS to SPS transfer lines and the new TT40 LHC extraction channel.

### INTRODUCTION

In order to be able to evaluate the quality of the LHC beam before its extraction from the CERN-SPS it was necessary to develop a beam intensity measurement capable of distinguishing between the individual LHC bunches spaced by 25ns. This system was also foreseen for beam optimisation, allowing the operators to see the intensity structure of the beam throughout the SPS cycle, providing information on where in the batch losses are occurring and at what time. Since the same system was to be installed in the PS to SPS transfer lines it was important that the same electronics was capable of measuring standard, 200MHz structure SPS fixed target beams. To this end a new beam current transformer (BCT) system has been developed and installed in the SPS and its transfer lines. This is comprised of a commercial fast BCT, a specially adapted housing, a calibration unit, an integrator card containing a fast 40MHz integrator ASIC and a digital acquisition readout. There are currently 4 such systems installed in the SPS, one at each end of the PS to SPS transfer lines, one in the SPS ring itself, and one in the TT40 extraction channel towards the LHC and CNGS. A further 4 systems will be installed over the coming years: 3 completing the layout for the LHC transfer lines and one in front of the CNGS target station.

### THE SPS FAST BCT SYSTEM

#### *The Fast Beam Current Transformer*

The new fast beam current measurement in the SPS makes use of commercially available Bergoz low-droop,

passive, fast beam current transformer (FBCT) as the detection device. The 40 winding core used has a frequency response up to ~400MHz and a droop of less than 0.1% per microsecond. This low droop is important if difficult baseline correction is to be avoided during the passage of the beam. The FBCT is installed in a specially designed housing aimed at maintaining a clean signal response (see Fig. 1). An 80nm titanium coating is applied to the vacuum side of the ceramic gap, giving a series resistance of ~20Ω and effectively damping any cavity resonances.

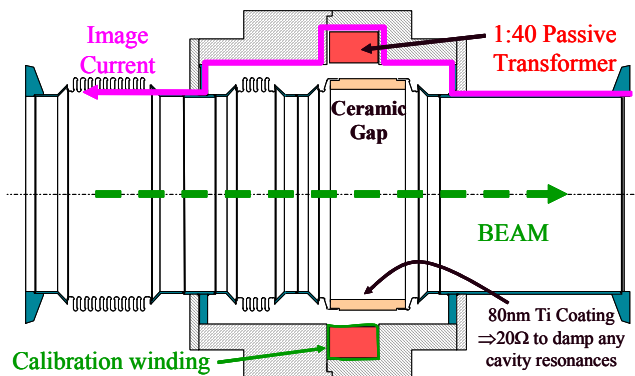


Figure 1. Schematic of the SPS Fast BCT

A calibration winding has been added to the transformer core to allow the injection of a 5μs, 128mA calibration pulse generated on demand by a switchable current source. This provides the absolute calibration for the system and corresponds to  $2 \times 10^{10}$  charges in 25ns.

Fig.2 shows the typical response of the FBCT to LHC type beam. Each of the 4 batches visible contain 72 bunches separated by 25ns.

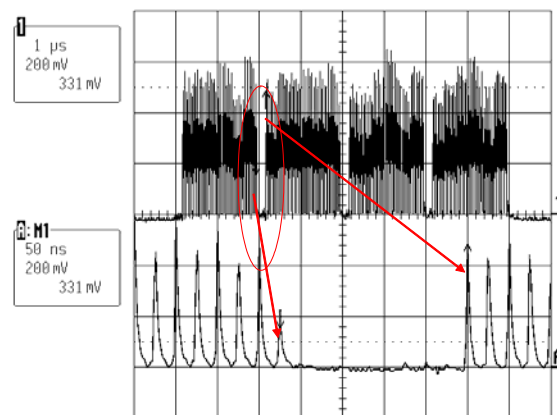


Figure 2. SPS Fast BCT response to LHC type beam.

<sup>#</sup>Rhodri.Jones@cern.ch

# CURRENT MEASUREMENTS OF LOW-INTENSITY BEAMS AT CRYRING

A. Paal, A. Simonsson, A. Källberg, Manne Siegbahn Laboratory of Physics, Stockholm, Sweden

J. Dietrich, I. Mohos, Institut für Kernphysik, Jülich, Germany

## Abstract

The demand for new ions species leads to an increasing number of cases in which the ions can only be produced in small quantities. thus weak ion currents below 1 nA quite often have to be handled and measured in low energy ion storage rings, like CRYRING.

-We have built a new amplifier with 86 dB gain and  $0.6 \text{ nV}/(\text{Hz})^{1/2}$  RMS input noise.

-It was moved close to the ICT.

In the Bunch Signal Processor the gain by 20 dB has been decreased to get lower slow offset.

-A low pass filter has been added (10 Hz, 100 Hz).

## INTRODUCTION

Various detector systems have been developed to measure such low intensity bunched and coasting beams by using the overlapping ranges of those systems (Fig.1).

### Bunched beam measurements

Bunched beam parameters:

Frequency range: 40 kHz-1.5 MHz

Duty cycle: 10%-50%

Pulse width: 60 ns-13  $\mu$ s

A Bergoz Beam Charge Monitor with Continuous Averaging (BCM-CA) and an Integrating Current Transformer (ICT) was installed 1997 to measure the bunched beam intensity with 200 A full scale range and 20 nA RMS resolution.

Modifications:

Result: The 200  $\mu$ A full scale range have been extended down to 5  $\mu$ A with 1 nA RMS resolution.

A bunched beam current measurement is shown in Fig.2.

The amplified sum signal of the capacitive pick up closest to the ICT can be used to set up the measuring windows for the BCM and for the second Gated Integrator. The RMS resolution is about 100 pA. The PU Amplifier [1] has  $1.2 \text{ nV}/(\text{Hz})^{1/2}$  RMS noise.

### Coasting beam measurements

To measure the coasting beam intensity, neutral particle detectors have been built [2, 3]. At high particle energies the RGBPMs are used [4]. Their fast Micro channel plate detectors can handle 1 Mcps count rate.

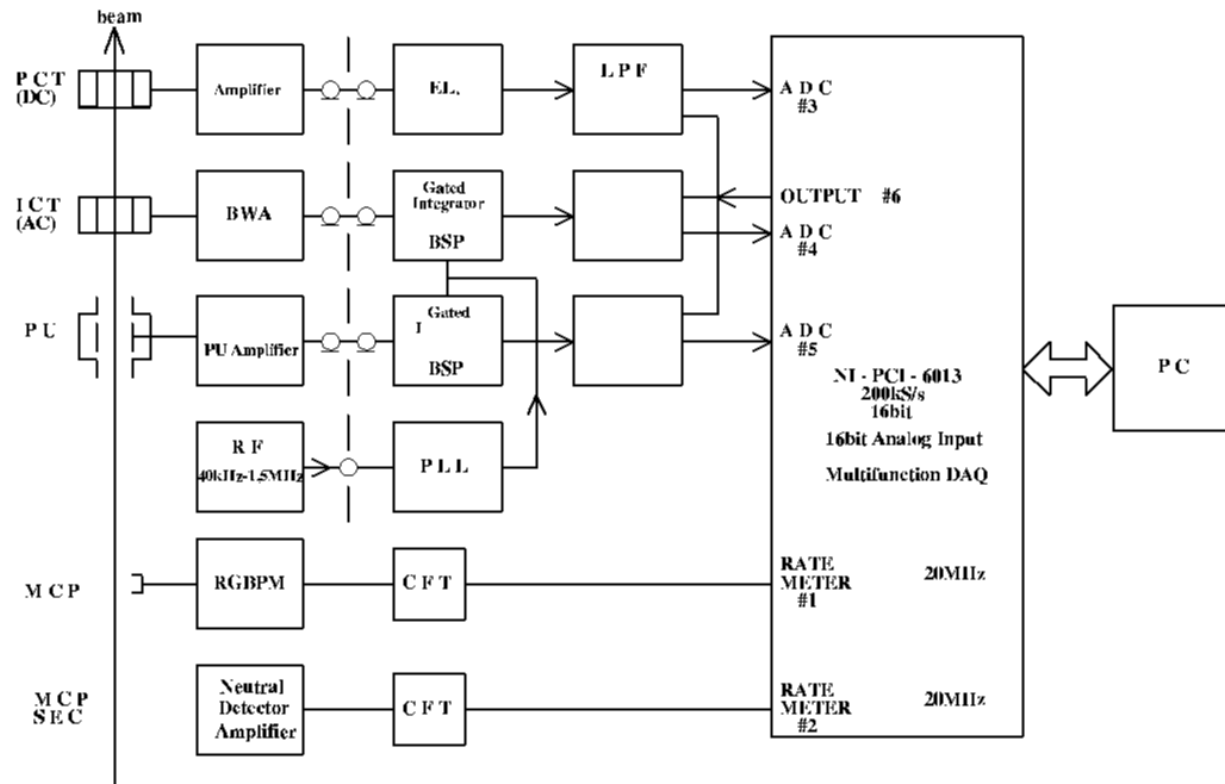


Figure 1: Beam Current Monitoring system of CRYRING

## DARK CURRENT MEASUREMENTS AT THE PITZ RF GUN

I. Bohnet, J. H. Han\*, M. Krasilnikov, F. Stephan, DESY Zeuthen, 15738 Zeuthen, Germany  
 K. Flöttmann, DESY Hamburg, 22603 Hamburg, Germany

### Abstract

For photocathode rf guns with electric fields of more than 40 MV/m at the photocathode and with an rf pulse length of 100  $\mu$ s or more, the amount of dark current might be comparable with the photoelectron beam. At the photoinjector test facility at DESY Zeuthen (PITZ) the dark current was measured with a Faraday cup for various settings of the solenoid fields at the rf gun. We discuss the dark current behavior for different photocathodes. Experimental results are compared with simulations.

### INTRODUCTION

The photoinjector test facility at DESY Zeuthen (PITZ) has been developed with the aim to achieve high quality electron beams and study their characteristics for future applications at free electron lasers and linear colliders. At PITZ, the photocathode rf gun is operated with a rf frequency of 1.3 GHz, a maximum electric field of 41 MV/m at the photocathode, a maximum rf pulse length of 900  $\mu$ s, and a maximum repetition rate of 10 Hz.

Due to the high electric field and the long field emission time, the amount of dark current might be comparable to the photoelectron beam. Such a strong dark current degrades the electron beam quality and impairs emittance and energy spread measurements. More seriously, a large dark current is a severe hazard for a superconducting linac as it may produce X-rays, cryogenic losses, and radioactive activation. In the following paper, the generation of dark current and its properties are studied with measurements and simulation.

### FIELD EMISSION AT THE RF GUN

The field emission of electrons is the main source of dark current. The field emission current at the rf gun can be parameterized in terms of the modified Fowler-Nordheim equation [1]

$$I_F = \frac{1.54 \times 10^{-6} \times 10^{4.52\phi^{-0.5}} A_e (\beta E)^2}{\phi} \times \exp\left(-\frac{6.53 \times 10^9 \phi^{1.5}}{\beta E}\right), \quad (1)$$

where  $E$  is the surface electric field in V/m,  $\phi$  is the work function of the emitting material in eV,  $\beta$  is a field enhancement factor, and  $A_e$  is the effective emitting area.

\*jhhan@ifh.de

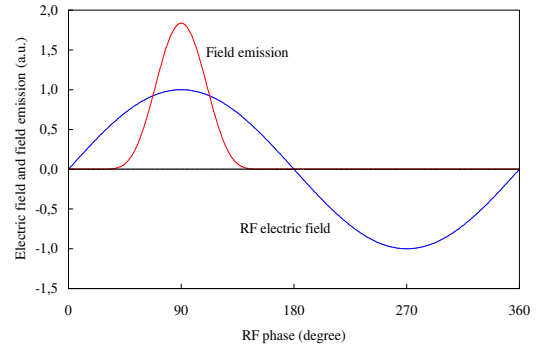


Figure 1: Intensity distribution of the field emission and the strength of the rf electric field for an rf cycle. The field emission curve was computed from the modified Fowler-Nordheim equation (Eq. 1) with an sinusoidal rf field and the typical  $\beta$  and  $\phi$  values of 200 and 4.5 eV, respectively.

Figure 1 shows that the field emission is concentrated on the maximum electric field region of an rf cycle. Therefore, the field emitted electrons produced on the cathode are preferably accelerated in forward direction by the rf electric field.

At the rf gun, the field emitted electrons from other sources, like the iris or the entrance to the coupler, cannot follow the downstream component of the accelerating field, because these electrons are not synchronized to the accelerating rf electric field. However, they are able to heat up the cavity surface and may create secondary electrons.

The average field emission current during one rf cycle is described as [1]

$$\bar{I}_F = \frac{5.7 \times 10^{-12} \times 10^{4.52\phi^{-0.5}} A_e (\beta E_0)^{2.5}}{\phi^{1.75}} \times \exp\left(-\frac{6.53 \times 10^9 \phi^{1.5}}{\beta E_0}\right), \quad (2)$$

where  $E_0$  is the amplitude of the sinusoidal macroscopic surface field in V/m.

### MEASUREMENTS

The experimental setup is shown in Fig. 2. A molybdenum (Mo) cathode is a circle with a radius of 8 mm and a cesium telluride ( $\text{Cs}_2\text{Te}$ ) cathode is a circle with a radius of 4 mm on a Mo substrate which has the same geometry as the Mo cathode except for the  $\text{Cs}_2\text{Te}$  coating. The

# IONISATION CHAMBERS FOR THE LHC BEAM LOSS DETECTION

E. Gschwendtner, R. Assmann, B. Dehning, G. Ferioli, V. Kain  
 CERN, Geneva, Switzerland

## Abstract

At the Large Hadron Collider (LHC) a beam loss system will be used to prevent and protect superconducting magnets against coil quenches and coil damages. Ionisation chambers will be mounted outside the cryostat to measure the secondary shower particles caused by lost beam particles.

Since the stored particle beam intensity is eight orders of magnitude larger than the lowest quench level and the losses should be detected with a relative error of two, the design and the location of the detectors have to be optimised. For that purpose a two-fold simulation was carried out: The longitudinal loss locations of the tertiary halo is investigated by tracking the halo through several magnet elements. These loss distributions are combined with simulations of the particle fluence outside the cryostat, which is induced by lost protons at the vacuum pipe.

The base-line ionisation chamber has been tested at the PS Booster in order to determine the detector response at the high end of the dynamic range.

## INTRODUCTION

The magnet coil quench and damage levels are time and energy dependent. This results in a large range of loss rate variations requiring observations of ionisation chamber currents between  $10^{-12}$  and  $10^{-3}$  A [1]. The required time resolution for the arc monitors is 2.5 ms and for all other detectors it is 89 $\mu$ s (i.e. 1 LHC turn).

These requirements show already that the demands on the design of a reliable beam loss detection system are extremely high. Here are three different design aspects of the loss system are investigated:

- The longitudinal beam loss distribution of the tertiary halo along the magnets. It is emitted by the secondary collimators and will be lost at aperture limits.
- Calculations of the particle fluences outside the cryostat, which is induced by lost protons. This defines the most suitable positions, the needed number and the impact on the dynamic range of the detectors.
- The signal response of the ionisation chamber in a high rate environment similar to the LHC.

First results are shown.

## TERTIARY HALO LOSS DISTRIBUTION STUDIES FOR 450 GeV

The longitudinal beam loss distribution was obtained by tracking particles populating the tertiary halo at 450GeV through parts of the LHC. The tertiary halo particles stem from the collimation insertion IR7 escaping

the secondary collimators. The halo particles were tracked with SIXTRACK and the scattering routine K2. The left plot in Fig. 1 shows the (X,Y)-distribution of the halo after the collimators. MAD-X in the ‘one-pass’ mode was applied to track the particles from the collimation insertion IR7 to the chain of the LHC magnet elements we investigate. Finally the linear tracking program SLICETRACK was used to slice the elements and calculate the longitudinal beam loss distribution.

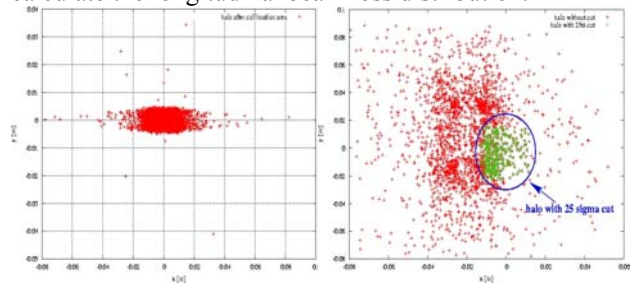


Figure 1: Left: Tertiary halo distribution after the collimation section IR7. Right: Halo tracked with MAD-X to the dispersion suppressor in IR1. Particles with amplitudes larger than  $25\sigma$  are cut.

The MAD-X tracking was based on the sequence V6.4.aperture containing information on apertures in the LHC. So particles exceeding these apertures get already lost during the transfer from the collimation section to the sliced chain of elements (e.g. tracking with MAD-X until IP5 results in the loss of all halo particles). But for the time being the LHC sequence does not contain all apertures and the particles can still reach unrealistic amplitudes in the tracking process. Thus we were forced to apply a cut in particle amplitudes before tracking through the sliced elements. Out of a geometrical argument we discarded particles with amplitudes exceeding  $25\sigma$  that is still quite large (see right plot in Fig. 1).

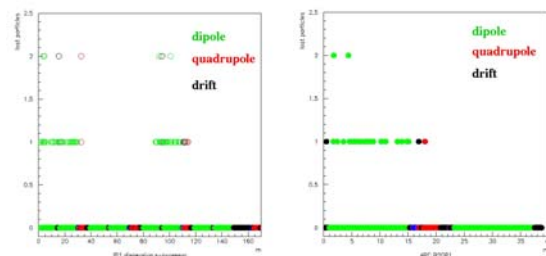


Figure 2: Loss distributions along the dispersion suppressor (left) and an arc short section (right) right of IP1. No beam excursions and misalignments are introduced.

We have investigated two cases: the loss distribution along the dispersion suppressor and along an arc short section, both right of IP1 for LHC beam1. SLICETRACK

## OPTICAL FIBRE DOSIMETER FOR SASE FEL UNDULATORS

H. Henschel, J. Kuhnhehn, Fraunhofer-INT, Euskirchen, Germany

M. Körfer\*, DESY, Hamburg, Germany

F. Wulf, HMI, Berlin, Germany

### ABSTRACT

Single pass Free Electron Lasers (FELs) based on self-amplified spontaneous-emission (SASE) are developed for high-brightness and short wavelength user applications. These light sources are related to short undulator periods which can be realized with permanent magnet designs. Unfortunately, the material is radiation sensitive and the undulators require a protection system. To monitor particle losses directly inside the undulator gap and to guarantee full magnetic performance for a long time, an optical fiber dosimeter has been developed and operated at the TESLA Test Facility (TTF). The dosimeter system allows online dose monitoring and beam particle loss optimisation.

### INTRODUCTION

High gain single pass SASE FELs require high peak current (kA), ultra-short (100  $\mu\text{m}$ ) and low emittance (few mm mrad normalized) electron bunches. The TTF achieved long bunch trains with 1800 bunches per second, a bunch charge of 4 nC and a bunch spacing down to 444 ns. The average beam power was 1.8 kW. To realize safe beam operation a machine protection system was necessary. Due to the radiation sensitive permanent magnet material a protection of the undulator with an upstream collimator system was installed. The necessarily tight tolerance of the magnetic field integrals is  $\leq 10 \text{ T mm}^2$  (rms). Therefore, local particle losses and resulting doses inside the radiation sensitive permanent magnet undulator were recorded with an online dosimeter system. The fibre sensor should be as close as possible to the magnet surface inside the undulator gap. Since the gap between magnetic yoke and the flat vacuum chamber is less than 1 mm conventional online dosimeters do not fit in such a geometry. Moreover, the strong magnetic field environment is not compatible with electrical sensor cabling. The TESLA collaboration developed an optical fibre dosimeter for SASE FEL undulators. At TTF, the fibre optical power-meter system and an Optical Time Domain Reflectometer (OTDR) system [1] has been successfully operated, which allows one to obtain the accumulated dose continuously.

### OPTICAL FIBRE DOSIMETER

The most obvious effect of ionising radiation in optical fibres is an increase of light attenuation. The radiation penetrates the fibre and creates additional colour-centres which cause a wavelength-dependent attenuation that can be measured with a power-meter (Fig.1).

#### *Radiation Effect on Optical Fibre*

The high purity of the modern fibre raw materials has reduced their radiation sensitivity. However, if the core material of Germanium (Ge)-doped Multi-Mode Gradient Index (MM-GI) fibres is co-doped with Phosphorus (P), their radiation-induced attenuation increases significantly so that these fibres are suitable for dosimeter purposes. A dedicated optical fibre for dosimeters shows (wavelength-dependent) a nearly linear increase of attenuation after irradiation. For the optical fibre used the calibration of dose D versus light attenuation A is valid up to 1000 Gy and independent of the dose-rate and source type. No systematic influence on the dose rate was observed between about 0.006 and 70 Gy/min.

#### *General Layout*

A LED is connected with an optical fibre (Fig. 1). Light passing through the fibre will be continuously measured with the power-meter. Due to the irradiated fibre part, the light intensity suffers absorption leading to an attenuation step. The trace of attenuation increase versus time can be displayed at the accelerator control desk.

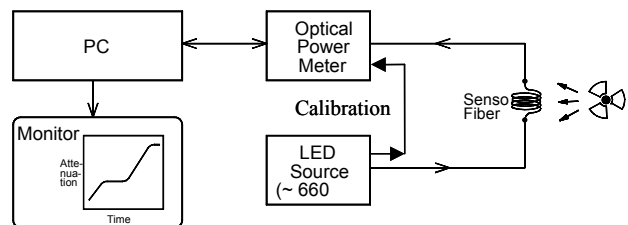


Figure 1: Scheme of an optical fibre dosimeter. The radiation produces absorbing "colour centres" in the sensor fibre. The light attenuation has been measured with an optical power-meter and allows one to determine the radiation dose.

\* corresponding author: markus.koerfer@desy.de

## BEAM LOSS DIAGNOSTICS BASED ON PRESSURE MEASUREMENTS

E.Badura, B.Franczak, W.Kaufmann, P.Horn, H.Reeg, H.Reich-Sprenger, P.Schütt, P.Spiller, K.Welzel, U.Weinrich, Gesellschaft für Schwerionenforschung mbH, Darmstadt, Germany

### Abstract

The GSI is operating a heavy ion synchrotron, which is currently undergoing an upgrade towards higher beam intensities. It was discovered that beam losses induce a significant pressure increase in the vacuum system. This effect can be used as beam loss diagnostics. In addition fast total pressure measurements were put into operation in order to detect the time constants of the pressure increase and decrease.

### 1 Measurement Principle

The energy loss per unit length of ions in matter depends on the kind, energy and charge state of the ions as well as on the target material. For heavy ions this energy deposition might be so high that effects like sputtering, melting, crack formation, etc. might occur. During such impacts a lot of gas molecules are released. The desorption yield, i.e. the number of gas molecules released per impact ion has been reported to be in the range from  $10^3$  to  $10^5$ . This effect has been studied at CERN [1] and is object to further investigations at GSI [2]. The typical value measured for the stainless steel vacuum chamber of the GSI heavy ion synchrotron SIS is  $10^4$ .

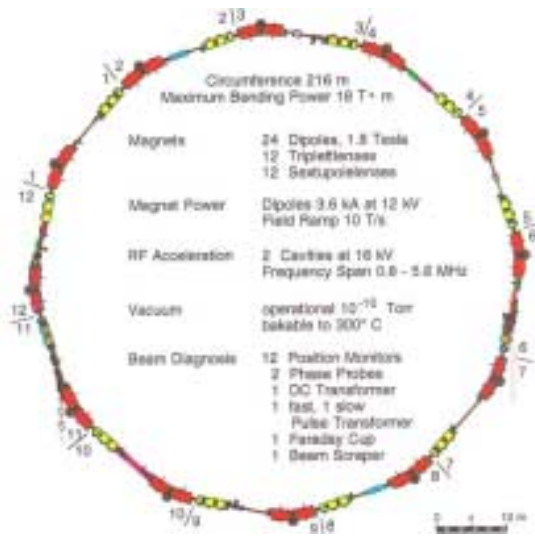


Fig. 1: The GSI heavy ion synchrotron SIS

The release of gas molecules increases the pressure in the vacuum system of the accelerator. The measurement of the pressure rise with pressure gauges contains the information about the amount of the lost ions as well as their impact point on the vacuum chamber. In the SIS the total pressure measurement is done with 12 IE514 extractor gauges from

Leybold equally distributed around the ring. These gauges can reliably measure down to a few  $10^{-12}$  mbar. The distance between two gauges is 18 m.

The pressure rise due to ion losses is immediate. There is also a typical pumping down time, which depends on the kind of gas molecules and the pumping system. In the SIS this pumping down time is the range from 10 ms to 10 s.

It is important to mention two cases: a constant loss rate and single loss events. One can consider a constant loss rate when the rate at which the losses take place is shorter than the pumping down time. In this case the pressure will increase to a kind of dynamic equilibrium. In the SIS this is the case for chemically inert gases in combination with short cycle times of the synchrotron. For the case of long cycling times and/or chemically active gases the released gas molecules are pumped away before the next significant ion loss appears.

### 2 Average total pressure and lifetime

Heavy ion circular accelerators operate at low pressure. The base pressure for the SIS for example is around  $2 \cdot 10^{-11}$  mbar. This corresponds to about a total of  $2 \cdot 10^{12}$  free gas molecules in the vacuum system. With the above mentioned desorption coefficient the amount of ions necessary to create a total pressure rise equivalent to the base pressure of the SIS can be estimated to about  $2 \cdot 10^8$ . If this amount of ions is lost in a short time the lifetime decreases by a factor of two. This is therefore about the detection limit for beam losses just from total average pressure or lifetime. The value of  $2 \cdot 10^8$  ions accelerated is close to the operation value for  $U^{28+}$ . Measurements of the total pressure and beam lifetime as function of the loss rate were done and are summarised in the following tables:

Beam type	Loss rate [ $10^7$ ions/s]	Pressure [ $10^{-11}$ mbar]	Lifetime [s]
no beam		1.96	
$U^{28+}$	1.2	2.13	5.0
$U^{28+}$	11.4	2.62	3.6
$U^{73+}$	0.88	1.99	14.4
$U^{73+}$	1.6	2.03	12.4
$U^{73+}$	2.2	2.22	12.3

Tab. 1: total pressure and lifetime as function of loss rate

## DAFNE BEAM LOSS MONITOR SYSTEM

G. Di Pirro, A. Drago, F. Sannibale, Laboratori Nazionali di Frascati INFN (LNF-INFN), Via E. Fermi 40, 00044 Frascati (RM), Italy

### Abstract

At the DAFNE collider a beam loss monitor system has been installed to continuously monitor the particle losses. The acquisition is based on 32 Bergoz beam loss monitors, of the Wittenburg type, installed close to the main rings vacuum chamber, buffer and monitoring circuitry and a scaler (SIS 3801) as acquisition board. We developed a front-end software that allows acquiring the integrated value of the BLM counts and a stream of 1000 point for each monitor, to cover a history of 3000 s. The operator program allows displaying the instantaneous BLM values over the machine together with a representation of the past history.

### 1 INTRODUCTION

DAFNE [1] is an electron/positron collider, composed by two rings and with two interaction regions. More than 1 A has been stored in collision. With beams at high current any beam loss along the machine pipe becomes a source of high background. To understand if we have anomalous beam losses we installed a beam loss monitor system on the machine pipe. The small size of the accelerator allows us to try a first installation with a low monitor number. A requirement to the installation is to allow upgrading the system in the future without any change in the software environment.

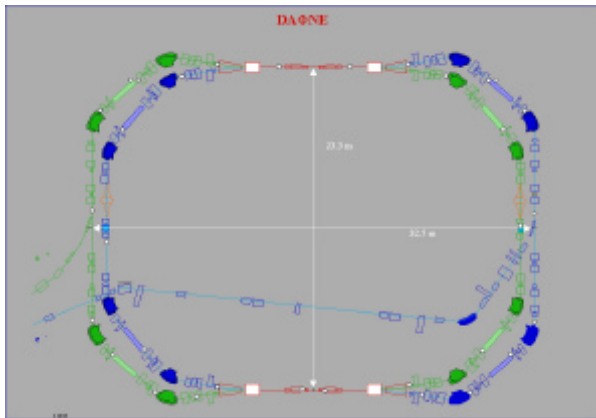


Fig.1 Dafne BLMs positions

We installed 31 monitors in total: 13 on the electron ring, 14 on the positron and 4 near the interaction region. The position has been chosen downstream already existing beam scrapers on the machine. Other monitors are placed at the point where the pipe is narrow near the splitter. Some other are near the dipoles and the wiggler. The BLMs are placed in equivalent positions in both rings. There are some monitors near the two experiments as well.

### 2 HARDWARE

The high density of elements installed on the DAFNE accelerator requires a compact beam loss monitor; moreover the monitor must be easy to install on the vacuum pipe. We chose the Beam Loss Monitor by Bergoz [3] for his compact size ( $33.5 \times 68.5 \text{ mm}^2$ ) and performances, a VME counter/scaler by Struck SIS 3801 [5] as acquisition board with an in house developed fan out. The acquisition board and the fan out are put inside a VME control system crate.

Fig 2 illustrates BLM operation. The BLM produces voltage pulses when the active area of a PIN photo-diode is struck by minimum ionizing particles (MIP), usually created by high energy particles striking residual gas molecules or a beam pipe obstruction. Presumably a MIP produces current flow in both detectors while a photon does not.

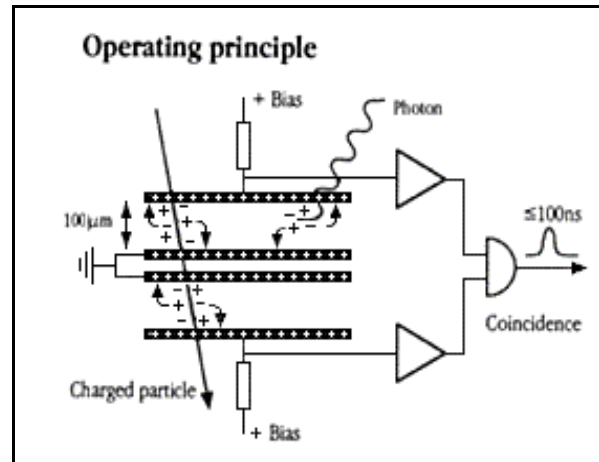


Fig 2 Operating principle (courtesy of Bergoz)

The acquisition board (SIS 3801) is a 100 MHz 32-channel scaler/counter. To synchronize the acquisition we use the 25 MHz internal clock which can be read on the first channel of the board. To the other 31 channels we connect the BLMs. A fan out board has been developed to interface the monitor with the acquisition board.

The beam loss monitor fan out is a VME module designed by the DAFNE electronics laboratory with the aim to interface mechanically and electrically the commercial parts and simplifies the test of the system. The fan out module is made of terminals to interface 32 Bergoz input sensors, 32 channel TTL buffers, 2 channel outputs with BNC connectors for diagnostics purpose, two manual knobs to select the channels to be monitored, and terminals to connect easily the SIS3800 counter. The diagnostics interface allows checking each input channel

## Discussion-Session

### Session 1: Wednesday (11:15–13:00 Hrs)

#### Machine Protection And Interlock Systems

K. Wittenburg, DESY, Deutsches Elektronen Synchrotron, Hamburg, Germany

e-mail: [kay.wittenburg@desy.de](mailto:kay.wittenburg@desy.de)

K. Scheid, ESRF, European Synchrotron Radiation Facility, Grenoble, France

e-mail: [scheidt@esrf.fr](mailto:scheidt@esrf.fr)

The purpose of a MPS is to protect the equipment against abnormal beam behaviour. High intense and high brilliant particle, photon and X-ray beams are capable of causing significant damage to components in a fraction of a second, i.e. too fast for any human reaction.

The aim of this session is to discuss existing and planned MPS with both their specific and their general requirements. Among points to be reviewed in the need for the MPS to be fail-proof are:

- the choice of sensors and components,
- the logic,
- the strategy, etc.

Some typical questions that will be raised are:

- What are the criteria for determining that an alarm situation has been reached?
- What is the subsequent action of the system?

Very often the MPS may allow different beam modes, depending on beam permit inputs:

- Which kind of beam modes exist?
- Which are the input signals?
- How are these systems integrated with the accelerator controls?
- What is the impact on their operation?

This session will include a few very brief presentations of existing and planned MPS' from different machines to illustrate the above questions and to stimulate the subsequent discussion.

**Discussion-Session**  
**Session 2: Wednesday (11:15–13:00 Hrs)**

**Global Accelerator Network, Control Systems And Beam Diagnostics**

U. Raich, CERN, Geneva, Switzerland

e-mail: Ulrich.Raich@cern.ch

H. Schmickler, CERN, Geneva, Switzerland

e-mail: Hermann.Schmickler@cern.ch

Falling funds force all accelerator centers to look for new sources of financing and for the most efficient way of implementing new projects. This very often leads to collaborations between institutes scattered around the globe, a problem well known to big high energy physics experiments. The collaborations working on big detectors e.g. for LHC started thinking about detector acquisition and control systems which can be remotely used from their respective home institutes with minimal support on the spot.

This idea was taken up by A. Wagner from DESY for the TESLA machine, who proposed the Global Accelerator Network (GAN) enabling users from around the world to run an accelerator remotely.

Questions around this subject that immediately come to mind

- Is the GAN only relevant to big labs? Or is it reasonable e.g. for operators or engineers in charge to do certain manipulations from home?
- Are our instruments ready for the GAN?
- Does the fact of being GAN ready increase the cost of the instruments?
- What are the advantages and disadvantages?
- Do we want these features? Or do inconveniences prime over advantages?
- Do any of the labs already have experience with GAN or any system going into this direction?
- What does GAN mean for the relationship between controls and beam diagnostics (a sometimes difficult chapter)?
- Can measurement systems be put onto the WEB and if yes, which ones?
- Where are the limitations?
- Can the scope of GAN be expanded to remote diagnostics and active maintenance of equipment, i.e. collaborating partners maintain their product in service after commissioning?
- What about common machine experiments with people sitting in different control rooms?
- What communication systems have to be put in place for this?
- Are there security issues and how do we deal with them?

**Discussion-Session**  
**Session 3: Wednesday (11:15–13:00 Hrs)**

**Beam Synchronous Timing Systems**

A. Peters, GSI, Gesellschaft für Schwerionenforschung, Darmstadt, Germany

e-mail: A.Peters@gsi.de

M. Ferianis, ELETTRA, Sincrotrone Trieste, Trieste, Italy

e-mail: mario.ferianis@elettra.trieste.it

For many beam diagnostics purposes beam synchronous timing systems are needed in addition to the timing systems supplied by the control systems of the different accelerators. The demands and techniques of different accelerator facilities will be discussed along the following aspects:

- Bunch and macro pulse synchronous timing systems
  - Solutions for different time scales from ps to ms
  - Coupling to the RF and control systems of the different accelerators
  - Electronics for the beam synchronous timing systems:
    - parameters,
    - techniques,
    - controlling.
- Use of industrial products for bunch synchronous timing systems, e.g. function generators
  - Distribution of the timing signals:
    - electronically via cables,
    - optically via fibres or
    - wireless
  - Coupling to and use of timing standards:
    - IRIG-B,
    - GPS,
    - ...

The participants should present and describe solutions from their facilities with some transparencies as a starting point for the discussion.